Accounts of Peptide Science Japan

Vol. 36, No. 1 | October 2025

The Japanese Peptide Society

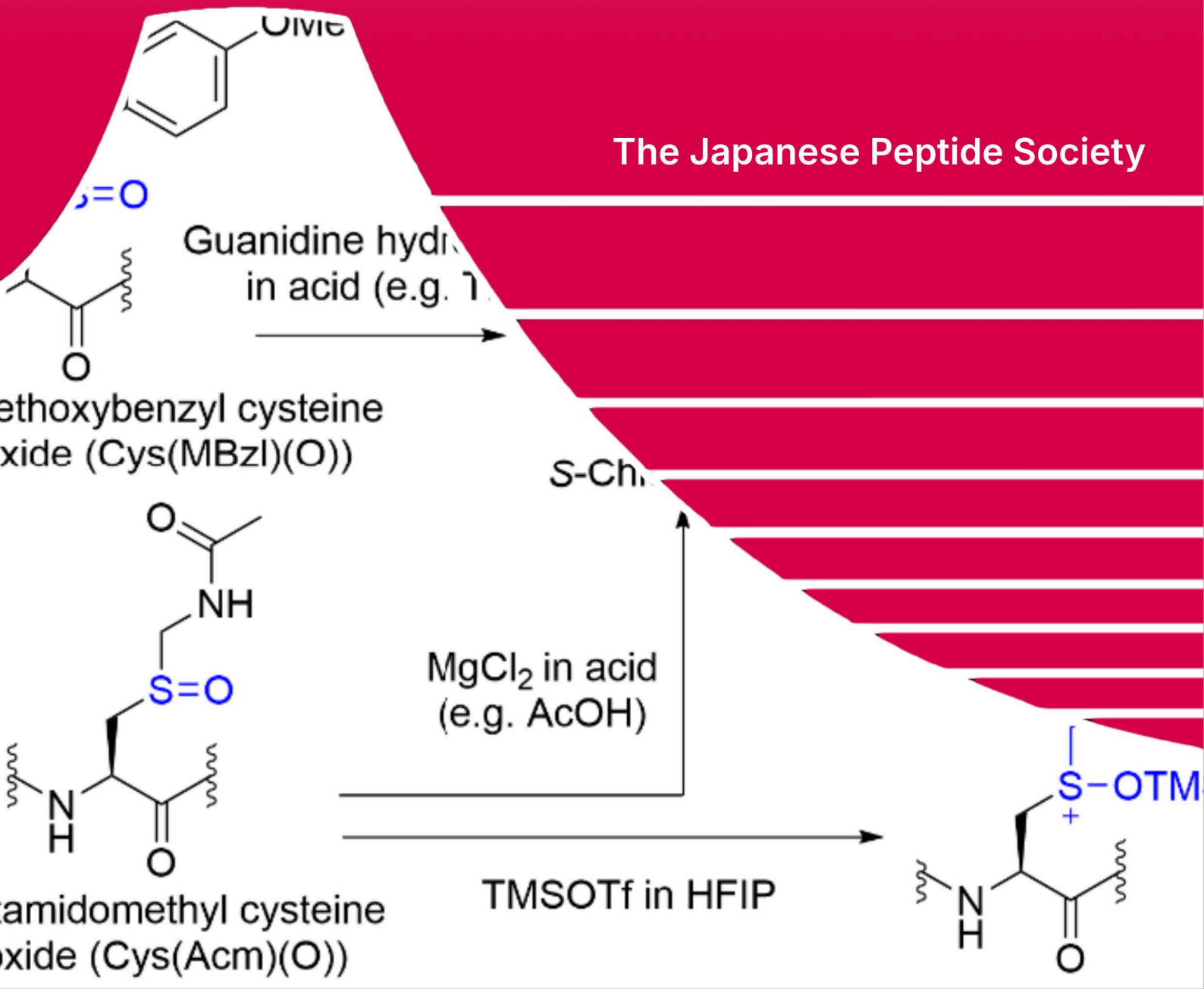

Accounts of Peptide Science Japan

Publisher

The Japanese Peptide Society
4-1-2 Ina, Minoo-shi, Osaka 562-0015, Japan

Published on October 1, 2025

Aims and scope

Accounts of Peptide Science Japan is an open access journal established through the integration of *Peptide Science* and *Peptide Newsletter Japan*. It is dedicated to sharing the scholarship of the Japanese Peptide Society with a global audience.

The journal centers on the article type *Account* – articles in which authors present an integrative account of their own research on a single theme, encompassing background, methodology, findings, significance, and future perspectives. The journal also publishes *Editorial* communicating the Society's activities and policies, *Essays* exploring topics of scholarly and societal relevance, and *Information* providing domestic and international updates on research, funding, and conferences. Together, these sections form an integrated platform that facilitates the sharing of knowledge across the community and broadens its international reach.

The scope of the journal spans the full breadth of peptide science, including, but not limited to: peptide synthesis and design; structural and physicochemical characterization; biological activity and mechanisms of action; drug discovery and delivery; peptidomimetics; computational and data science; analytical methodologies; biomaterials; and practical applications in the life sciences, medicine, and materials science. The journal welcomes contributions from researchers across academia, industry, and related fields, to promote international exchange and advance peptide science worldwide.

Information for Subscribers

Accounts of Peptide Science Japan is published online in three issues per year. This journal is available online for free.

Copyright and Copying (in any format)

Disclaimer

Table of Contents

Editorial

Accounts of Peptide Science Japan: Showcasing Japan's Excellence in Peptide Research
Akira Otaka III

Accounts of Peptide Science Japan 発刊に際し
大高 章 IV

Account

S-protected cysteine sulfoxide, a side product in peptide synthesis, finds an unprecedented usage: From peptide stapling and modification to insulin synthesis
Akira Otaka 1

Design of Tau-derived peptides for modulating structures and functions of microtubules
Hiroshi Inaba 11

Biomembrane research utilizing functional peptides: Stoichiometric analysis of oligomeric states of membrane proteins and sensing analysis of membrane curvature of extracellular vesicles
Kenichi Kawano 22

Essay

The 29th American Peptide Symposium and the 15th International Peptide Symposium 参加報告
新城（永原）紳吾 33

Information

第 62 回ペプチド討論会のご案内 ～ようこそ福岡へ～
伊東 祐二、野瀬 健、松島 綾美 36

Announcement of the 62nd Japanese Peptide Symposium – Welcome to Fukuoka
Yuji Ito, Takeru Nose, Ayami Matsushima 37

第 57 回若手ペプチド夏の勉強会開催報告
傳田 将也、猪熊 翼 38

第 27 回ペプチドフォーラム 開催報告
伊東 祐二、吉矢 拓 39

学会からのお知らせ 40

訃報　中嶋 暉躬 先生 41

Accounts of Peptide Science Japan: Showcasing Japan's Excellence in Peptide Research

As the President of the Japanese Peptide Society, it is my pleasure to announce the launch of *Accounts of Peptide Science Japan*, a publication that represents a significant step forward in disseminating Japan's peptide research achievements.

Since 1963, the Japanese Peptide Society has been publishing *PEPTIDE CHEMISTRY* (1963–1996) and *PEPTIDE SCIENCE* (1997–2024), journals dedicated to compiling abstracts from academic presentations at the Peptide (Chemistry) Symposium. In 1990, the Society introduced *PEPTIDE NEWSLETTER JAPAN*, which has served as an invaluable resource for updates and insights within the peptide research community.

Recognizing the evolving trends in academic communication, we have decided to unify *PEPTIDE SCIENCE* and *PEPTIDE NEWSLETTER JAPAN* into a single, dynamic publication. This new journal, *Accounts of Peptide Science Japan*, builds upon the strengths of its predecessors while introducing a significant new feature: English-language Accounts authored by Japan's peptide researchers. This addition aims to present the groundbreaking work of Japanese scientists to a global audience, thereby fostering international collaboration and recognition.

Accounts of Peptide Science Japan will be freely available via J-STAGE, an Open-Access journal that ensures accessibility to researchers and students worldwide.

We hope that this new academic journal will contribute to the advancement of peptide science worldwide.

Akira Otaka
President,
The Japanese Peptide Society

Accounts of Peptide Science Japan 発刊に際し

これまで日本ペプチド学会の会員の皆様に親しまれてきた通称「Green Book」こと「PEPTIDE SCIENCE」ですが、2024 年発刊の「PEPTIDE SCIENCE 2023」をもって休刊とし、今後は 1990 年の日本ペプチド学会設立を契機に創刊された「PEPTIDE NEWSLETTER JAPAN」と発展的に統合する形で、新たに「Accounts of Peptide Science Japan」としてスタートを切る運びとなりました。

「PEPTIDE SCIENCE」の起源は、1962 年に開催された蛋白質研究所セミナー第一集「ペプチドの合成」にまで遡ります。その後、1963 年からは「PEPTIDE CHEMISTRY」、1997 年からはペプチド研究領域の拡大に伴い現在の「PEPTIDE SCIENCE」へと改名し、ペプチド（化学）討論会の英文要旨集として、日本のペプチド研究成果を広く発信する役割を担ってきました。

しかし近年、多くの学術誌がペプチド研究を取り上げるようになった影響で、「PEPTIDE SCIENCE」への投稿数が減少傾向にありました。こうした背景の中、その存続意義が議論されることが増え、時代の変化に対応する必要性が認識されるようになりました。

このような状況を受け、理事会での議論の結果、「PEPTIDE SCIENCE」と「PEPTIDE NEWSLETTER JAPAN」を発展的に統合し、新たな学術誌「Accounts of Peptide Science Japan」を発刊することが決定されました。そして、このたび創刊号をお届けする運びとなりました。

新学術誌は以下のような原稿区分で構成される予定です：

- **巻頭言**：学会の方針、活動報告、社会との関わりなど
- **英文 Account**：一つの主題に基づき、著者自身の研究を総合的にまとめた英文記述
- **和文 Account**：一つの主題に基づき、著者自身の研究を総合的にまとめた和文記述
- **Information**：国内外の学術情報、研究資金情報、学会報告など、研究活動支援を目的とした記述
- **Essay**：関連分野の学術的・社会的意義を有する内容の記述

さらに、日本のペプチド科学を広く世界に発信する目的で、英文および和文の「Account」には DOI（Digital Object Identifier）を付与し、J-STAGE を通じた Open Access 形式を採用します。

「Accounts of Peptide Science Japan」は、まさに新たに産声を上げたばかりの学術誌です。会員の皆様のご支援とご協力を賜りながら、本誌が世界のペプチド科学において重要な情報源としての役割を果たすことを心より願っております。

日本ペプチド学会
会長　大高 章

S-protected cysteine sulfoxide, a side product in peptide synthesis, finds an unprecedented usage: From peptide stapling and modification to insulin synthesis

Received: May 14, 2025

Accepted: July 4, 2025

Published: October 1, 2025

Akira Otaka

Institute of Biomedical Sciences and Graduate School of Pharmaceutical Sciences, Tokushima University, Tokushima 770-8505, Japan

e-mail: aotaka@tokushima-u.ac.jp

Keywords: S-protected cysteine sulfoxide; sulfenylation of amino acids; disulfide formation; peptide lipidation; sactipeptide

Abstract

Peptide chain elongation induces the oxidation of amino acid side chains. The most profound oxidative modification occurs on the sulfide of a methionine residue to give methionine sulfoxide. An S-protected cysteine possessing a sulfide functionality undergoes the same modification to the corresponding S-protected cysteine sulfoxide. On treating the *S*-*p*-methoxybenzyl (MBzl) cysteine sulfoxide [Cys(MBzl)(O)] under acidic conditions in the presence of a large excess of an electron-rich aromatic compound, the sulfoxide works as an electrophile (i.e., a cysteine umpolung) to participate in an aromatic electrophilic substitution reaction (S_EAr), affording an *S*-aryl compound, while the *S*-acetoamidemethyl cysteine sulfoxide [Cys(Acm)(O)] is converted to the corresponding disulfide by treatment with a thiol nucleophile. Although these two observations were made about 40 years ago, there has been little practical application of the research in peptide chemistry, except in a disulfide-forming reaction confined to single disulfide-bonding peptides. This is partly due to a lack of information on which of the reaction intermediates resulting from acid-activated sulfoxides are suitable for use in subsequent reactions, including *S*-arylation or disulfide formation. The clue to active application came from the development of sp^2(C–H) sulfenylation of the indole of tryptophan (Trp). We found that treatment of Cys(MBzl)(O) under acidic conditions (e.g., trifluoroacetic acid; TFA) in the presence of guanidine hydrochloride (Gn·HCl) as a chloride anion source facilitates the formation of *S*-chlorocysteine, which then selectively reacts with Trp among the aromatic amino acids to yield 2'-sulfenyl-Trp. Cys(Acm)(O) can also be converted to *S*-chlorocysteine under TFA conditions in the presence of Gn·HCl. This conversion additionally occurs under milder acidic conditions in the AcOH system in the presence of $MgCl_2$, while Cys(MBzl)(O) remains intact. In contrast, the reaction of Cys(Acm)(O) under trimethylsilyl trifluoromethanesulfonate (TMSOTf) in TFA or hexafluoroisopropanol (HFIP) conditions in the absence of chloride anion sources may lead to the formation of a silylated dicationic species as a plausible intermediate involved in the S_EAr reaction with tyrosine (Tyr). The *S*-chlorocysteine preferentially reacts with S-protected Cys residues, including Cys(Acm) and Cys(MBzl), over Trp to afford the corresponding S-protection-attached sulfenyl sulfonium cations, which are converted to disulfide with release of the S-protection as a cation. The ease of the cation leaving depends on the acidity of the reaction: the Cys(Acm)-derived sulfonium cation easily converts to disulfide under mild acidic conditions, while the Cys(MBzl)-derived one requires strong acidity. The difference in acidity that facilitates the conversion of Cys(Acm)(O) or Cys(MBzl)(O) to the corresponding *S*-chlorocysteine led us to discover that use of a Cys(Acm)(O)/Cys(Acm) or Cys(MBzl)(O)/Cys(MBzl) pair with the acidity of the reaction increasing stepwise allows one-pot/stepwise disulfide bond formation in a regioselective manner. This reaction was successfully applied to the unprecedented synthesis of insulin including a lipidated analog. Lastly, the synthesis of a model sactipeptide possessing a sactionine linkage was achieved based on the observation in insulin synthesis that an S-modified sulfonium cation derived from a Cys(Acm) derivative easily loses the Acm group as the cation under acidic conditions where no protonation occurs on the amide moiety of the Acm group. In this article, we briefly summarize the chemistry of S-protected cysteine sulfoxides, emphasizing the sulfenylation of amino acid side chains, including Trp, Tyr, and S-protected cysteine.

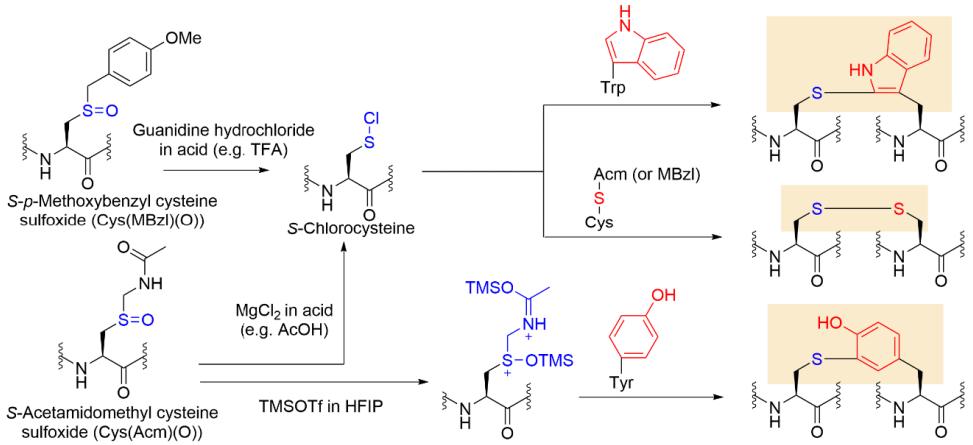

Part of the research eligible for the 2023 The Japanese Peptide Society Award is described in this article.

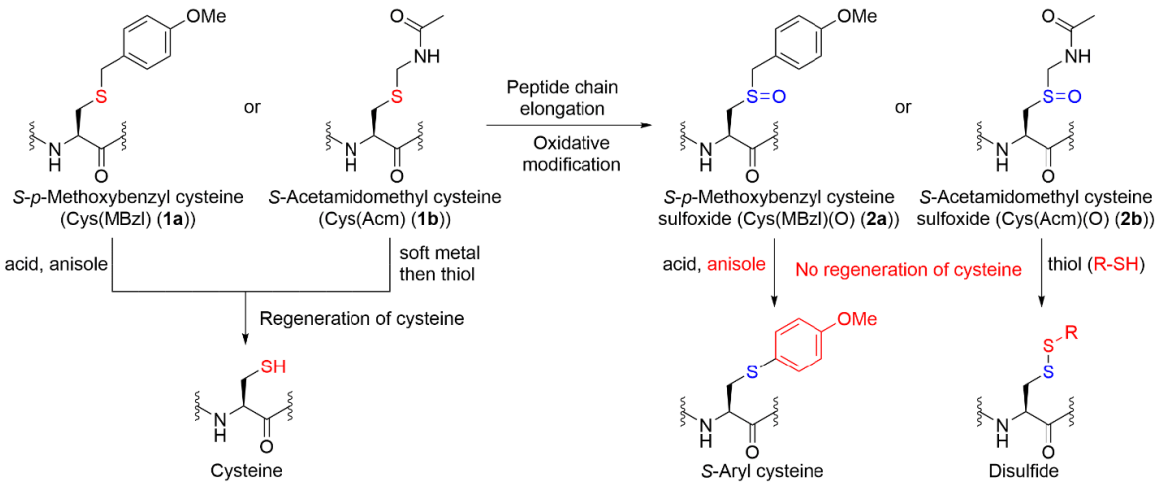

Figure 1. Oxidative modification of S-protected cysteine [Cys(MBzl) (**1a**) or Cys(Acm) (**1b**)] during peptide chain assembly and chemical behavior of the resulting sulfoxides (**2a** or **2b**). Nucleophilic and electrophilic characters are indicated in red and blue, respectively.

Introduction

The peptide chain assembly process, whether in a liquid or solid phase, is susceptible to several side reactions including epimerization and termination, as has been well-documented in literature. Moreover, the sulfide of an S-protected cysteine residue **1** undergoes oxidation to the corresponding sulfoxide **2**, a process observed in the methionine (Met) side chain. Nevertheless, the formation of the S-protected cysteine sulfoxide **2** has not been widely recognized in the scientific community. About 40 years ago, Yajima and colleagues[1] demonstrated that an S-protected cysteine sulfoxide **2**, such as *S*-*p*-methoxybenzyl cysteine sulfoxide [Cys(MBzl)(O) (**2a**)], does not regenerate the parent cysteine upon acidic final deprotection to afford the desired peptide (Figure 1). The reaction of **2a** with hydrogen fluoride (HF) in the presence of a large excess of anisole or phenol gives an *S*-aryl compound in which the acid-activated sulfoxide works as an electrophilic sulfenylation agent of aromatic compounds. Furthermore, *S*-acetamidomethyl cysteine sulfoxide [Cys(Acm)(O) (**2b**)] is converted to the disulfide compound upon reacting with thiol, with the Acm group released as a cation[2]. The finding that the a sulfoxide **2** with a releasable S-substituent such as MBzl or Acm serves as a sulfenylation reagent of a nucleophilic counterpart led us to evaluate the potential utility of **2** in disulfide-forming reactions in combination with an S-protected cysteine **1**, based on the mechanism depicted in Figure 2[3].

We reasoned that free cysteine **4**, which should be regenerated from the protected cysteine under appropriate acidic conditions, will react with an acid-activated sulfoxide **3** to yield a sulfenyl cysteine sulfonium cation **5**, which is then converted to a disulfide with the release of the $\mathbf{P^1}$ protection on sulfoxide **2**. While the synthesis of a peptide containing a disulfide bond was successfully achieved, utilizing this sulfoxide-mediated disulfide formation in the synthesis of a peptide containing multiple disulfide bonds did not yield any positive outcomes. However, the reason for this failure did not become clear until our recent discovery that copper-mediated disulfide formation proceeds between thiazolidine-4-carbonyl (Thz) and Cys(Acm) residues (**6** and **1b**) (Figure 3)[4].

The Thz residue **6** as an N,S-protected cysteine derivative[5] has served as an N-terminal Cys indispensable for C-to-N directed sequential native chemical ligation[6] required for chemical synthesis of proteins. Typically, treatment with methoxyamine under mildly acidic conditions (~pH 4–5) cleaves the thioaminal ring[5]. However, we found that the Thz ring is opened by the action of Cu(II) irrespective of the presence of ascorbate to yield the N-terminal Cys[4a,7]. Moreover, when Cys(Acm) is present alongside Thz in the absence of ascorbate, disulfide bonds readily form between the Cys(Acm) **1b** and Thz **6** residues[4b]. The detailed reaction mechanism involving disulfide formation has not been elucidated. We hypothesized that the Cu(II) salt is likely to act as a Lewis acid to promote Thz ring opening, and the resulting Cys will be oxidized to the corresponding cysteine sulfenic acid [Cys(OH) (**7**)] via the Cys-thiyl radical through the action of Cu(II)[4b,8]. Consequently, as an umpolung cysteine, the resulting Cys(OH)

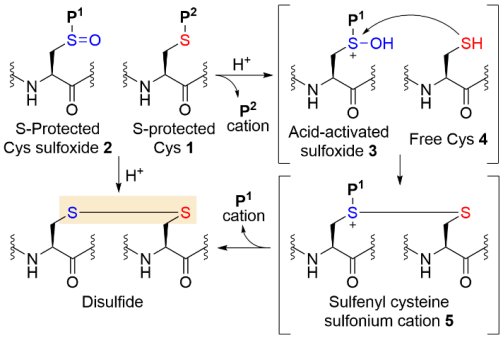

Figure 2. Initially envisioned reaction mechanism of acid-activated sulfoxide-mediated disulfide formation.

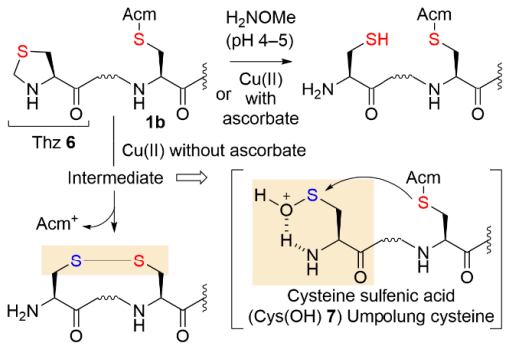

Figure 3. An umpolung cysteine, resulting from Thz **6** by the action of a Cu(II) salt in the absence of ascorbate under atmospheric conditions, might be involved in the formation of a disulfide bond between Thz and the Cys(Acm) residue.

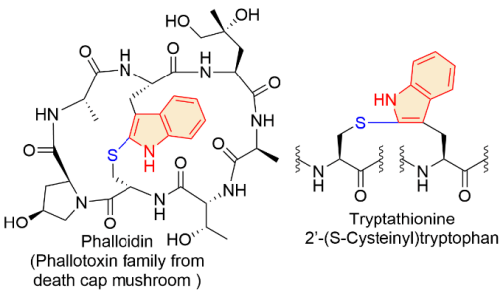

Figure 4. Example of tryptathionine-containing toxin from the death cap mushroom.

7 might electrophilically attack Cys(Acm) to yield disulfide with release of the Acm group as a cation. The experimental finding that such an electrophilic cysteine umpolung **7** would participate in disulfide formation evoked our interest in acid-activated S-protected cysteine sulfoxide as an electrophilic cysteine umpolung.

In addition, the complete chemical synthesis of the peptidic toxin amanitin, which contains 2'-(*S*-cysteinyl)tryptophan (termed tryptathionine)[9], has been recently achieved (Figure 4)[10]. Based on Yajima and co-worker's[1] finding that an *S*-aryl compound is generated from the reaction of Cys(MBzl)(O) (**2a**) in the presence of phenol under acidic conditions, we reasoned that the reaction of Trp with S-protected cysteine sulfoxide **2** under appropriate acidic conditions should yield tryptathionine. Research on S-protected cysteine sulfoxides resumed with the construction of a tryptathionine moiety in peptides.

In this article, we describe recent advances in the chemistry of acid-activated S-protected cysteine sulfoxides, including side chain sulfenylation that occurs selectively at Trp[11–13], Tyr[14], or S-protected cysteine[15] under varying reaction conditions.

sp²(C–H) sulfenylation of the indole of Trp using acid-activated S-protected cysteine sulfoxide[11,12]

The hypothesis that an acid-activated S-protected cysteine sulfoxide might act as an sp²(C–H) sulfenylation agent for Trp prompted us to investigate the feasibility of thioether formation between Trp and Cys residues in a model substrate peptide [Ac-Trp-**GAL**-Cys(MBzl)(O)-**R**-NH_2 (**8**)] using the sulfoxide system. Initially, the reaction of **8** in 1 M trifluoromethanesulfonic acid (TFMSA) in trifluoroacetic acid (TFA)[16] unambiguously yielded the desired Cys–Trp-linked peptide **9** containing tryptathionine. However, significant amounts of **9** + 120-Da products, related to MBzl cation adducts, were also observed by HPLC analysis. We speculated that potential alkylation sites in the product peptide might be present in the thioether of tryptathionine and in tryptathionine itself; alternatively, the guanidine group of arginine might provide a site, although this seemed less likely. Because a sulfide or aromatic compound as a cation scavenger slows the progress of sulfenylation, the addition of guanidine hydrochloride (Gn·HCl) was tried without much expectation. Surprisingly, however, Gn·HCl markedly altered the reaction outcomes, such that the reaction of **8** in 1 M TFMSA in TFA in the presence of 4 M Gn·HCl proceeded efficiently to yield **9** as a main product. In addition, the presence of Gn·HCl facilitated the quantitative sulfenylation of Trp with Cys(MBzl)(O) under less acidic conditions, such as 1 M methanesulfonic acid (MSA) in TFA. Notably, $(Gn)_2{\cdot}H_2SO_4$ was ineffective in the reaction, and no sulfenylation proceeded. This observation allowed us to conclude that Gn·HCl has dual functions as (1) a cation scavenger and (2) a chloride anion source to yield the *S*-chlorocysteine intermediate **10**, known as a Trp sulfenylation agent[17] (Figure 5). Among the proteogenic amino acids, the resulting *S*-chlorocysteine **10** modified Trp via an aromatic electrophilic substitution (S_EAr) reaction in a highly Trp-selective manner, even in the presence of a Tyr residue possessing an electron-rich aromatic ring. Kinetically, the sulfide side chain of a Met residue underwent sulfenylation more preferentially than a co-existing Trp residue[12,18] however, the resulting sulfenyl Met sulfonium cation **11** either reverted to *S*-chlorocysteine and Met, or reacted with Trp to yield the sulfenyl Trp (Figure 6). The *S*-chlorocysteine, which results from the reaction of Cys(MBzl)(O) under acidic conditions stronger than TFA in the presence of amine hydrochloride such as Gn·HCl, enabled Trp-selective sulfenylation to occur not only in an intramolecular manner, but also in an intermolecular manner. Consequently, Trp-selective sulfenylation utilizing acid-activated Cys(MBzl)(O) showed utility in peptide stapling[19], bicyclic peptide synthesis, and peptide lipidation[12].

sp²(C–H) sulfenylation of the phenol of Tyr using acid-activated S-protected cysteine sulfoxide[14]

As mentioned above, use of Cys(MBzl)(O) for the sulfenylation of sp²(C–H) Trp requires Gn·HCl, which acts as an MBzl cation scavenger and chloride anion source. Under this reaction condition, sulfenylation occurs only on Trp, and the modification of Tyr does not proceed. As Tyr-selective sulfenylation probably requires an S-protection alternative to the MBzl group, we evaluated the utility of *S*-Acm[20] for S-protection of the S-protected cysteine sulfoxide. The Acm group was selected because it exhibits chemical behavior during its removal that differs from

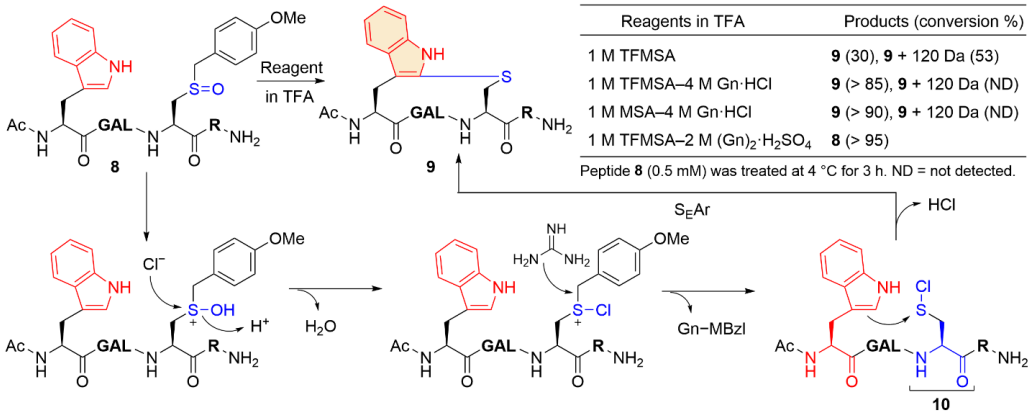

Reagents in TFA	Products (conversion %)
1 M TFMSA	**9** (30), **9** + 120 Da (53)
1 M TFMSA–4 M Gn·HCl	**9** (> 85), **9** + 120 Da (ND)
1 M MSA–4 M Gn·HCl	**9** (> 90), **9** + 120 Da (ND)
1 M TFMSA–2 M $(Gn)_2{\cdot}H_2SO_4$	**8** (> 95)

Peptide **8** (0.5 mM) was treated at 4 °C for 3 h. ND = not detected.

Figure 5. Plausible mechanism of the reaction for affording a sulfenyl tryptophan (tryptathionine) residue.

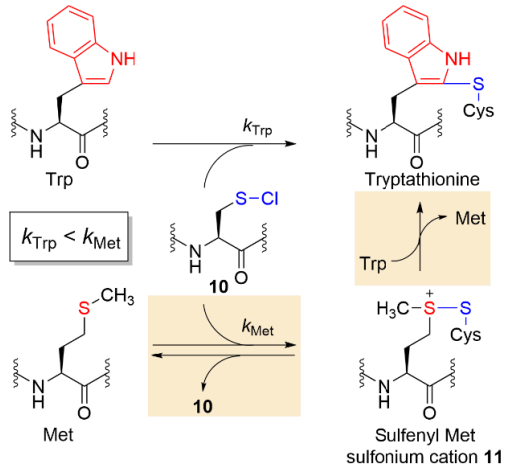

Figure 6. Methionine preferentially reacts with *S*-chlorocysteine in a kinetic manner.

that of the MBzl group, which becomes more susceptible to deprotection as the acidity of the reaction increases. Initially, the attempted reaction of the model Cys(Acm)(O) and Tyr-containing peptide **12** under TFA conditions without a chloride anion source gave a mixture of the desired Cys–Tyr-linked **13** and dimer **14** peptides, along with the remaining substrate (Figure 7a). Gratifyingly, the addition of MSA at a concentration of 1 M enabled the reaction to yield the desired Cys–Tyr-linked peptide **13** in quantitative amounts. We reasoned that dual protonation on the *S*-Acm oxide moiety under 1 M MSA conditions is likely to contribute to the favorable reaction outcome. Under TFA conditions, mono protonation occurs only on the sulfoxide, allowing facile removal of the Acm group as a cation to generate the cysteine sulfenic acid **7** that can function as a nucleophile and electrophile. The S_EAr reaction of the resulting **7** with Tyr allowed formation of the desired Cys–Tyr-linked peptide **13**. Otherwise, the sulfenic acid **7** self-dimerized to give dimer peptides **14**. Under more acidic conditions containing MSA, by contrast, protonation occurred on both the sulfoxide and the amide moiety of the Acm group, forming the dicationic intermediate **15**. Thereby, the positive charge on the Acm group may prevent its release as a cation, and the resulting dicationic intermediate **15** might participate in the S_EAr reaction of the Tyr residue. In summary, we tentatively established reaction conditions suitable for the sulfoxide-mediated Tyr-sulfenylation of peptides possessing only Tyr as an aromatic residue; however, Tyr- or Trp-selective sulfenylation remained to be achieved.

Tyr- or Trp-selective sp²(C–H) sulfenylation using acid-activated Cys(Acm)(O)[14]

Evaluations of the Tyr- and Trp-containing model Cys(Acm)(O) peptide **16** under various reaction conditions uncovered a reagent system facilitating the discrimination of Tyr and Trp residues in sulfenylation (Figure 7b). As described above, treating the Tyr-containing Cys(Acm)(O) peptide **12** with TFA resulted in a mixture of Cys–Tyr-linked and dimer peptides, possibly involving a Cys sulfenic acid intermediate. However, the presence of Trp changed the reaction outcomes significantly. When **16** was reacted with TFA, no Cys–Tyr or dimer peptides were formed. Instead, a Cys–Trp-linked peptide was selectively obtained, although the reaction was not fully completed. The addition of Gn·HCl to the reaction in TFA allowed

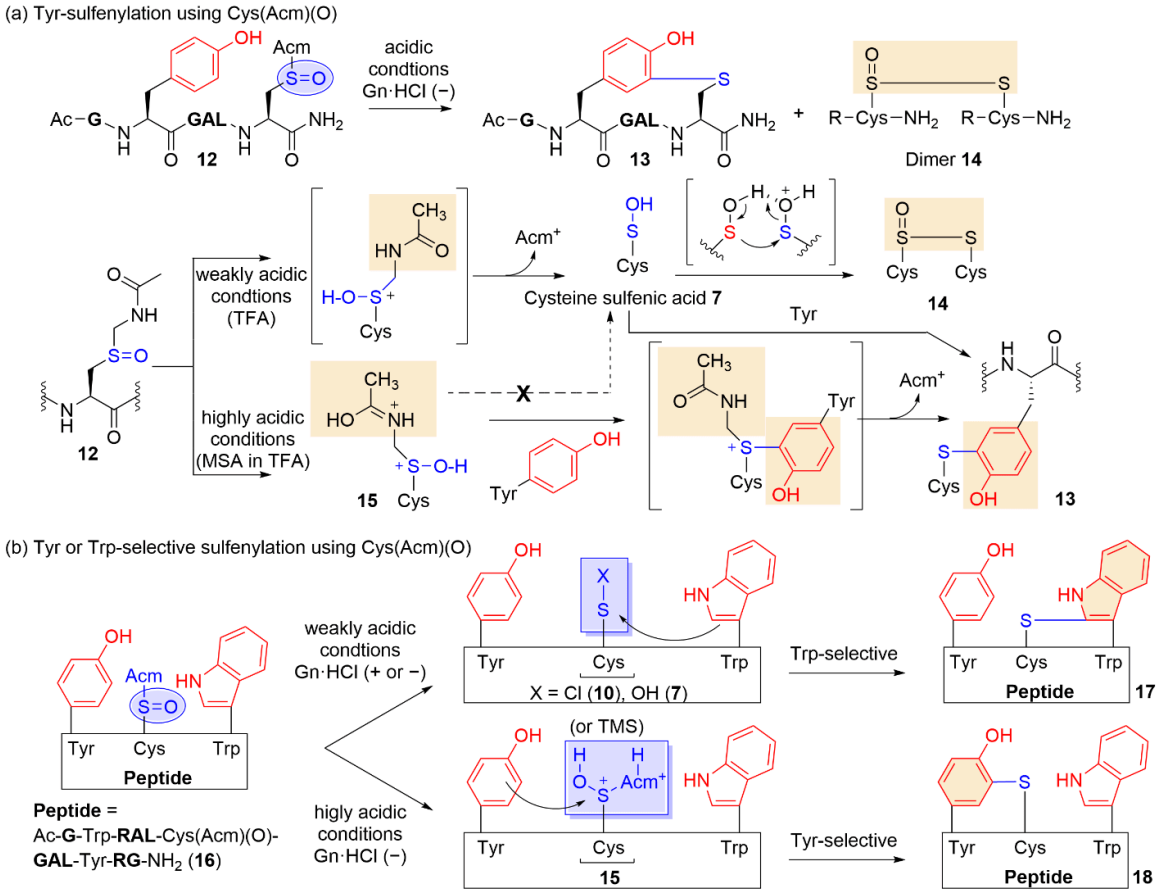

Figure 7. (a) Plausible mechanism of the reaction for affording a sulfenyl tyrosine residue. (b) The Trp- or Tyr-selective sulfenylation reaction.

the Cys–Trp-linked peptide **17** to form in an entirely Trp-selective manner in almost quantitative conversion. Both reaction conditions involved a neutral reaction intermediate such as the cysteine sulfenic acid **7** or *S*-chlorocysteine **10**; therefore, we concluded that a neutral species for the sp^2(C–H) sulfenylation is likely to contribute to Trp-selective sulfenylation even in the presence of a Tyr residue.

Regarding sulfenylation of Tyr, the dicationic intermediate **15**, envisioned in the reaction under 1 M MSA in TFA conditions, might be responsible for the reaction that affords the Cys–Tyr linkage. Therefore, we hypothesized that the desired Tyr-selective sulfenylation might occur if the dicationic intermediate **15** remains stable during the sulfenylation reaction; consequently, we used a strong acid (TFMSA) or strong Lewis acidic silylating agent (trimethylsilyl trifluoromethanesulfonate; TMSOTf)[21] to anticipate a long-lasting cationic intermediate. The attempted sulfenylation of peptide **16** proceeded in a highly Tyr-selective manner to yield the desired Cys–Tyr-linked peptide **18**, although Acm cation adducts also formed. Lastly, the addition of guanidium trifluoromethanesulfonate (Gn·HOTf) was found to effectively suppress this alkylation without affecting residue selectivity. Thus, Trp- or Tyr-selective sulfenylation using acid-activated Cys(Acm)(O) proceeded in a highly residue-selective fashion to yield the desired Cys–Trp- or Cys–Tyr-linked peptides (**17** and **18**) by selecting the neutral intermediate such as *S*-chlorocysteine for Trp sulfenylation or the dicationic intermediate for Tyr sulfenylation.

Encouraged by our success in residue-selective sulfenylation, we attempted to synthesize a stapled glucagon-like peptide 1 (GLP-1)[22] with lipid modification (Figure 8)[23]. Upon food intake, secreted GLP-1 stimulates insulin secretion, contributing to efficient use of glucose. Therefore, GLP-1 **19** has been receiving increasing interest not only as a therapeutic agent for type II diabetes but also as an anti-obesity agent. In addition, lipidated GLP-1 analogs, represented by Liraglutide or Semaglutide, occupy a large market share as diabetes drugs,

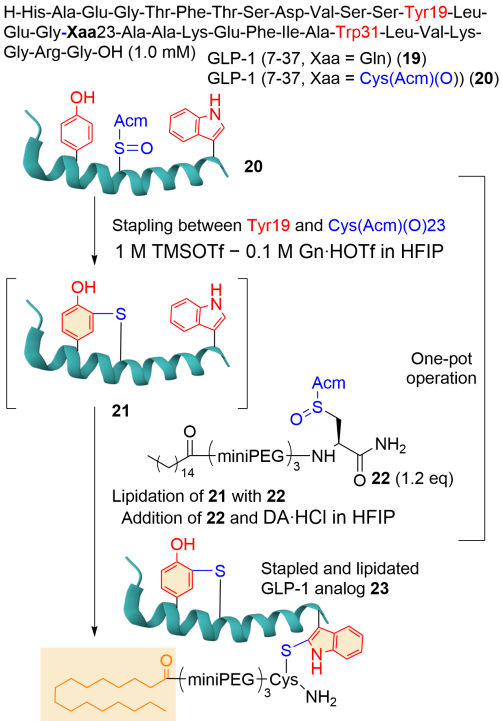

Figure 8. One-pot/stepwise stapling and lipidation sequence for preparation of a GLP-1 analog.

and they interact with their receptor through an α-helical active conformation. Given this context, we synthesized the stapled and lipidated GLP-1 analog **23** in a one-pot/sequential manner utilizing the developed residue-selective sulfenylation reaction. To utilize Tyr19 in GLP-1 (7–37) as a stapling pair in the i and i + 4 relationship, Gln23 was replaced with Cys(Acm)(O) as another stapling pair. The reaction of the Cys(Acm)(O)-substituted peptide **20** in 1 M TMSOTf–0.1 M Gn·HOTf in hexafluoroisopropanol (HFIP) allowed selective incorporation of the stapling Cys–Tyr linkage between Tyr19 and Cys22, with Trp31 remaining intact. Next, addition of a solution of the Cys(Acm)(O)-modified lipid **22** and diisopropylamine hydrochloride (DA·HCl) as a chloride anion source in HFIP to the reaction resulted in Trp-selective incorporation of the lipid moiety through intermolecular Cys–Trp sulfenylation to yield the desired stapled and lipidated GLP-1 analog **23** in a one-pot/sequential manner. The resulting **23** was shown to significantly reduce blood glucose levels in a long-lasting manner.

Trp-sulfenylation under conditions benign to protein molecules[13]

Whether using Cys(MBzl)(O) or Cys(Acm)(O), Trp sulfenylation requires strong acidic conditions (e.g., TFA) and a chloride anion source. In modifying proteins, it is important to use reaction conditions that are benign to a wide variety of proteins to prevent their denaturation. Comparison of *S*-Acm with *S*-MBzl suggested that the resulting Acm-derived hydroxyl sulfonium cation **24b**, upon protonation of the sulfoxide, might be more susceptible in weak acid to become *S*-chlorocysteine **10** in the presence of a chloride anion source; therefore, we evaluated Cys(Acm)(O) as the Trp-sulfenylation agent under mildly acidic conditions. We employed nonaqueous AcOH as a solvent in the presence of metal chloride as a Lewis acid because water decomposes the *S*-chlorocysteine, which is indispensable for Trp sulfenylation. Among various metal chlorides, magnesium chloride ($MgCl_2$) was found to be the best additive: intermolecular sulfenylation of a model Trp peptide with a Cys(Acm)(O) peptide under AcOH conditions in the presence of 30 mM $MgCl_2$ at 25 °C for 15 h went to completion, yielding the desired Trp sulfenyl peptide. In addition, the inclusion of 0.1% TFA in the AcOH mixture resulted in a faster reaction,

Table 1. Conversion of S-protected cysteine sulfoxide to *S*-chlorocysteine **10**

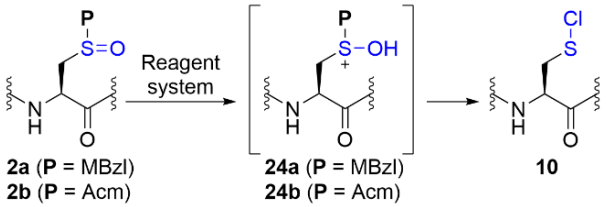

Acidity	Reagent system	P	
		Acm	MBzl
Low	30 mM $MgCl_2$, 0.1% TFA in AcOH	**10**	intact
	30 mM $MgCl_2$, 0.1% TFA in 2% BMPy·OTf/AcOH		
	30 mM $MgCl_2$, 0.1% TFA in 1% H_2O/BMPy·OTf		
High	Amine·HCl in TFA (or + strong acid)	**10**	**10**

completing within 5 hours. Moreover, the addition of an ionic liquid (BMPy·OTf, 2%) significantly enhanced the solubility of slightly soluble peptides in AcOH, leading to synthesis of the corresponding sulfenyl peptides. Furthermore, reaction in the ionic liquid system[24] containing 30 mM $MgCl_2$, 1–5% H_2O, and 0.05–0.1% TFA allowed Trp sulfenylation of the antibody trastuzumab while retaining the affinity of the modified protein, although the reaction remained incomplete. As mentioned above, Cys(Acm)(O) can be converted under mildly acidic conditions (e.g., 0.1% TFA in AcOH) in the presence of $MgCl_2$ to *S*-chlorocysteine **10**, which then reacts with Trp. In contrast, the Cys(MBzl)-derived hydroxyl sulfonium cation **24a** under AcOH conditions cannot release the MBzl cation due to the low acidity of the reaction and fails to become *S*-chlorocysteine.

Hence, we reasoned that Cys(Acm)(O) and Cys(MBzl)(O) were converted stepwise in this order to the corresponding *S*-chlorocysteine, which is responsible for the sulfenylation of Trp, with the acidity of the reaction increasing. This rationale encouraged us to develop a linker molecule that would allow the one-pot/sequential heterodimerization of Trp-containing peptides. The developed linker **25**, possessing Cys(Acm)(O) and Cys(MBzl)(O) at its termini, enabled the connection of Trp-containing MAX and MYC as DNA-binding peptide peptides in a one-pot/sequential fashion, with the acidity increasing during the reaction.

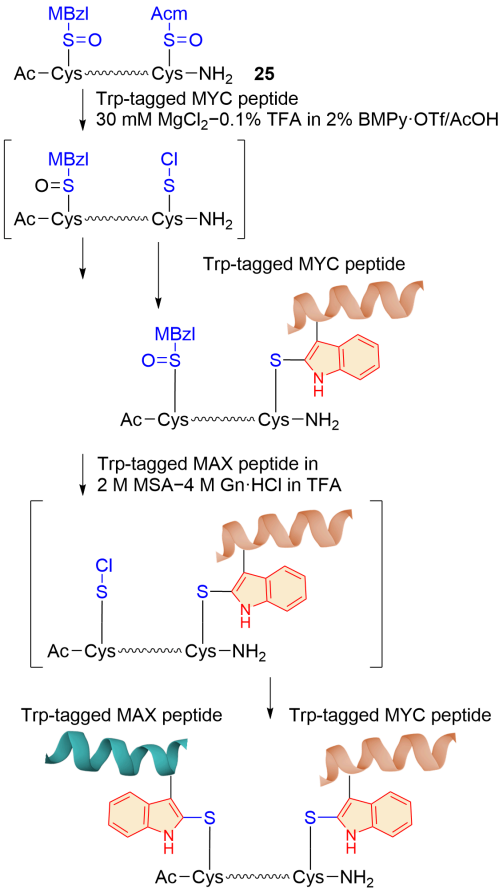

Figure 9. One-pot/stepwise dimerization of Trp-containing peptides using S-protected cysteine sulfoxide.

Application of S-protected cysteine sulfoxides to the synthesis of disulfide-bonding peptides including insulin[15]

As shown in Figure 6, *S*-chlorocysteine **10** preferentially reacts with Met over Trp to reversibly afford the sulfenyl Met sulfonium cation **11**. However, the resulting **11** cannot release the methyl group as a cation and so fails to become a disulfide product. In other words, a cation-releasable sulfide, including an S-protected cysteine derivative, might be involved in the disulfide bond that forms upon reaction with *S*-chlorocysteine (Figure 10a). Therefore, we implemented an unprecedented one-pot/sequential disulfide-forming strategy to challenge insulin synthesis[25,26]. This approach is based on two key experimental findings in the Trp-sulfenylation evaluation: (1) under low acidic conditions (e.g., 0.1% TFA in AcOH) in the presence of $MgCl_2$, Cys(Acm)(O) can be transformed to *S*-chlorocysteine **10**, while Cys(MBzl)(O) remains unaffected (Table 1); and (2) the conversion of Cys(MBzl)(O) to **10** occurs under high acidic conditions (e.g., TFA–Gn·HCl). To advance these promising results to insulin synthesis, we evaluated potential S-protected cysteine pairs that might react with Cys(Acm)(O) or Cys(MBzl)(O) to afford the disulfide selectively under each *S*-chlorocysteine-forming condition. Gratifyingly, we found that two pairs, Cys(Acm)(O)/Cys(Acm) and Cys(MBzl)(O)/Cys(MBzl), met our demands (Figure 10b). Under low acidic conditions (AcOH in the presence of $MgCl_2$), the *S*-chlorocysteine **10** resulting from Cys(Acm)(O), but not from Cys(MBzl)(O), reacted with Cys(Acm) or Cys(MBzl) to give the corresponding sulfenyl sulfonium cations (**11'a** and **11'b**). Among these cations, the Cys(Acm)-derived cation **11'a** converted to a disulfide with release of the *S*-Acm group; however, this was not the case for the Cys(MBzl)-derived cation **11'b** because the MBzl group does not leave as the cation under weakly acidic AcOH conditions. Instead, **11'b** either reverted to the starting *S*-chlorocysteine **10** and *S*-MBzl species, or it progressed to the sulfonium cation **11'a** through a reaction with Cys(Acm). Consequently, only the Cys(Acm)(O)/Cys(Acm) pair forms disulfide under low acidic conditions, while the reaction of Cys(MBzl)(O) with Cys(MBzl) in TFA in the presence of Gn·HCl gives a disulfide. This was successfully applied to unprecedented synthesis of insulin and its lipidated analog. In the synthesis of the Trp-lipidated insulin analog **26** shown in Figure 11, the difference in chemical behavior between the Cys(Acm)/Cys(Acm)(O) and Cys(MBzl)/Cys(MBzl)(O) pairs relevant to disulfide formation allowed for a one-pot/stepwise interchain disulfide formation connecting the oxidized A chain **27** and the B chain **28**. A stepwise increase in acidity of the reaction resulted in regioselective disulfide formation between the Cys(Acm)(O) and Cys(Acm) residues, giving two disulfide-containing peptides **29**. This was followed by the formation of the Trp-incorporated insulin analog **30** through disulfide formation between Cys(MBzl)(O) and Cys(MBzl). Rather than reacting with the Trp residue incorporated in the B chain, the *S*-chlorocysteine **10** is preferentially involved in the stepwise disulfide formation by reacting with the S-protected cysteine as sulfide. Next, the addition of the Cys(Acm)(O)-decorated fatty acid unit **22** to the disulfide-forming reaction mixture allowed the fatty acid to be installed on the non-modified Trp residue by *S*-chlorocysteine-mediated indole sulfenylation. Consequently, the lipidated insulin[27] analog **26** was obtained in 16% isolated yield, calculated from the oxidized A chain **27**, in a one-pot/stepwise disulfide-bonding and lipidation sequence. A key feature of our insulin synthesis is that the single oxidation step for providing the oxidized A

chain **27** possessing one disulfide bond and two sulfoxide units contributes to the stepwise formation of three disulfide bonds, a process that has conventionally required three independent oxidation steps such as a dipyridyl disulfide or iodine-mediated oxidative protocol. The oxidation state garnered in the sulfoxide moiety step wisely participates in disulfide formation after conversion to the *S*-chlorocysteine. Another indispensable feature in the success of insulin synthesis is that modification of the sulfur atom of the *S*-Acm group by a thiophilic agent results in facile removal of *S*-Acm even under mild conditions. This feature led us to attempt α-carbon modification by a sulfur atom as described in the next section.

Oxidation of a peptide α-carbon by a sulfur atom[28,29]

Although unrelated to the use of S-protected cysteine sulfoxides, we will briefly describe the synthesis of α-carbon oxidized peptides with a sulfur atom. This reaction scheme drew from the experimental insights gained during insulin synthesis. Peptides containing a sulfur (Cys)-to-α-carbon (another amino acid) thioether cross-linkage (sactionine linkage), named sactipeptides, belong to the family of ribosomally synthesized and post-translationally modified peptides (RiPPs), and have been receiving significant attention in recent years[30–32].

One insight was that modifying the *S*-Acm group with a thiophilic agent facilitates removal of this group under mildly acidic conditions, leading to success in insulin synthesis (Figures 10 and 11, Table 1). Another insight came from the observation that an N-terminal glycyl hydroxamic acid (GlyHA **31**) can be converted to a 2-oxo-glyoxylyl moiety **32** by a Lossen rearrangement-mediated intramolecular redox reaction (Figure 12a). We found that regioselective *O*-acylation of the N-terminal GlyHA residue, followed by Lossen rearrangement, allowed conversion of GlyHA to the isocyanate unit **33**, which finally resulted in the aldehyde **32** through successively

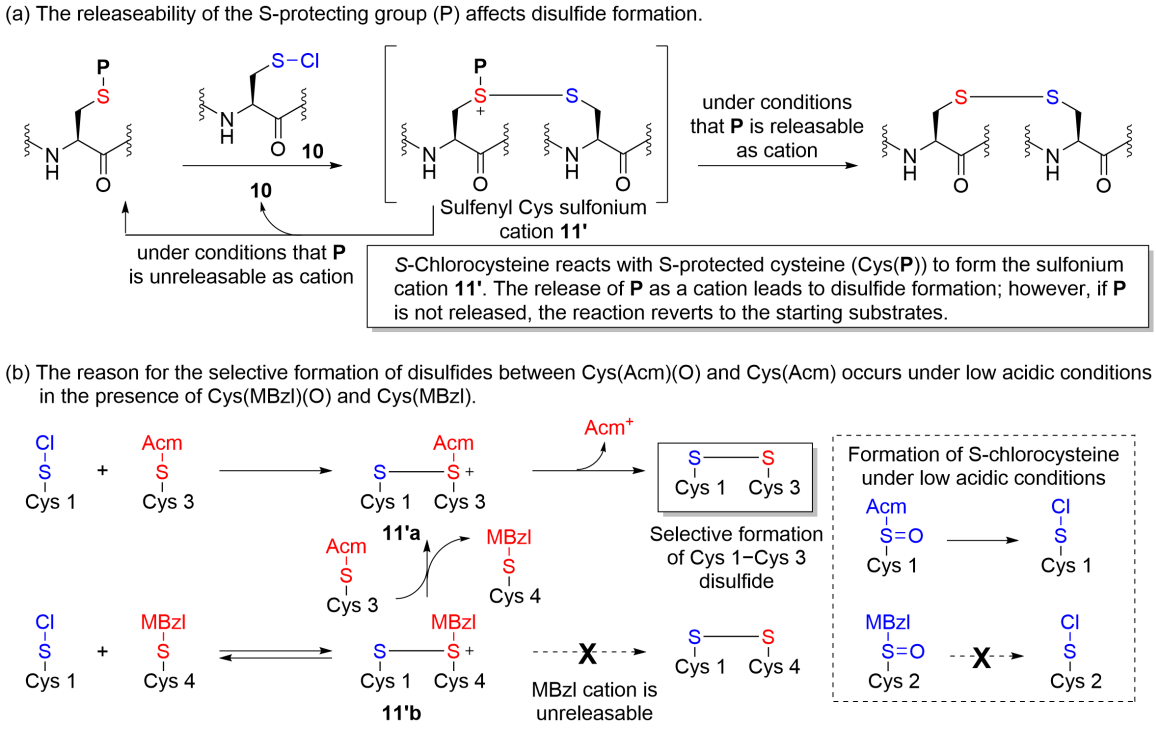

Figure 10. (a) Disulfide bond formation between S-protected cysteine and *S*-chlorocysteine, and (b) the reason for selective disulfide formation between Cys(Acm)(O) and Cys(Acm) under low acidic conditions in the presence of Cys(MBzl)(O) and Cys(MBzl).

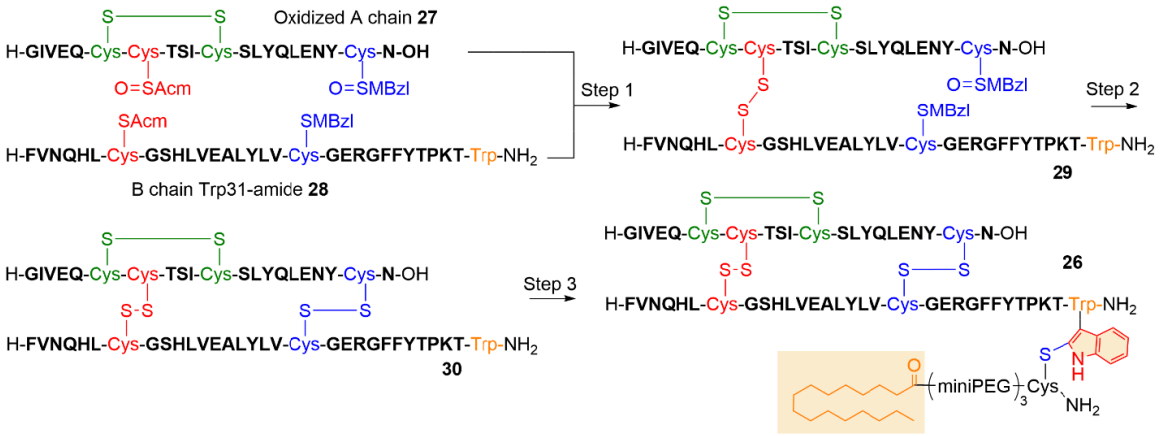

Figure 11. Synthesis of a Trp-lipidated insulin analog. Step 1: weakly acidic conditions, 30 mM $MgCl_2$, 5% BMPy·OTf, and 0.4 M LiCl in 0.1% TFA/AcOH, 37 °C for 7 h. Step 2: TFA, 4 M Gn·HCl, highly acidic conditions. Step 3: TFA/AcOH (1:1) 37 °C for 2 h 100 mM anisole, followed by addition of the reaction mixture to Cys(Acm)(O)-modified fatty acid **23** at 25 °C for 1 h.

occurring hydrolysis via an aminal structure possessing α-amino glycine (Gly(NH_2) **34**). The sequence of reactions also occurred at an internal GlyHA residue within the peptide sequence, yielding a peptide containing **34**. Conversion of **34** to an α-sulfenyl glycine (Gly(SR) **35**) is possible by a sequence of reactions consisting of $NaNO_2$-mediated oxidation of **34** and subsequent nucleophilic attack of a thiol to the resulting iminium ion or its equivalent **36**. However, formation of the sactionine linkage by intramolecular nucleophilic attack of thiols is impossible because the free Cys residue that coexists with Gly(NH_2) in molecule **37** is affected by oxidative modification during the $NaNO_2$-mediated conversion of Gly(NH_2) to the acyl iminium equivalent. This limitation was solved by subjecting the Cys(Acm)-substituted analog **38** for the free Cys residue. *S*-Alkylation of the *S*-Acm moiety with the acyl iminium equivalents **36** under TFA–Gn·HCl conditions resulted in the facile and efficient formation of the sactionine linkage with release of the Acm group from the transiently formed *S*-Acm-derived alkylated sulfonium cation **39**. The reaction sequence, consisting of the Lossen rearrangement-mediated intramolecular redox reaction and the following *S*-alkylation of Cys(Acm) with the acyl iminium equivalent, facilitated synthesis of the model sactipeptide **40** using a late-stage sactionine linkage-forming strategy.

Conclusion

S-Protected cysteine sulfoxides, initially recognized as a side product in peptide synthesis, have found significant appeal in peptide and protein chemistry. Cys(MBzl)(O) is converted to the corresponding *S*-chlorocysteine in the presence of a chloride anion source under acidic conditions, facilitating release of the MBzl group as the cation. The resulting *S*-chlorocysteine selectively reacts with Trp to afford the tryptathionine unit even in the presence of Tyr. In contrast, Cys(Acm)(O) under acidic conditions becomes *S*-chlorocysteine or a dicationic intermediate, depending on the reaction conditions. On the one hand, treatment under acidic conditions in the presence of a chloride anion source results in the formation of *S*-chlorocysteine. On the other hand, under highly acidic conditions that enable protonation or silylation of the amide of the *S*-Acm group, a dicationic intermediate is formed that selectively reacts with Tyr to yield the sulfenyl Tyr. It is also worth noting that weakly acidic conditions in the presence of $MgCl_2$, which does not affect Cys(MBzl)(O), allow for the conversion of Cys(Acm)(O) to the corresponding *S*-chlorocysteine. This difference in reactivity between Cys(Acm)(O) and Cys(MBzl)(O) has led to the development of a linker that enables the one-pot/stepwise linking of two Trp-containing peptides. The fact that the *S*-chlorocysteine reacts with S-protected cysteine to yield a disulfide with release of the *S*-protection and that regioselective disulfide formation can be performed by selecting appropriate conditions for the Cys(Acm)(O)/Cys(Acm) and Cys(MBzl)(O)/Cys(MBzl) pairs with successful application to the synthesis of insulin is notable. The combination of the unique chemical character of the *S*-Acm group, which is susceptible to release upon *S*-alkylation, and the Lossen rearrangement-mediated intramolecular redox reaction of GlyHA is paving the way for unprecedented synthetic access to sactipeptides.

Acknowledgments

I acknowledge Daishiro Kobayashi (Ph.D.), Kento Ohkawachi (Ph.D.), Junya Hayashi (Ms.), Kota Hidaka (Ms.), Naoto Naruse

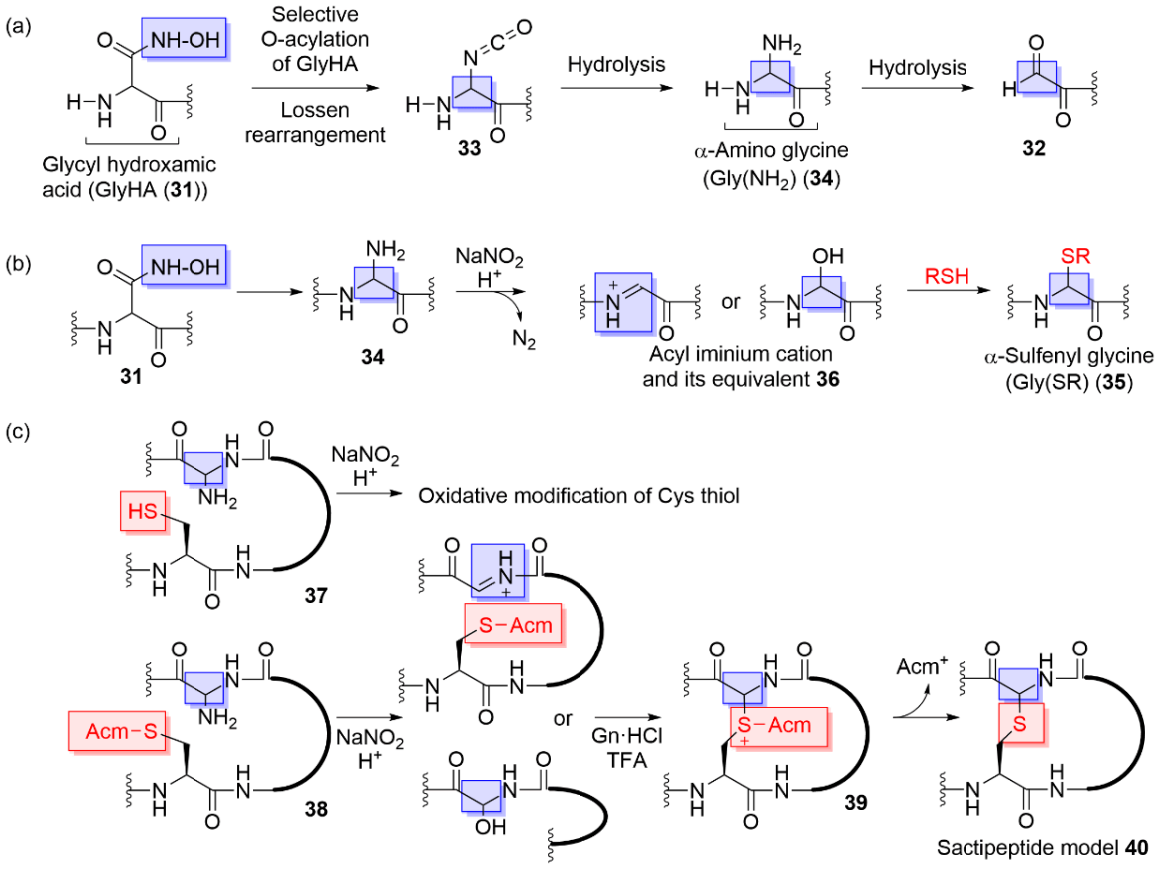

Figure 12. (a) Lossen rearrangement of an N-terminal GlyHA residue. (b) Lossen rearrangement of an internal GlyHA residue in a peptide sequence, followed by nucleophilic attack of a thiol. (c) Synthesis of a model sactipeptide using a late-stage sactionine linkage-forming strategy.

(Ph.D.), and Masaya Denda (Ph.D.) for their great contributions to the presented work. These studies were supported in part by The Canon Foundation and by JSPS KAKENHI (23 K18187 and 23H02609) (for A.O.).

Conflict of Interests

The author declares no conflict in interest.

References

1. Funakoshi, S.; Fujii, N.; Akaji, K.; Irie H.; Yajima, H. Studies on Peptides. LXXXIII. Behavior of S-Substituted Cysteine Sulfoxides under Deprotecting Conditions in Peptide Synthesis. *Chem. Pharm. Bull. (Tokyo)* **1979**, *27*, 2151–2156.
2. Yajima, H.; Akaji, K.; Funakoshi, S.; Fujii, N.; Irie, H. Studies on Peptides. XCVI. Behavior of S-Acetamidomethylcysteine Sulfoxide under Deprotecting Conditions in Peptide Synthesis. *Chem. Pharm. Bull. (Tokyo)* **1980**, *28*, 1942–1945.
3. (a) Fujii, N.; Otaka, A.; Watanabe, T.; Arai, H.; Funakoshi, S.; Bessho, K.; Yajima, H. Sulphoxide-directed disulphide bond-forming reaction for the synthesis of cystine peptides. *J. Chem. Soc., Chem. Commun.* **1987**, 1676–1678.
4. (a) Naruse, N.; Kobayashi, D.; Ohkawachi, K.; Shigenaga, A.; Otaka, A. Copper-Mediated Deprotection of Thiazolidine and Selenazolidine Derivatives Applied to Native Chemical Ligation. *J. Org. Chem.* **2020**, *85*, 1425–1433. (b) Kobayashi, D.; Naruse, N.; Denda, M.; Shigenaga, A.; Otaka, A. Deprotection of S-acetamidomethyl cysteine with copper(ii) and 1,2-aminothiols under aerobic conditions. *Org. Biomol. Chem.* **2020**, *18*, 8638–8645.
5. Bang, D.; Kent, S. B. H. A One-Pot Total Synthesis of Crambin. *Angew. Chem. Int. Ed.* **2004**, *43*, 2534–2538.
6. (a) Dawson, P.; Muir, T.; Clark-Lewis, I.; Kent, S. Synthesis of proteins by native chemical ligation. *Science* **1994**, *266*, 776–779.
7. (a) Jbara, M.; Maity, S. K.; Brik, A. Palladium in the Chemical Synthesis and Modification of Proteins. *Angew. Chem. Int. Ed. Engl.* **2017**, *56*, 10644–10655.
8. Kobayashi, D.; Kohmura, Y.; Hayashi, J.; Denda, M.; Tsuchiya, K.; Otaka, A. Copper(ii)-mediated C–H sulphenylation or selenylation of tryptophan enabling macrocyclization of peptides. *Chem. Commun.* **2021**, *57*, 10763–10766.
9. May, J. P.; Perrin, D. M. Tryptathionine bridges in peptide synthesis. *Peptide Sci.* **2007**, *88*, 714–724.
10. (a) Siegert, M.-A. J.; Knittel, C. H.; Süssmuth, R. D. A Convergent Total Synthesis of the Death Cap Toxin α-Amanitin. *Angew. Chem. Int. Ed.* **2020**, *59*, 5500–5504.
11. Kobayashi, D.; Kohmura, Y.; Sugiki, T.; Kuraoka, E.; Denda, M.; Fujiwara, T.; Otaka, A. Peptide Cyclization Mediated by Metal-Free S-Arylation: S-Protected Cysteine Sulfoxide as an Umpolung of the Cysteine Nucleophile. *Chem. Eur. J.* **2021**, *27*, 14092–14099.
12. Kobayashi, D.; Kuraoka, E.; Hayashi, J.; Yasuda, T.; Kohmura, Y.; Denda, M.; Harada, N.; Inagaki, N.; Otaka, A. S-Protected Cysteine Sulfoxide-Enabled Tryptophan-Selective Modification with Application to Peptide Lipidation. *ACS Med. Chem. Lett.* **2022**, *13*, 1125–1130.
13. Kobayashi, D.; Denda, M.; Hayashi, J.; Hidaka, K.; Kohmura, Y.; Tsunematsu, T.; Nishino, K.; Yoshikawa, H.; Ohkawachi, K.; Nigorikawa, K.; et al. Sulfoxide-Mediated Cys-Trp-Selective Bioconjugation that Enables Protein Labeling and Peptide Heterodimerization. *ChemistryEurope* **2024**, *2*, e202400014.
14. Ohkawachi, K.; Anzaki, K.; Kobayashi, D.; Kyan, R.; Yasuda, T.; Denda, M.; Harada, N.; Shigenaga, A.; Inagaki, N.; Otaka, A. Residue-Selective C−H Sulfenylation Enabled by Acid-Activated S-Acetamidomethyl Cysteine Sulfoxide with Application to One-Pot Stapling and Lipidation Sequence. *Chem. Eur. J.* **2023**, *29*, e202300799.
15. Hidaka, K.; Kobayashi, D.; Hayashi, J.; Denda, M.; Otaka, A. Advanced Insulin Synthesis by One-pot/Stepwise Disulfide Bond Formation Enabled by S-Protected Cysteine Sulfoxide. *Chem. Eur. J.* **2024**, e202401003.
16. Yajima, H.; Fujii, N. Studies on peptides. 103. Chemical synthesis of a crystalline protein with the full enzymic activity of ribonuclease A. *J. Am. Chem. Soc.* **1981**, *103*, 5867–5871.
17. Anderson, M. O.; Shelat, A. A.; Guy, R. K. A Solid-Phase Approach to the Phallotoxins: Total Synthesis of [Ala7]-Phalloidin. *J. Org. Chem.* **2005**, *70*, 4578–4584.
18. Shida, H.; Taguchi, A.; Tokita, Y.; Cui, Y.; Sakamaki, M.; Konno, S.; Taniguchi, A.; Yun, Y. S.; Fujikawa, Y.; Kaneko, H.; Nakaminami, H.; Hayashi, Y., Tryptophan-Selective Chemical Modification of Peptides by Thioether-Mediated Sulfenylation. *ChemistryEurope* **2025**, *3*, e2500059.
19. (a) Lau, Y. H.; de Andrade, P.; Wu, Y.; Spring, D. R. Peptide stapling techniques based on different macrocyclisation chemistries. *Chem. Soc. Rev.* **2015**, *44*, 91–102.
20. Veber, D.; Milkowski, J.; Varga, S.; Denkewalter, R.; Hirschmann, R. Acetamidomethyl. A Novel Thiol Protecting Group for Cysteine. *J. Am. Chem. Soc.* **1972**, *94*, 5456–5461.
21. Fujii, N.; Otaka, A.; Ikemura, O.; Akaji, K.; Funakosho, S.; Hayashi, Y.; Kuroda, Y.; Yajima, H. Trimethylsilyl trifluoromethanesulphonate as a useful deprotecting reagent in both solution and solid phase peptide syntheses. *J. Chem. Soc., Chem. Commun.* **1987**, 274–275.
22. Mima, A.; Nomura, A.; Fujii, T. Current findings on the efficacy of incretin-based drugs for diabetic kidney disease: A narrative review. Biomed. *Pharmacotherapy* **2023**, *165*, 115032.
23. Zhang, L.; Bulaj, G. Converting Peptides into Drug Leads by Lipidation. *Curr. Med. Chem.* **2012**, *19*, 1602–1618.
24. El-Shaffey, H. M.; Gross, E. J.; Hall, Y. D.; Ohata, J. An Ionic Liquid Medium Enables Development of a Phosphine-Mediated Amine–Azide Bioconjugation Method. *J. Am. Chem. Soc.* **2021**, *143*, 12974–12979.
25. Review on chemical synthesis of insulin; see. Karas, J. A.; Wade, J. D.; Hossain, M. A. The Chemical Synthesis of Insulin: An Enduring Challenge. *Chem. Rev.* **2021**, *121*, 4531–4560.
26. Representative conventional insulin synthesis; see. (a) Akaji, K.; Fujino, K.; Tatsumi, T.; Kiso, Y. Total synthesis of human insulin by regioselective disulfide formation using the silyl chloride-sulfoxide method. *J. Am. Chem. Soc.* **1993**, *115*, 11384–11392.
27. (a) Soran, H.; Younis, N. Insulin detemir: a new basal insulin analogue. *Diabetes, Obesity and Metabolism* **2006**, *8*, 26–30.
28. Hayashi, J.; Kobayashi, D.; Namikawa, C.; Denda, M.; Otaka, A. Synthesis of N-Glyoxylyl Peptides Enabled by a Lossen Rearrangement-Induced Intramolecular Redox Reaction of N-Terminal Glycyl Hydroxamic Acid. *Org. Lett.* **2024**, *26*, 4246–4250.
29. Hayashi, J.; Kobayashi, D.; Denda, M.; Otaka, A. Late-Stage Formation of a Sactionine Linkage Enabled by Lossen Re-

arrangement of Glycyl Hydroxamic Acid. *Org. Lett.* **2024**, *26*, 5167–5171.
30. Chen, Y.; Wang, J.; Li, G.; Yang, Y.; Ding, W. Current Advancements in Sactipeptide Natural Products. Front. Chem. **2021**, *9*, 595991.
31. Milewska, K. D.; Malins, L. R. Synthesis of Amino Acid α-Thioethers and Late-Stage Incorporation into Peptides. *Org. Lett.* **2022**, *24*, 3680–3685.
32. Zhang, Y.; Saha, S.; Esser, Y. C. C.; Ting, C. P. Total Synthesis and Stereochemical Assignment of Enteropeptin A. *J. Am. Chem. Soc.* **2024**, *146*, 17629–17635.

Biography

Dr. Akira Otaka was born in Osaka, Japan in 1960, and received his bachelor's degree from Kyoto University in 1984. He obtained his Ph.D. from Kyoto University in 1989 under the direction of the late Professor Haruaki Yajima. He obtained an Assistant Professor position in Professor Nobutaka Fujii's group at Kyoto University in 1989. After a one-year visiting scientist position in NCI, NIH (1992–1993), he was promoted to Associate Professor in the Fujii's group in 1995. He is currently a Professor at Tokushima University (since 2005) and President of the Japanese Peptide Society (since 2024). He has received the Japan Peptide Society Award for Young Scientists (1997), the Pharmaceutical Society of Japan Award for Young Scientists (1999), the Society of Synthetic Organic Chemistry, Japan, Astellas Award for Organic Chemistry in Life Sciences (2012), the Pharmaceutical Society of Japan Award (2022), and The Japanese Peptide Society Award (2023). His research interests include peptide and protein chemistry, chemical biology, and medicinal chemistry.

Design of Tau-derived peptides for modulating structures and functions of microtubules

Received: May 1, 2025

Accepted: July 4, 2025

Published: October 1, 2025

Hiroshi Inaba [1,2]

[1]Department of Chemistry and Biotechnology, Graduate School of Engineering, Tottori University, 4-101 Koyama-Minami, Tottori 680-8552, Japan.
[2]Center for Research on Green Sustainable Chemistry, Tottori University, 4-101 Koyama-Minami, Tottori 680-8552, Japan.

e-mail: hinaba@tottori-u.ac.jp

Keywords: Microtubules; Tau-derived peptide; Encapsulation; Active matter; Superstructures

Abstract

Microtubules are nanotubular cytoskeleton structures composed of tubulin proteins that are essential for mechanical support, molecular transport, cell division, and various other cellular functions. The motility of microtubules coupled with motor proteins such as kinesin and dynein enables the construction of microtubule-based, motile nanomaterials. Modulation of microtubule structures and functions is crucial for advancing our understanding of microtubule biophysics, cell manipulation strategies, and nanotechnological applications. In nature, the properties of microtubules such as their size, dynamics, and superstructures are modulated by the binding of diverse groups of proteins. In addition to the well-studied microtubule-associated proteins (MAPs) that bind to the outside of microtubules, microtubule inner proteins (MIPs) that bind to the inside of microtubules and act as modulators have recently been discovered. Thus, the inside of microtubules is an intriguing space for modulating microtubules by introducing nanomaterials. However, unlike conjugation of molecules to the outside of microtubules, methods of introducing exogenous molecules to the inside of microtubules are not well established. We developed a Tau-derived peptide (TP) that binds to the inside of microtubules as a means of functionalizing microtubules. In this account, we summarize our approaches for TP-based modulation of microtubules for encapsulation of nanomaterials, cell manipulation, and construction of microtubule superstructures. First, TP was designed, and the binding property with microtubules was analyzed. In addition, cyclic TPs were developed for enhanced binding to microtubules and stabilization of microtubules. Second, photocontrol of microtubule structures was achieved by conjugating TP with photoresponsive molecules. The system was applied to cause light-induced cell death. Third, the TP-based methods were used for constructing metal nanoparticle-encapsulating microtubules, creating new types of nanomaterials such as magnetotactic microtubules. Fourth, structural changes were induced in microtubules by TP-based encapsulation of proteins. Fifth, various microtubule superstructures were constructed by displaying TP on the outer surface of microtubules. This TP-based technology opens up new research possibilities via modulating microtubules to understand their properties and their applications in biological and nanotechnological fields.

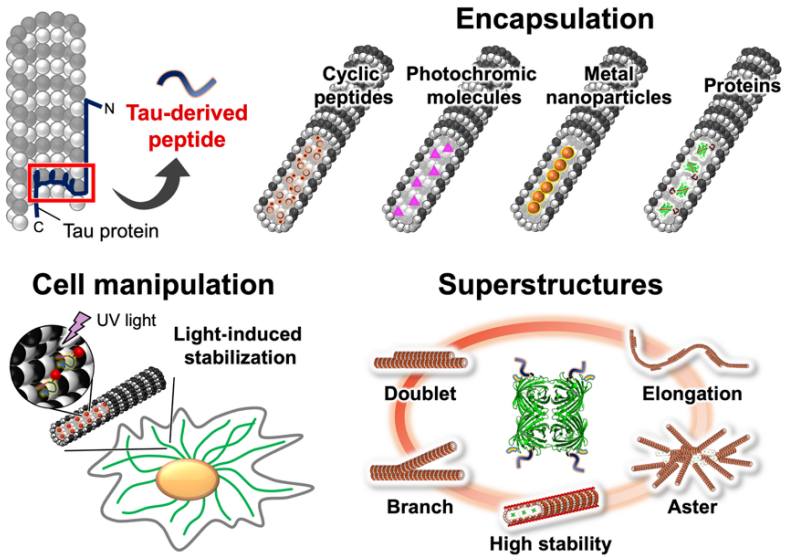

Part of the research eligible for 2024 Award for Young Investigator, The Japanese Peptide Society is described in this article.

Introduction

Microtubules are tubular cytoskeleton structures with a 15 nm inner diameter that are important for mechanical support, molecular transport by motor proteins, and cell division (Figure 1a)[1–6]. Microtubule dynamics, the formation (polymerization) and dissociation (depolymerization) of microtubules, are regulated by the binding of GTP to tubulin proteins and the hydrolysis of GTP[7]. Motor proteins such as kinesin and dynein use the energy from ATP hydrolysis to walk along microtubules and transport molecules. Microtubules are able to form various structures with different diameters, lengths, stability, and superstructures[8]. Compared with the typical single hollow tubular structures (singlet microtubules), microtubule superstructures are complicated multiple tubular structures such as doublets, branches, and asters (Figure 1b)[5,9,10]. Doublet microtubules, a famous superstructure consisting of a complete singlet microtubule (A-tubule) and an incomplete microtubule (B-tubule) tethered to the A-tubule, contribute to the mechanical strength and motility of flagella and cilia[5,10].

Owing to their diverse structures and functions, microtubules are targeted in various research fields[11]. For example, microtubule-targeted drugs have been developed to manipulate cellular functions, mainly by disturbing microtubule dynamics[12–14]. One of the best-known microtubule-targeted drugs is taxol (paclitaxcel), which shows anti-cancer activity by binding to the inner pocket of microtubules and stabilizing their structures. Recently, photocontrol of intracellular microtubules by microtubule-targeted drugs with photoresponsive molecules has been reported[15–18]. Another large research field is the use of microtubules as components for nanomaterials. Microtubules show ATP-driven, unidirectional motility on a substrate coated with kinesin motors (Figure 1c). This unique motile property of microtubules is used for constructing dynamic nanomaterials such as active matter and molecular robots[19–27].

The structures and characteristics of microtubules, such as length, diameter, rigidity, dynamics, velocity, and superstructure, are controlled in nature by the binding of various proteins. For instance, microtubule-associated proteins (MAPs) are a well-known group of microtubule-binding proteins that bind to the outside of microtubules and modify their properties[28–30]. Recently, a group of proteins that bind to the inside of microtubules has been identified and named as microtubule inner proteins (MIPs)[6,10,31–39]. Although the functions of MIPs remain to be elucidated, they are expected to contribute to the stability and strength of microtubules and the formation of doublet microtubules. Engineering microtubules by chemical approaches is important not only for their applications in biological and nanotechnological fields but also for understanding their biophysical properties in nature. Chemical modification of lysine residues located on the outer surface of microtubules is widely used for conjugation of molecules such as fluorescent dyes; however, the inside of microtubules has been overlooked for a long time. As shown by MIPs, the inside of microtubules could be a novel space for modulating microtubules, possibly enabling encapsulation of nanomaterials such as proteins and metal nanoparticles. For this purpose, molecular units that bind to the inside of microtubules are required.

Peptides are unique molecular tools with powerful molecular recognition capabilities based on optimization of their sequences of natural and non-natural amino acids by rational design, screening methods, and *in silico* methods[40–47]. On the basis of the microtubule-binding protein Tau, we designed a peptide to bind to the inside of microtubules and modulate them. This new concept of peptide-based modulation of microtubules from the inside is described in our reviews and books[6,48–51]. Here, we summarize the latest developments in the Tau-derived peptide (TP) derivatives, the TP-based encapsulation of metal nanoparticles and proteins inside microtubules, and the construction of microtubule superstructures by displaying TP.

Design of Tau-derived peptides binding to the inside of microtubules

We constructed a Tau-derived peptide (TP) that binds to a pocket inside microtubules known as the 'taxol-binding pocket' (Figure 2)[52]. Tau is an intrinsically disordered protein that binds to microtubules through various binding modes. It was reported that preincubation of Tau with tubulin and subsequent polymerization leads to binding of the Tau repeat sequences (R1–R4) to the taxol-binding pocket of microtubules[53]. Another study revealed that certain regions of Tau, the R1-interrepeat (267–284) and R2-interrepeat (298–315), adopt a hairpin conformation upon binding to microtubules[54]. On the basis of these reports, we developed four peptides consisting of the R1-interrepeat or R2-interrepeat with a cysteine residue linked at the N- or C-terminal via a glycine residue (Figure 2). All tetramethylrhodamine (TMR)-labeled peptides bind to tubulin with different K_d (3.4–40.0 μM). For the preparation of microtubules in the subsequent experiments, GTP was used to analyze the effects of the TP constructs on microtubule formation and stability. In contrast, a slowly hydrolyzable GTP analog, guanosine-5'-[(α,β)-methyleno]triphosphate (GMPCPP), was used for the analysis of the binding of the TP constructs and the structures of microtubules, because GMPCPP is commonly used to form stable microtubules. Among the designed four peptides, the peptide that we refer to as TP (CGGGKKHVPGGGSVQIVYKPVDL) was labeled with TMR and observed to be bound to the taxol-binding pocket following preincubation with tubulin and subsequent polymerization

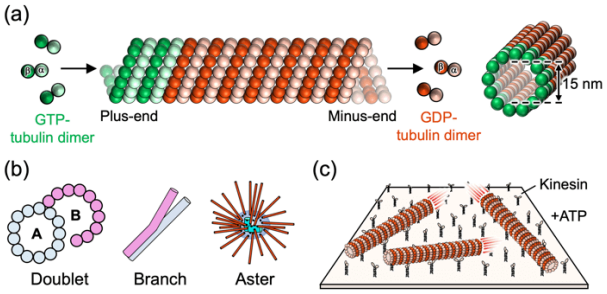

Figure 1. (a) Structures of microtubules. (b) Examples of microtubule superstructures. (c) ATP-driven motility of microtubules on a kinesin-coated substrate.

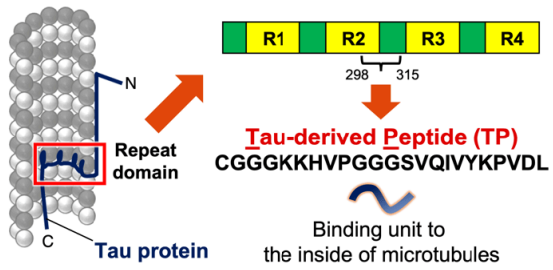

Figure 2. Design of Tau-derived peptide (TP) from the sequence (298–315) of binding repeats (R1–R4) in Tau.

by GMPCPP to form microtubules. When TP was instead incubated with preformed microtubules, the main binding site was changed to the outside of microtubules. The other three peptides mainly bind to the outside of microtubules even when incubated with tubulin prior to polymerization. Thus, we concluded that TP is useful as a binding unit to the inside of microtubules when incubated with tubulin before polymerization. TP is highly amenable to conjugation of small molecules, metal nanoparticles, and proteins by sequence modification, chemical modification, and genetic engineering. TP was used to introduce various nanomaterials into microtubules as illustrated in this report and our previous reviews and books[6,48–51].

The affinity of TMR-labeled TP to tubulin is moderate (K_d = 6.0 μM)[52], and therefore we developed Tau-derived cyclic peptides (TCPs) to enhance the binding affinity to tubulin and stabilize the microtubules[55]. We designed TMR-labeled TCPs with different numbers of glycine linkers (TCPn-TMR, n = 1, 3). TCPn-TMR was synthesized by reacting the N-terminal chloroacetyl moiety and a C-terminal cysteine residue, deprotection of the S-acetamidomethyl group, and subsequent labeling of the deprotected cysteine residue with TMR (Figure 3a). The binding affinity of TCP3-TMR (K_d = 0.97 μM) was higher than that of TMR-labeled TP (K_d = 6.0 μM), whereas the affinity of TCP1-TMR (K_d = 7.2 μM) was lower than that of TMR-labeled TP. A turbidity assay showed that TCP3-TMR enhanced the formation of microtubules compared with TCP1-TMR and TMR-labeled TP, reflecting the high binding affinity of TCP3-TMR to tubulin. Because microtubules prepared with GTP are typically unstable *in vitro* due to the hydrolysis of GTP to GDP, GTP-microtubules were used to evaluate the stabilization effect of the cyclic peptides on microtubules. Confocal laser scanning microscopy (CLSM) images showed that the pretreatment of tubulin with TCP1-TMR or TCP3-TMR and subsequent polymerization using GTP resulted in the formation of microtubules similar to treatment with taxol, indicating the stabilization of microtubules (Figure 3b). Thus, the cyclic peptides, especially TCP3-TMR, bound to tubulin with strong affinity and showed stabilization of microtubules in a similar manner to taxol.

Photocontrol of microtubule structures by TP derivatives

Control of microtubule structures by external stimuli, especially by light, enables modulation of active matter properties and manipulation of cellular functions[25,26,56]. For example, development of photochromic molecules mimicking microtubule-binding drugs and conjugation of photoresponsive molecules to microtubule-binding drugs has enabled photocontrol of intracellular microtubule structures[15–18]. Another approach is the conjugation of azobenzene-bearing DNA to the outside of microtubules for the photocontrol of microtubule assembly/disassembly and cargo pickup/release by a light-induced change in the DNA moiety's hybridization[57,58]. Peptides conjugated with photoresponsive molecules have great potential to modulate biological functions[59]. We have developed TPs with photoresponsive molecules to photocontrol microtubule structures[60,61]. We first focused on the photoaffinity labeling agent diazirine (DA), which generates a carbene upon ultraviolet (UV) light (365 nm) irradiation by forming a covalent bond with a nearby residue in the target protein. TP conjugated with DA at the N-terminus (DA-TP) was designed for light-induced stabilization of microtubules by formation of a covalent bond to microtubules upon UV light irradiation (Figure 4a)[60]. TMR-labeled DA-TP (DA-TP-TMR) bound to the taxol-binding pocket of microtubules and formed a covalent bond to microtubules upon UV light irradiation. Incorporation of DA-TP into microtubules and subsequent UV light irradiation led to the formation of longer and more rigid GTP-microtubules compared with no UV light irradiation, indicating that there was light-induced stabilization of microtubules by the covalent bond formation (Figure 4b). Because the binding of TP to intracellular microtubules was previously

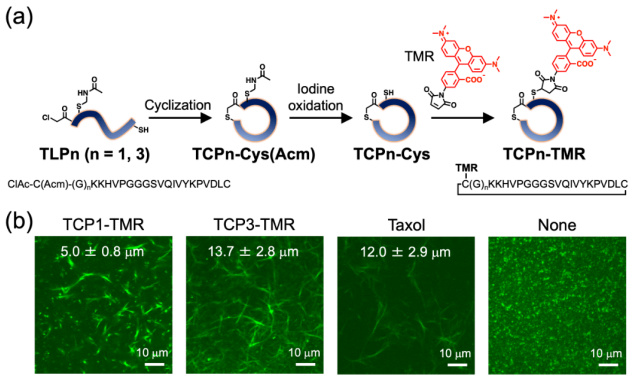

Figure 3. (a) Synthesis of tetramethylrhodamine (TMR)-labeled cyclic TPs (TCPn-TMR) (n = 1, 3). (b) Confocal laser scanning microscopy (CLSM) images of GTP-microtubules preincubated with TCP1-TMR, TCP3-TMR, or Taxol and without any additive. Reproduced and modified from ref. 55 with permission from Springer Nature.

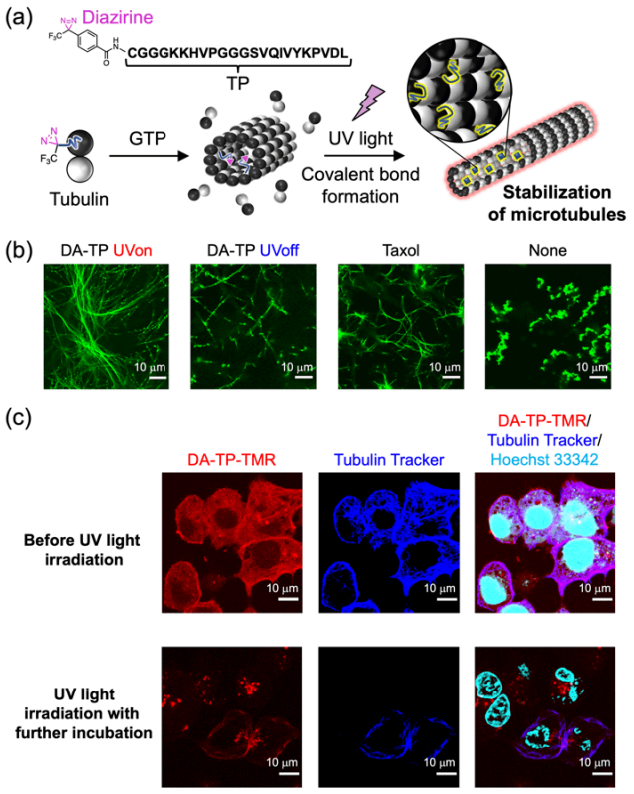

Figure 4. (a) UV light (365 nm)-induced stabilization of microtubules by diazirine-conjugated TP (DA-TP). (b) CLSM images of GTP-microtubules preincubated with DA-TP with and without UV light irradiation, with Taxol, and without any additive. (c) CLSM images of HepG2 cells upon introduction of TMR-labeled DA-TP (DA-TP-TMR) (top) and after UV light irradiation (5 min) and further incubation for 15 h (bottom). Intracellular microtubules were stained with Tubulin Tracker Deep Red, and cell nuclei were stained with Hoechst 33342. Reproduced and modified from ref. 60 with permission from Royal Society of Chemistry.

shown[62], we applied this system for light-induced stabilization of intracellular microtubules. DA-TP-TMR was incorporated into intracellular microtubules in HepG2 cells by depolymerizing the existing microtubules, introducing DA-TP-TMR, and incubating during microtubule assembly (Figure 4c). UV light irradiation and further incubation led to abnormally shaped cells with nuclear defects (Figure 4c). Cell viability analysis also showed that treatment with DA-TP-TMR and subsequent UV light irradiation induced significant cell death. These results demonstrated that UV light-induced stabilization of intracellular microtubules by DA-TP-TMR can be used to inhibit normal cell growth.

The DA-based photoaffinity labeling system is irreversible. For the reversible control of microtubule structures by light, we next developed a photochromic spiropyran (SP)-conjugated TP (Figure 5a)[61]. SP converts to merocyanine (MC) upon UV light irradiation, and MC returns to SP upon visible light irradiation. Because of the different properties of SP (nonionic and hydrophobic, smaller dipole moment) and MC (zwitterionic and hydrophilic, larger dipole moment) and the reversible conversion by light irradiation, the SP/MC system can be used for various photoswitching applications[59,63]. We synthesized four TMR-labeled, SP-conjugated TPs that have SP conjugated to cysteine residues at different positions in TP. Among them, the peptide conjugated with SP at the N-terminus (TMR-1-TP-SP) stabilized GTP-microtubules, whereas the same peptide in the MC form (TMR-1-TP-MC) showed no stabilization effect. The distinct effects of TMR-1-TP-SP and TMR-1-TP-MC were used for the reversible photocontrol of the formation and dissociation of microtubules. UV light (365 nm) irradiation of TMR-1-TP-SP-stabilized GTP-microtubules to induce the conversion of TMR-1-TP-SP to TMR-1-TP-MC led to the dissociation of microtubules, and subsequent visible light (505 nm) irradiation to induce the conversion of TMR-1-TP-MC to TMR-1-TP-SP led to the reformation of microtubules (Figure 5b). Interestingly, the light-induced formation and dissociation of microtubules was a reversible and repeatable process. The on-demand structural change of microtubules by light could have applications in the manipulation of cell fate and spatiotemporal control of active matter.

Encapsulation/growth of metal nanoparticles inside microtubules

The inner diameter of microtubules (typically 15 nm) is suitable for encapsulating nanomaterials, and the incorporation of nano-sized materials could be used for the modulation of microtubule structures and functions. We introduced gold[52,64], cobalt-platinum (CoPt)[65], and silver nanoparticles[66] into microtubules using TP. First, we encapsulated gold nanoparticles (AuNPs) inside microtubules using TP-conjugated AuNPs (TP-AuNPs) prepared by a simple reaction between cysteine in TP and gold[52,64]. Preincubation of TP-AuNPs with tubulin and subsequent polymerization resulted in the encapsulation of TP-AuNPs in microtubules as observed by transmission electron microscopy (TEM)[52]. Later, we investigated the effects of particle size (5 or 10 nm), TP density (1, 10, 50 equivalents), and surface functional groups (citrate-capped, hydroxy group, amino group) of TP-AuNPs on microtubules[64]. The rigidity of microtubules was enhanced by increasing the density of TP on the AuNPs. Among TP-AuNPs, citrate-capped TP-AuNP (10 nm) with 50 equivalents of TP efficiently enhanced the rigidity and stability of microtubules, whereas the TP-AuNPs with hydroxy and amino groups showed no significant effects. Thus, the TP density and surface properties of TP-AuNPs affect microtubules.

Next, we used TP to introduce ferromagnetic CoPt nanoparticles into microtubules and construct magnetotactic microtubules[65]. The combination of the inherent motility of microtubules and the magnetic alignment of CoPt nanoparticles make it possible to construct magnetotactic microtubules that align and move in accordance with a magnetic field. Natural magnetotactic bacteria possess magnetic nanoparticles called 'magnetosomes' that they use to align to and move along the geomagnetic field[67]. We mimicked this natural system with a peptide consisting of CoPt-binding peptide, CBP (HYPTLPLGSSTY)[68], and TP (CBP-TP) to introduce ferromagnetic CoPt nanoparticles into microtubules. CBP-TP was incorporated into microtubules and incubated with metal sources ($Co(CH_3COO)_2$) and ($(NH_4)_2PtCl_4$) and a reductant ($NaBH_4$) to form CoPt nanoparticles inside microtubules (Figure 6a). Linear-chain assembly of CoPt nanoparticles was observed by TEM, indicating the *in situ* nucleation and growth of CoPt nanoparticles inside microtubules. The microtubules with CoPt nanoparticles showed remarkable alignment along the direction of a weak magnetic field (0.37 T) (Figure 6b). By contrast, such magnetic alignment was not observed when CoPt nanoparticles without TP were formed in microtubules or accumulated on the outer surface of microtubules. Thus, the linear-chain assembly of CoPt nanoparticles in microtubules leads them to behave like ferromagnetic nanowires, which is important for the alignment in response to magnetic fields. A motility assay showed that the CoPt nanoparticle-encapsulating microtubules had increased velocity (0.40 $\mu m\ s^{-1}$) compared with normal microtubules (0.34 $\mu m\ s^{-1}$), whereas the velocity was decreased when CoPt nanoparticles were accumulated on the outer surface (0.28 $\mu m\ s^{-1}$). Thus, the formation

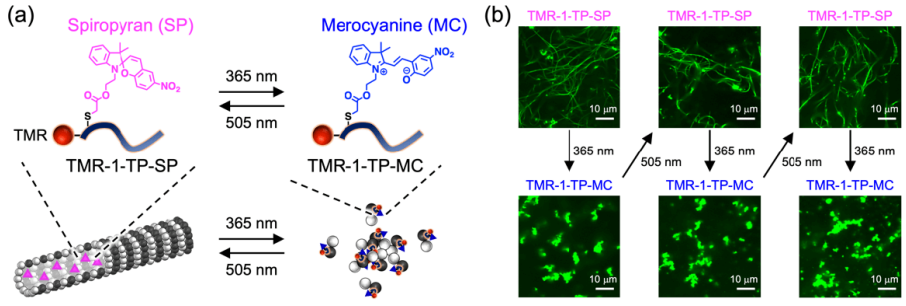

Figure 5. (a) Light-induced, reversible structural changes of microtubules via TMR-labeled spiropyran (SP)-conjugated TP (TMR-1-TP-SP) and TMR-labeled merocyanine (MC)-conjugated TP (TMR-1-TP-MC). (b) CLSM images of GTP-microtubules incorporating TMR-1-TP-SP and upon repeated irradiation with UV light (365 nm) and visible light (505 nm) at 37 °C for 2 min. Reproduced and modified from ref. 61 with permission from John Wiley and Sons.

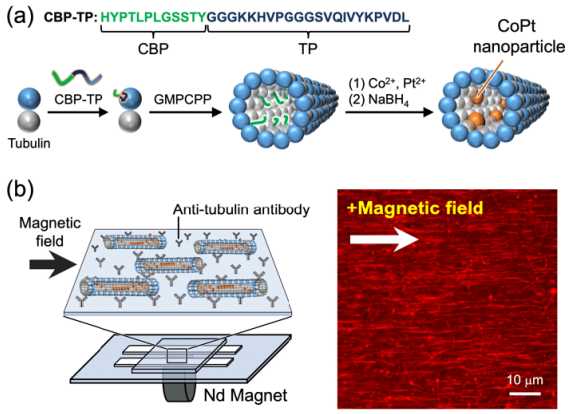

Figure 6. (a) Formation of magnetic CoPt nanoparticles inside microtubules *in situ*. (b) Alignment of CoPt NP-encapsulating microtubules with a magnetic field generated by a neodymium magnet. Reproduced and modified from ref. 65 with permission from American Chemical Society.

of CoPt nanoparticles inside microtubules using CBP-TP is a useful method for constructing magnetotactic microtubules with significant magnetic alignment and increased velocity.

This same method of *in situ* formation of metal nanoparticles inside microtubules was applied to generate silver nanoparticles (AgNPs) and nanowire-like structures inside microtubules[66]. A peptide consisting of silver-binding peptide, AG4 (NPSSLFRYLPSD)[69], and TP (AG4-TP) was introduced into microtubules. Then, AG4-TP was incubated with $AgNO_3$ and $NaBH_4$ to form AgNPs inside microtubules (Figure 7a). The incubation step with $AgNO_3$ and $NaBH_4$ was repeated to grow AgNPs. The density of AgNPs increased with increased concentrations of $AgNO_3$ and $NaBH_4$, and the formation of nanowire-like structures was observed by TEM (Figure 7b), showing the concentration dependent formation of AgNPs and growth of nanowire-like structures in microtubules. When metal nanoparticles were grown on the outside of microtubules by general methods, the formation of aggregates was frequently observed. Our TP-based method to grow nanoparticles inside of microtubules is useful to form uniform metal nanoparticles without aggregation.

Structural change of microtubules by encapsulation of proteins

In nature, MIPs with various shapes and sizes bind to the inside of microtubules to modulate the structures and functions of microtubules[6,10,31,32]. By mimicking MIPs, we encapsulated GFP[70] and tetrameric Azami-Green (AG)[71] inside microtubules with our TP-based approach. First, TP-conjugated GFP (TP-GFP) was prepared using a split GFP system with the truncated N-terminal region of superfolder GFP and a peptide consisting of the C-terminal fragment and TP[70]. The binding of TP-GFP to microtubules was achieved by preincubation with TMR-labeled tubulin (TMR-tubulin) and subsequent polymerization (Figure 8a). The binding site was confirmed to be the inside of microtubules by a competitive binding assay using fluorescently-labeled anti-GFP and anti-tubulin antibodies. There was no binding of GFP alone to microtubules, indicating that the TP moiety of TP-GFP was important for the binding to microtubules. The TP-GFP-encapsulating microtubules had increased contour length (1.7-fold), persistence length (an indicator of microtubule rigidity, 4.0-fold), and velocity (1.2-fold), showing that the encapsulation can cause structural changes in microtubules (Figure 8b). A turbidity assay showed enhanced tubulin polymerization by TP-GFP similar to taxol. The peptide moiety without the GFP scaffold showed a moderate effect on tubulin polymerization, indicating the importance of both the TP and GFP moieties of TP-GFP for induction of structural changes and stabilization of microtubules. Further experiments showed the binding of genetically-fused TP-GFP to plant microtubules in *Arabidopsis thaliana*[72]. Thus, the encapsulation of TP-fused proteins in microtubules can be used for modulation of intracellular microtubules.

Next, we constructed a tetrameric fluorescent protein, AG[73], fused with TP at the C-terminus (TP-AG) (Figure 9a)[71]. TP-AG possesses four TPs in the tetrameric form and is approximately four-fold larger than TP-GFP. The binding site of TP-AG can be changed to the inside of microtubules by preincubation with tubulin and subsequent polymerization or to the outside of microtubules by incubation with preformed microtubules. This was confirmed by digestion of the C-terminal tail, located on the outside of microtubules, and binding of an anti-AG antibody. A turbidity assay showed that TP-AG dramatically induced tubulin polymerization compared with taxol and TP-GFP (Figure 9b). Because AG alone and a

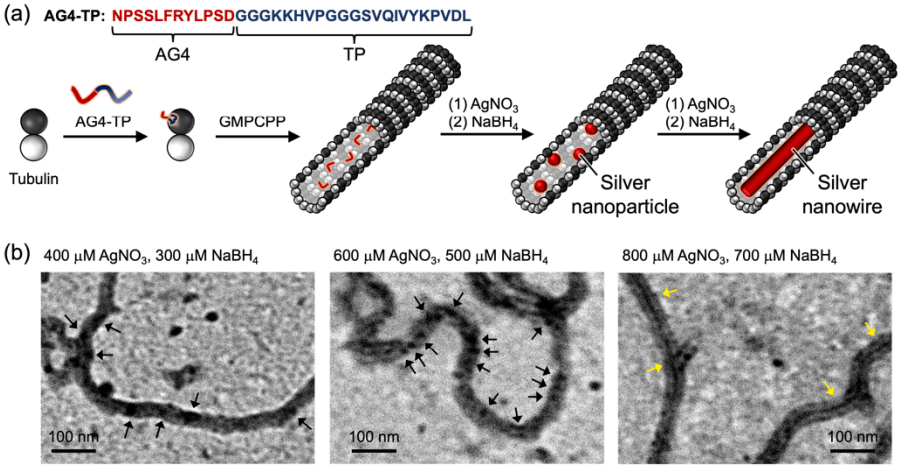

Figure 7. (a) Formation of silver nanoparticles and nanowire-like structures inside microtubules *in situ* and (b) TEM images with different concentrations of $AgNO_3$ and $NaBH_4$. Black arrows indicate representative AgNPs in microtubules, and yellow arrows indicate representative nanowire-like structures in microtubules. Reproduced and modified from ref. 66 with permission from Oxford University Press.

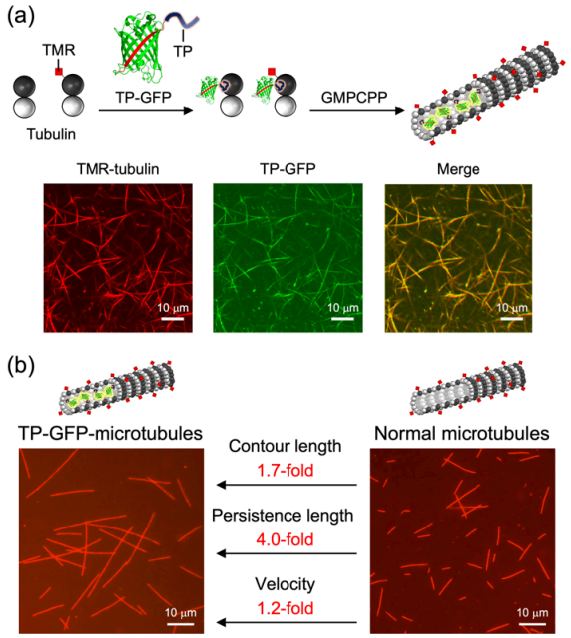

Figure 8. (a) Encapsulation of TP-conjugated GFP (TP-GFP) in microtubules and CLSM images. (b) Comparison of properties of TP-GFP-encapsulated microtubules and normal microtubules. Reproduced and modified from ref. 70 with permission from Royal Society of Chemistry.

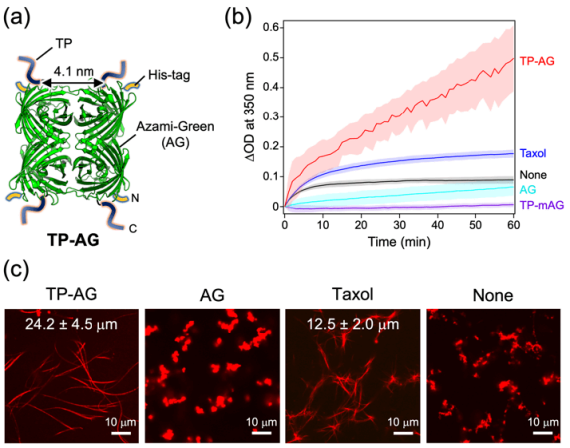

Figure 9. (a) TP-fused Azami-Green (TP-AG). (b) Turbidity change due to tubulin polymerization. (c) CLSM images of GTP-microtubules preincubated with TP-AG, AG, or Taxol and without any additive. Reproduced and modified from ref. 71 with permission from AAAS.

monomeric version of AG fused with TP showed no enhancement of tubulin polymerization, the TP moiety and tetrameric structure of TP-AG are important for the enhanced polymerization. The stabilization of GTP-microtubules by TP-AG was also confirmed by CLSM (Figure 9c) and SDS-PAGE analysis. TP-GFP and TP-AG serve as examples that the introduction of exogenous proteins to the inside of microtubules alters their structure and especially their stability. Similar to the different MIPs, the stronger stabilization by TP-AG compared with TP-GFP indicates that the effects on microtubules depend on the encapsulated protein.

Formation of microtubule superstructures by displaying TP on the outside of microtubules

Microtubule superstructures such as doublets, branches, and asters possess unique functions compared with the general singlet microtubules. For example, cilia and flagella possess complex microtubule superstructures containing doublets and branches to provide high mechanical strength and motility[5,10]. It has been suggested that the formation of doublet microtubules is induced by binding of specific MIPs to microtubules to fix and stabilize B-tubules. This natural mechanism inspired us to form microtubule superstructures artificially by binding TP-AG to the outside of microtubules[71]. TP-AG bound to the outside of microtubules recruits free tubulin via exposed TP moieties, inducing the formation of doublets and branched structures (Figure 10a). Treatment with TP-AG induced the formation of various microtubule superstructures, such as doublets, multiplets, and branches, as observed by TEM and cryo-TEM. The percentage of superstructures was higher when TP-AG was bound to the outside than when it was bound to the inside, indicating the importance of free tubulin recruitment to the outside by TP-AG for the generation of microtubule superstructures. The growth of the branched microtubules was observed by time-lapse imaging using total internal reflection fluorescence microscopy. Furthermore, other microtubule superstructures such as motile, aster-like structures (Figure 10b) and extremely long microtubules were formed dependent on the complexation conditions of TP-AG and microtubules. These conditions include the number of equivalents of TP-AG, the usage of GTP or GMPCPP for forming microtubules, and the incubation with TP-AG before or after microtubule polymerization. This is the first example of a single exogenous protein generating various types of microtubule superstructures.

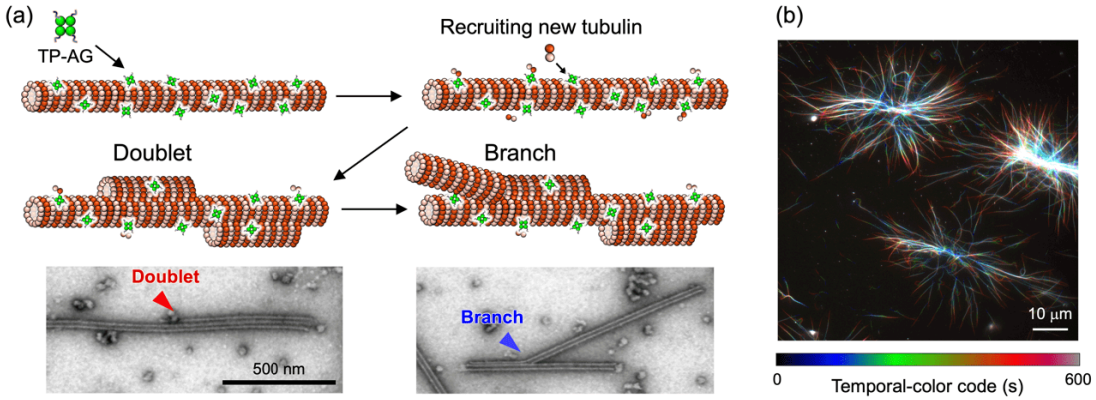

Figure 10. (a) Formation of microtubule superstructures by binding of TP-AG and TEM images of doublet and branched microtubules induced by TP-AG. (b) Motile asters of TP-AG-incorporated microtubules on a kinesin-coated substrate using a temporal-color code. Reproduced and modified from ref. 71 with permission from AAAS.

On the basis of the successful generation of microtubule superstructures by TP-AG, we next designed the TP-fused, photoswitchable protein Dronpa (TP-Dronpa) for photocontrol of the formation and dissociation of microtubule superstructures (Figure 11a)[74]. Tetrameric Dronpa exhibits green fluorescence and is converted to the monomeric state when irradiated with approximately 500 nm light, whereas the monomeric Dronpa exhibits no fluorescence and is converted to the tetrameric state when irradiated with approximately 400 nm light[75]. Tetrameric TP-Dronpa induced the formation of bundles, doublets, and motile asters of microtubules as observed by CLSM and TEM, whereas the microtubules bound with monomeric TP-Dronpa remained dispersed. Irradiation at 505 nm of accumulated microtubules with tetrameric TP-Dronpa induced dispersion of microtubules, while irradiation at 405 nm of dispersed microtubules with monomeric TP-Dronpa induced accumulation of microtubules (Figure 11b). These light-responsive behaviors were used to create light-induced "swarming" movement of microtubules. Irradiation at 405 nm of monomeric TP-Dronpa-bound dispersed microtubules with random movement on a kinesin-coated substrate induced associated movement of microtubules by converting monomeric TP-Dronpa to tetrameric TP-Dronpa and cross-linking microtubules. This photocontrol of formation/dissociation of microtubule superstructures by TP-Dronpa is useful for nanotechnological applications of microtubule superstructures.

The above examples of microtubule superstructure generation by TP-fused proteins are based on mimicking the functions of MIPs. Here the question arises whether protein scaffolds are essential for the generation of microtubule superstructures. To answer this question, we developed a peptide-based method for the construction of microtubule superstructures by displaying TP on microtubules. KA7 peptide (KAKAKAKAKAKAKA) was used to bind to the C-terminal tails of tubulin that are located on the outside of microtubules[76]. A KA7-connected TP (KA7-TP) was designed to bind the KA7 moiety to the outside of microtubules and recruit free tubulin at the TP moiety to generate microtubule superstructures (Figure 12a)[77]. Three KA7-TPs with flexible (GGGS and $(GGGS)_3$) and rigid ($(EAAAK)_2$) linkers were designed. All TMR-labeled KA7-TP showed binding to microtubules and their main binding site was the outer surface of microtubules as confirmed by digestion analysis of the C-terminal tails of tubulin. When KA7-TP-bound, TMR-labeled microtubules were incubated with Alexa Fluor 488-labeled tubulin (AF-tubulin) prior to polymerization, efficient co-localization of the TMR- and AF-labeled microtubules was observed (Figure 12b), indicating the formation of microtubule superstructures by growth of AF-labeled microtubules on TMR-labeled microtubules. KA7 and TP alone showed low co-localization, indicating the importance of the linkage of KA7 and TP. TEM observation showed the formation of bundles and doublets of microtubules induced by the KA7-TP with a $(GGGS)_3$ linker. Peeled structures and sheet-like structures were also observed, presumably due to detachment of layers of microtubules because the connecting B-tubules of doublet microtubules are not as stable as A-tubules. Thus, the peptide-based approach is useful for studying the formation/dissociation mechanisms of microtubule superstructures. It is important to note that the simple peptide-based approach of displaying TP on microtubules is sufficient to induce the formation of doublet microtubules.

Conclusion

Microtubules are important not only as modulators of cell functions but also as intriguing components for constructing nanomaterials such as active matter. Despite the attention given to microtubules in a wide range of areas, methods to

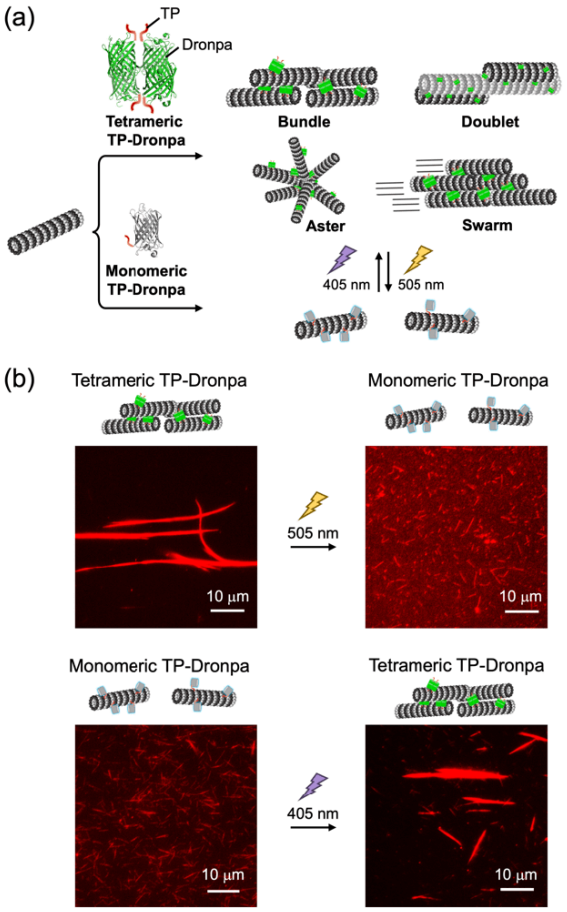

Figure 11. (a) Photocontrol of microtubule superstructures by TPfused, photoresponsive protein Dronpa (TP-Dronpa). (b) Light-induced conversion of tetrameric/monomeric TP-Dronpa to change accumulation/dispersion of microtubules. Reproduced and modified from ref. 74 with permission from American Chemical Society.

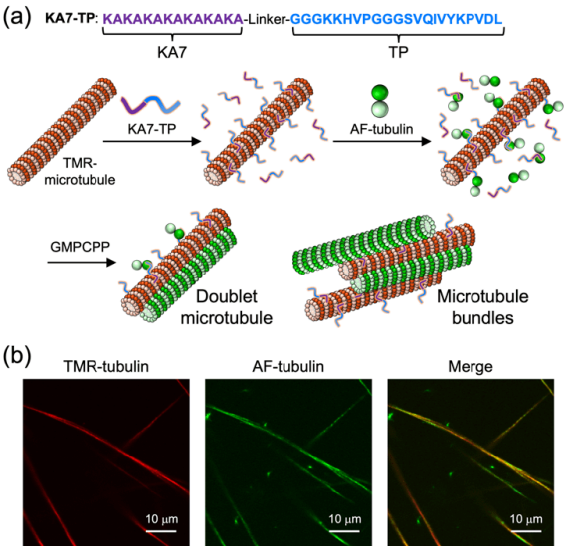

Figure 12. (a) Peptide-based display of the TP moiety on the outside of microtubules for the formation of microtubule superstructures and (b) CLSM images. Reproduced and modified from ref. 77 with permission from Royal Society of Chemistry.

modulate the structures and functions of microtubules are in their infancy. This is especially so for the inside of microtubules, which have not received much attention to date. The discovery of various proteins inside of microtubules shone a light on the possibility of modulating microtubules from the inside. This account summarizes the development of our TP-based technology for modulating microtubules. TP is a useful peptide to introduce various molecules and nanomaterials inside microtubules. Importantly, the structures and properties of microtubules (e.g., length, rigidity, stability, and velocity) were changed depending on the encapsulated nanomaterials. Thus, we demonstrated proof-of-concept for artificial modulation of microtubules from the inside similar to MIPs in nature. In addition, binding of TP to intracellular microtubules to induce structural changes could have applications for cell manipulation. TP is useful not only for the encapsulation of nanomaterials but also for the recruitment of free tubulin on the outer surface of microtubules to generate microtubule superstructures. As shown in this report, TP-fused tetrameric proteins induced the generation of microtubule superstructures such as doublets, branches, bundles, and asters. In the latest research, the peptide-based display of TP on the outer surface of microtubules was shown to be sufficient for the formation of microtubule superstructures. The artificial construction of microtubule superstructures *in vitro* could be important for understanding the formation mechanisms of natural microtubule superstructures and for nanotechnological applications. Furthermore, the photocontrol of microtubule structures was achieved by conjugating TP with photoresponsive molecules and proteins. Recently, other approaches were developed for introducing molecules inside of microtubules, such as the genetic modification of tubulin[78,79] and the use of antibody fragments[80]. The modulation of microtubules, especially by targeting their inside, is a recently-emerged research field, and there is much potential for providing insight into the biological functions of microtubules and for various applications in biological and nanotechnological fields.

Acknowledgments

The author sincerely thanks Prof. Kazunori Matsuura (Tottori University, Japan) and the colleagues and students of Matsuura Laboratory, especially those who are listed in the cited references, for their intensive efforts and achievements. I appreciate Dr. Arif Md. Rashedul Kabir (Macquarie University, Australia), Prof. Kazuki Sada (Hokkaido University, Japan), and Prof. Akira Kakugo (Kyoto University, Japan) for their continuous support of the experiments of microtubules. I appreciate Ms. Noriko Matsuura and Dr. Takashi Iwasaki (Tottori University, Japan) for the help of the protein expression and purification. I appreciate Dr. Muneyoshi Ichikawa (Fudan University, China) and Prof. Tomoya Tsukazaki (Nara Institute of Science and Technology, Japan) for the EM measurements of microtubules, and Dr. Hideki Shigematsu (Japan Synchrotron Radiation Research Institute, Japan) for the help of the cryo-EM measurements of microtubules. I appreciate Dr. Tomonori Tamura and Prof. Itaru Hamachi (Kyoto University, Japan) for the analysis of photoaffinity labeling. I appreciate Dr. Kazusato Oikawa and Prof. Keiji Numata (Kyoto University, Japan) for the analysis of protein expression in plants. I thank the technical staff of the Chemical Bio-Life Division, Technical Department, Tottori University for technical assistance. This work was supported by KAKENHI (No. 17K14517, 19K15699, JP23K04931) and JP24H01721 in a Grant-in-Aid for Transformative Research Areas "Materials Science of Meso-Hierarchy" from the Japan Society for the Promotion of Science (JSPS), ACT-X (JPMJAX2012) and FOREST Program (JPMJFR2034) from the Japan Science and Technology Agency (JST), the Inamori Foundation, and Konica Minolta Science and Technology Foundation for Konica Minolta Imaging Science Encouragement Award, Advanced Technology Institute Research Grants 2022 (for H. I.). I thank Hunter Barbee, PhD, from Edanz (https://jp.edanz.com/ac) for editing a draft of this manuscript.

Conflict of Interests

The author declares no conflict on interest.

References

1. *The Role of Microtubules in Cell Biology, Neurobiology, and Oncology*; Fojo, T., Ed.; Humana Press: Totowa, NJ, 2008. 978-1-58829-294-0.
2. Conde, C.; Cáceres, A. Microtubule Assembly, Organization and Dynamics in Axons and Dendrites. *Nat. Rev. Neurosci.* **2009**, *10*, 319–332.
3. Fletcher, D.A.; Mullins, R.D. Cell Mechanics and the Cytoskeleton. *Nature* **2010**, *463*, 485–492.
4. Brouhard, G.J.; Rice, L.M. Microtubule Dynamics: An Interplay of Biochemistry and Mechanics. *Nat. Rev. Mol. Cell Biol.* **2018**, *19*, 451–463.
5. Janke, C.; Magiera, M.M. The Tubulin Code and Its Role in Controlling Microtubule Properties and Functions. *Nat. Rev. Mol. Cell Biol.* **2020**, *21*, 307–326.
6. Inaba, H.; Matsuura, K. Modulation of Microtubule Properties and Functions by Encapsulation of Nanomaterials Using a Tau-Derived Peptide. *Bull. Chem. Soc. Jpn.* **2021**, *94*, 2100–2112.
7. Gudimchuk, N.B.; McIntosh, J.R. Regulation of Microtubule Dynamics, Mechanics and Function through the Growing Tip. *Nat. Rev. Mol. Cell Biol.* **2021**, *22*, 777–795.
8. Chaaban, S.; Brouhard, G.J. A Microtubule Bestiary: Structural Diversity in Tubulin Polymers. *Mol. Biol. Cell* **2017**, *28*, 2924–2931.
9. Lüders, J.; Stearns, T. Microtubule-Organizing Centres: A Re-Evaluation. *Nat. Rev. Mol. Cell Biol.* **2007**, *8*, 161–167.
10. Ichikawa, M.; Bui, K.H. Microtubule Inner Proteins: A Meshwork of Luminal Proteins Stabilizing the Doublet Microtubule. *BioEssays* **2018**, *40*, 1700209.
11. *Microtubules: Methods and Protocols*; Inaba, H., Ed.; Methods in Molecular Biology; Springer US: New York, NY, 2022; Vol. 2430. 978-1-07-161982-7.
12. Jordan, M.A.; Wilson, L. Microtubules as a Target for Anticancer Drugs. *Nat. Rev. Cancer* **2004**, *4*, 253–265.
13. Dumontet, C.; Jordan, M.A. Microtubule-Binding Agents: A Dynamic Field of Cancer Therapeutics. *Nat. Rev. Drug Discov.* **2010**, *9*, 790–803.
14. Steinmetz, M.O.; Prota, A.E. Microtubule-Targeting Agents: Strategies To Hijack the Cytoskeleton. *Trends Cell Biol.* **2018**, *28*, 776–792.
15. Borowiak, M.; Nahaboo, W.; Reynders, M.; Nekolla, K.; Jalinot, P.; Hasserodt, J.; Rehberg, M.; Delattre, M.; Zahler, S.; Vollmar, A.; et al. Photoswitchable Inhibitors of Microtubule Dynamics Optically Control Mitosis and Cell Death. *Cell* **2015**, *162*, 403–411.
16. Müller-Deku, A.; Meiring, J.C.M.; Loy, K.; Kraus, Y.; Heise, C.; Bingham, R.; Jansen, K.I.; Qu, X.; Bartolini, F.; Kapitein, L.C.; et al. Photoswitchable Paclitaxel-Based Microtubule

Stabilisers Allow Optical Control over the Microtubule Cytoskeleton. *Nat. Commun.* **2020**, *11*, 4640.
17. Gao, L.; Meiring, J.C.M.; Varady, A.; Ruider, I.E.; Heise, C.; Wranik, M.; Velasco, C.D.; Taylor, J.A.; Terni, B.; Weinert, T.; et al. In Vivo Photocontrol of Microtubule Dynamics and Integrity, Migration and Mitosis, by the Potent GFP-Imaging-Compatible Photoswitchable Reagents SBTubA4P and SBTub2M. *J. Am. Chem. Soc.* **2022**, *144*, 5614–5628.
18. Schmitt, C.; Mauker, P.; Vepřek, N.A.; Gierse, C.; Meiring, J.C.M.; Kuch, J.; Akhmanova, A.; Dehmelt, L.; Thorn-Seshold, O. A Photocaged Microtubule-Stabilising Epothilone Allows Spatiotemporal Control of Cytoskeletal Dynamics. *Angew. Chem. Int. Ed.* **2024**, *63*, e202410169.
19. Goel, A.; Vogel, V. Harnessing Biological Motors to Engineer Systems for Nanoscale Transport and Assembly. *Nat. Nanotechnol.* **2008**, *3*, 465–475.
20. Hawkins, T.; Mirigian, M.; Selcuk Yasar, M.; Ross, J.L. Mechanics of Microtubules. *J. Biomech.* **2010**, *43*, 23–30.
21. Malcos, J.L.; Hancock, W.O. Engineering Tubulin: Microtubule Functionalization Approaches for Nanoscale Device Applications. *Appl. Microbiol. Biotechnol.* **2011**, *90*, 1–10.
22. Bachand, G.D.; Spoerke, E.D.; Stevens, M.J. Microtubule-Based Nanomaterials: Exploiting Nature's Dynamic Biopolymers. *Biotechnol. Bioeng.* **2015**, *112*, 1065–1073.
23. Hess, H.; Ross, J.L. Non-Equilibrium Assembly of Microtubules: From Molecules to Autonomous Chemical Robots. *Chem. Soc. Rev.* **2017**, *46*, 5570–5587.
24. Needleman, D.; Dogic, Z. Active Matter at the Interface between Materials Science and Cell Biology. *Nat. Rev. Mater.* **2017**, *2*, 17048.
25. Saper, G.; Hess, H. Synthetic Systems Powered by Biological Molecular Motors. *Chem. Rev.* **2020**, *120*, 288–309.
26. Kabir, A.M.R.; Inoue, D.; Kakugo, A. Molecular Swarm Robots: Recent Progress and Future Challenges. *Sci. Tech. Adv. Mater.* **2020**, *21*, 323–332.
27. Kawamata, I.; Nishiyama, K.; Matsumoto, D.; Ichiseki, S.; Keya, J.J.; Okuyama, K.; Ichikawa, M.; Kabir, A.M.R.; Sato, Y.; Inoue, D.; et al. Autonomous Assembly and Disassembly of Gliding Molecular Robots Regulated by a DNA-Based Molecular Controller. *Sci. Adv.* **2024**, *10*, eadn4490.
28. Mandelkow, E.; Mandelkow, E.-M. Microtubules and Microtubule-Associated Proteins. *Curr. Opin. Cell Biol.* **1995**, *7*, 72–81.
29. Goodson, H.V.; Jonasson, E.M. Microtubules and Microtubule-Associated Proteins. *Cold Spring Harb. Perspect. Biol.* **2018**, *10*, a022608.
30. Bodakuntla, S.; Jijumon, A.S.; Villablanca, C.; Gonzalez-Billault, C.; Janke, C. Microtubule-Associated Proteins: Structuring the Cytoskeleton. *Trends Cell Biol.* **2019**, *29*, 804–819.
31. Cuveillier, C.; Boulan, B.; Ravanello, C.; Denarier, E.; Deloulme, J.-C.; Gory-Fauré, S.; Delphin, C.; Bosc, C.; Arnal, I.; Andrieux, A. Beyond Neuronal Microtubule Stabilization: MAP6 and CRMPS, Two Converging Stories. *Front. Mol. Neurosci.* **2021**, *14*, 665693.
32. Tsuji, C.; Dodding, M.P. Lumenal Components of Cytoplasmic Microtubules. *Biochem. Soc. Trans.* **2022**, *50*, 1953–1962.
33. Ma, M.; Stoyanova, M.; Rademacher, G.; Dutcher, S.K.; Brown, A.; Zhang, R. Structure of the Decorated Ciliary Doublet Microtubule. *Cell* **2019**, *179*, 909–922.e12.
34. Leung, M.R.; Zeng, J.; Wang, X.; Roelofs, M.C.; Huang, W.; Zenezini Chiozzi, R.; Hevler, J.F.; Heck, A.J.R.; Dutcher, S.K.; Brown, A.; et al. Structural Specializations of the Sperm Tail. *Cell* **2023**, *186*, 2880–2896.e17.
35. Wang, X.; Fu, Y.; Beatty, W.L.; Ma, M.; Brown, A.; Sibley, L.D.; Zhang, R. Cryo-EM Structure of Cortical Microtubules from Human Parasite Toxoplasma Gondii Identifies Their Microtubule Inner Proteins. *Nat. Commun.* **2021**, *12*, 3065.
36. Chen, Z.; Shiozaki, M.; Haas, K.M.; Skinner, W.M.; Zhao, S.; Guo, C.; Polacco, B.J.; Yu, Z.; Krogan, N.J.; Lishko, P.V.; et al. De Novo Protein Identification in Mammalian Sperm Using in Situ Cryoelectron Tomography and AlphaFold2 Docking. *Cell* **2023**, *186*, 5041–5053.e19.
37. Andersen, J.S.; Vijayakumaran, A.; Godbehere, C.; Lorentzen, E.; Mennella, V.; Schou, K.B. Uncovering Structural Themes across Cilia Microtubule Inner Proteins with Implications for Human Cilia Function. *Nat. Commun.* **2024**, *15*, 2687.
38. Chakraborty, S.; Martinez-Sanchez, A.; Beck, F.; Toro-Nahuelpan, M.; Hwang, I.-Y.; Noh, K.-M.; Baumeister, W.; Mahamid, J. Cryo-ET Suggests Tubulin Chaperones Form a Subset of Microtubule Lumenal Particles with a Role in Maintaining Neuronal Microtubules. *Proc. Natl. Acad. Sci. USA* **2025**, *122*, e2404017121.
39. Doran, M.H.; Niu, Q.; Zeng, J.; Beneke, T.; Smith, J.; Ren, P.; Fochler, S.; Coscia, A.; Höög, J.L.; Meleppattu, S.; et al. Evolutionary Adaptations of Doublet Microtubules in Trypanosomatid Parasites. *Science* **2025**, *387*, eadr5507.
40. Sawada, T.; Mihara, H.; Serizawa, T. Peptides as New Smart Bionanomaterials: Molecular-Recognition and Self-Assembly Capabilities. *Chem. Rec.* **2013**, *13*, 172–186.
41. Pelay-Gimeno, M.; Glas, A.; Koch, O.; Grossmann, T.N. Structure-Based Design of Inhibitors of Protein–Protein Interactions: Mimicking Peptide Binding Epitopes. *Angew. Chem. Int. Ed.* **2015**, *54*, 8896–8927.
42. Hamley, I.W. Small Bioactive Peptides for Biomaterials Design and Therapeutics. *Chem. Rev*. **2017**, *117*, 14015–14041.
43. Inaba, H.; Matsuura, K. Peptide Nanomaterials Designed from Natural Supramolecular Systems. *Chem. Rec.* **2019**, *19*, 843–858.
44. Vinogradov, A.A.; Yin, Y.; Suga, H. Macrocyclic Peptides as Drug Candidates: Recent Progress and Remaining Challenges. *J. Am. Chem. Soc.* **2019**, *141*, 4167–4181.
45. Watson, J.L.; Juergens, D.; Bennett, N.R.; Trippe, B.L.; Yim, J.; Eisenach, H.E.; Ahern, W.; Borst, A.J.; Ragotte, R.J.; Milles, L.F.; et al. De Novo Design of Protein Structure and Function with RFdiffusion. *Nature* **2023**, *620*, 1089–1100.
46. Abramson, J.; Adler, J.; Dunger, J.; Evans, R.; Green, T.; Pritzel, A.; Ronneberger, O.; Willmore, L.; Ballard, A.J.; Bambrick, J.; et al. Accurate Structure Prediction of Biomolecular Interactions with AlphaFold 3. *Nature* **2024**, *630*, 493–500.
47. Pacesa, M.; Nickel, L.; Schellhaas, C.; Schmidt, J.; Pyatova, E.; Kissling, L.; Barendse, P.; Choudhury, J.; Kapoor, S.; Alcaraz-Serna, A.; et al. One-Shot Design of Functional Protein Binders with BindCraft. *Nature* **2025**.
48. Inaba, H. Development of Dynamic Bionanostructures Based on Peptides: Molecular Encapsulation Inside Microtubules and Light-Induced Propulsion of Microspheres. *Chem. Lett.* **2023**, *52*, 459–468.

49. Inaba, H. Construction of Functional Microtubules and Artificial Motile Systems Based on Peptide Design. *Polym. J.* **2023**, *55*, 1261–1274.
50. Inaba, H.; Matsuura, K. Functionalization of Microtubules by Tau-Derived Peptides: Encapsulation, Cell Manipulation, and Construction of Superstructures. In *Amino Acids, Peptides and Proteins: Volume 45*; Ryadnov, M., Matsuura, K., Eds.; Royal Society of Chemistry, 2024; Vol. 45, pp. 27–44. 978-1-83916-705-8
51. Inaba, H.; Matsuura, K. Encapsulation of Nanomaterials Inside Microtubules by Using a Tau-Derived Peptide. In *Microtubules: Methods and Protocols*; Inaba, H., Ed.; Methods in Molecular Biology; Springer US: New York, NY, 2022; Vol. 2430, pp. 243–260. 978-1-07-161983-4
52. Inaba, H.; Yamamoto, T.; Kabir, A.M.R.; Kakugo, A.; Sada, K.; Matsuura, K. Molecular Encapsulation Inside Microtubules Based on Tau-Derived Peptides. *Chem. Eur. J.* **2018**, *24*, 14958–14967.
53. Kar, S.; Fan, J.; Smith, M.J.; Goedert, M.; Amos, L.A. Repeat Motifs of Tau Bind to the Insides of Microtubules in the Absence of Taxol. *EMBO J.* **2003**, *22*, 70–77.
54. Kadavath, H.; Jaremko, M.; Jaremko, Ł.; Biernat, J.; Mandelkow, E.; Zweckstetter, M. Folding of the Tau Protein on Microtubules. *Angew. Chem. Int. Ed.* **2015**, *54*, 10347–10351.
55. Inaba, H.; Nagata, M.; Miyake, K.J.; Kabir, A.M.R.; Kakugo, A.; Sada, K.; Matsuura, K. Cyclic Tau-Derived Peptides for Stabilization of Microtubules. *Polym. J.* **2020**, *52*, 1143–1151.
56. Lian, Y.-L.; Lin, Y.-C. The Emerging Tools for Precisely Manipulating Microtubules. *Curr. Opin. Cell Biol.* **2024**, *88*, 102360.
57. Keya, J.J.; Suzuki, R.; Kabir, A.M.R.; Inoue, D.; Asanuma, H.; Sada, K.; Hess, H.; Kuzuya, A.; Kakugo, A. DNA-Assisted Swarm Control in a Biomolecular Motor System. *Nat. Commun.* **2018**, *9*, 453.
58. Akter, M.; Keya, J.J.; Kayano, K.; Kabir, A.M.R.; Inoue, D.; Hess, H.; Sada, K.; Kuzuya, A.; Asanuma, H.; Kakugo, A. Cooperative Cargo Transportation by a Swarm of Molecular Machines. *Sci. Robot.* **2022**, *7*, eabm0677.
59. Matsuura, K.; Inaba, H. Photoresponsive Peptide Materials: Spatiotemporal Control of Self-Assembly and Biological Functions. *Biophysics Rev.* **2023**, *4*, 041303.
60. Watari, S.; Inaba, H.; Tamura, T.; Kabir, A.M.R.; Kakugo, A.; Sada, K.; Hamachi, I.; Matsuura, K. Light-Induced Stabilization of Microtubules by Photo-Crosslinking of a Tau-Derived Peptide. *Chem. Commun.* **2022**, *58*, 9190–9193.
61. Inaba, H.; Sakaguchi, M.; Watari, S.; Ogawa, S.; Kabir, A.M.R.; Kakugo, A.; Sada, K.; Matsuura, K. Reversible Photocontrol of Microtubule Stability by Spiropyran-Conjugated Tau-Derived Peptides. *ChemBioChem* **2023**, *24*, e202200782.
62. Inaba, H.; Yamamoto, T.; Iwasaki, T.; Kabir, A.M.R.; Kakugo, A.; Sada, K.; Matsuura, K. Fluorescent Tau-Derived Peptide for Monitoring Microtubules in Living Cells. *ACS Omega* **2019**, *4*, 11245–11250.
63. Klajn, R. Spiropyran-Based Dynamic Materials. *Chem. Soc. Rev.* **2014**, *43*, 148–184.
64. Inaba, H.; Kabir, A.M.R.; Kakugo, A.; Sada, K.; Matsuura, K. Structural Changes of Microtubules by Encapsulation of Gold Nanoparticles Using a Tau-Derived Peptide. *Chem. Lett.* **2022**, *51*, 348–351.
65. Inaba, H.; Yamada, M.; Rashid, M.R.; Kabir, A.M.R.; Kakugo, A.; Sada, K.; Matsuura, K. Magnetic Force-Induced Alignment of Microtubules by Encapsulation of CoPt Nanoparticles Using a Tau-Derived Peptide. *Nano Lett.* **2020**, *20*, 5251–5258.
66. Inaba, H.; Hori, Y.; Kabir, A.M.R.; Kakugo, A.; Sada, K.; Matsuura, K. Construction of Silver Nanoparticles inside Microtubules Using Tau-Derived Peptide Ligated with Silver-Binding Peptide. *Bull. Chem. Soc. Jpn.* **2023**, *96*, 1082–1087.
67. Faivre, D.; Schüler, D. Magnetotactic Bacteria and Magnetosomes. *Chem. Rev.* **2008**, *108*, 4875–4898.
68. Naik, R.R.; Jones, S.E.; Murray, C.J.; McAuliffe, J.C.; Vaia, R.A.; Stone, M.O. Peptide Templates for Nanoparticle Synthesis Derived from Polymerase Chain Reaction-Driven Phage Display. *Adv. Funct. Mater.* **2004**, *14*, 25–30.
69. Naik, R.R.; Stringer, S.J.; Agarwal, G.; Jones, S.E.; Stone, M.O. Biomimetic Synthesis and Patterning of Silver Nanoparticles. *Nat. Mater.* **2002**, *1*, 169–172.
70. Inaba, H.; Yamamoto, T.; Iwasaki, T.; Kabir, A.M.R.; Kakugo, A.; Sada, K.; Matsuura, K. Stabilization of Microtubules by Encapsulation of the GFP Using a Tau-Derived Peptide. *Chem. Commun.* **2019**, *55*, 9072–9075.
71. Inaba, H.; Sueki, Y.; Ichikawa, M.; Kabir, A.M.R.; Iwasaki, T.; Shigematsu, H.; Kakugo, A.; Sada, K.; Tsukazaki, T.; Matsuura, K. Generation of Stable Microtubule Superstructures by Binding of Peptide-Fused Tetrameric Proteins to inside and Outside. *Sci. Adv.* **2022**, *8*, eabq3817.
72. Inaba, H.; Oikawa, K.; Ishikawa, K.; Kodama, Y.; Matsuura, K.; Numata, K. Binding of Tau-Derived Peptide-Fused GFP to Plant Microtubules in Arabidopsis Thaliana. *PLOS ONE* **2023**, *18*, e0286421.
73. Karasawa, S.; Araki, T.; Yamamoto-Hino, M.; Miyawaki, A. A Green-Emitting Fluorescent Protein from Galaxeidae Coral and Its Monomeric Version for Use in Fluorescent Labeling. *J. Biol. Chem.* **2003**, *278*, 34167–34171.
74. Watari, S.; Inaba, H.; Lv, Q.H.; Ichikawa, M.; Iwasaki, T.; Wang, B.; Tadakuma, H.; Kakugo, A.; Matsuura, K. Optical Control of Microtubule Accumulation and Dispersion by Tau-Derived Peptide-Fused Photoresponsive Protein. *JACS Au* **2025**, *5*, 791–801.
75. Ando, R.; Mizuno, H.; Miyawaki, A. Regulated Fast Nucleocytoplasmic Shuttling Observed by Reversible Protein Highlighting. *Science* **2004**, *306*, 1370–1373.
76. Drechsler, H.; Xu, Y.; Geyer, V.F.; Zhang, Y.; Diez, S. Multivalent Electrostatic Microtubule Interactions of Synthetic Peptides Are Sufficient to Mimic Advanced MAP-like Behavior. *Mol. Biol. Cell* **2019**, *30*, 2953–2968.
77. Inaba, H.; Kageyama, D.; Watari, S.; Tateishi, M.; Kakugo, A.; Matsuura, K. Peptide-Mediated Display of Tau-Derived Peptide for Construction of Microtubule Superstructures. *RSC Chem. Biol.* **2025**, *6*, 737–745.
78. Kleiner, R.E.; Ti, S.-C.; Kapoor, T.M. Site-Specific Chemistry on the Microtubule Polymer. *J. Am. Chem. Soc.* **2013**, *135*, 12520–12523.
79. Nihongaki, Y.; Matsubayashi, H.T.; Inoue, T. A Molecular Trap inside Microtubules Probes Luminal Access by Soluble Proteins. *Nat. Chem. Biol.* **2021**, *17*, 888–895.
80. Joshi, F.M.; Viar, G.A.; Pigino, G.; Drechsler, H.; Diez, S. Fabrication of High Aspect Ratio Gold Nanowires within the Microtubule Lumen. *Nano Lett.* **2022**, *22*, 3659–3667.

Biography

Dr. Hiroshi Inaba obtained his Ph.D. from Kyoto University in 2015. During his Ph.D., he worked as a Research Fellow of the Japan Society for the Promotion of Science (JSPS) for Young Scientists at the Institute for Integrated Cell-Material Sciences (iCeMS), Kyoto University. In 2015, he joined the Department of Chemistry at the University of Illinois Urbana-Champaign as a postdoctoral research associate. In 2016, he moved to the Department of Chemistry and Biotechnology at Tottori University as an assistant professor and was promoted to an associate professor in 2021. In 2021, he was selected as a researcher for the JST FOREST program.

Biomembrane research utilizing functional peptides: Stoichiometric analysis of oligomeric states of membrane proteins and sensing analysis of membrane curvature of extracellular vesicles

Received: May 14, 2025

Accepted: July 4, 2025

Published: October 1, 2025

Kenichi Kawano

Graduate School of Pharmaceutical Sciences, Kyoto University, Kyoto 606-8501, Japan.

e-mail: kawano.kenichi.2u@kyoto-u.ac.jp

Keywords: fluorescent / Förster resonance energy transfer; coiled-coil labeling method; membrane proteins; curvature-sensing peptides; extracellular vesicles

Abstract

This study describes two functional peptides analyzing oligomer formation of membrane proteins, and sensing extracellular vesicles (EVs) with highly curved membranes.

Many membrane proteins are responsible for signaling and ion transport, which are necessary for maintaining biological functions. The study of membrane protein oligomerization is crucial for developing new medical drugs. However, existing destructive methodologies are not suitable for precisely determining oligomeric states. In this study, a coiled-coil tag–probe labeling method was combined with spectral imaging to establish a new methodology based on fluorescent / Förster resonance energy transfer (FRET) for stoichiometric analysis of the oligomeric states of membrane proteins in living cells (in-cell FRET methodology). After validating the method for mono-, di-, and tetrameric standard membrane proteins, it was used to investigate full-length M2 proton-selective channels of the influenza A virus. We revealed that the full-length M2 proteins formed proton-conducting dimers at neutral pH and they were converted to tetramers at acidic pH, indicating that the minimal functional unit is a dimer. On the other hand, typical class-A G-protein-coupled receptors (GPCRs), which are a key class of drug targets for treating various diseases, do not form constitutive homo-oligomers, and it is not necessary for their receptor functions. Conversely, the epidermal growth factor receptor (EGFR), which is involved in the pathogenesis and progression of cancers, exhibits dynamic ligand-induced dimerization followed by autophosphorylation. These results demonstrate that our in-cell FRET methodology is a powerful tool for stoichiometrically analyzing the oligomeric states of membrane proteins in biomembranes.

EVs carry various biologically informative components, including signaling molecules, transcriptional proteins, lipids, and nucleic acids. EVs have shown great promise as pharmaco-targeting vesicles and have attracted the attention of researchers in various fields because of their importance as diagnostic and prognostic markers. However, the detection, isolation, and purification of EVs from cell-cultured media and bodily fluids remain challenging. We developed curvature-sensing peptides for the sensitive detection of EVs in cultured media and achieved rapid screening and identification of genes involved in bacterial EV production. The flexible structure of curvature-sensing peptides was revealed to be an important for binding to the lipid packing defects of curved membranes. Moreover, we successfully developed a novel methodology, an EV catch-and-release isolation system (EV-CaRiS) using a net-charge invertible curvature-sensing peptide (NIC). The NIC was designed to capture and release EVs reversibly in a pH-dependent manner. It allowed us to achieve reproducible EV isolation from three human cell lines and single-particle imaging of EVs containing the ubiquitous exosome markers CD63 and CD81. The EV-CaRiS is a simple and convenient method for EV isolation.

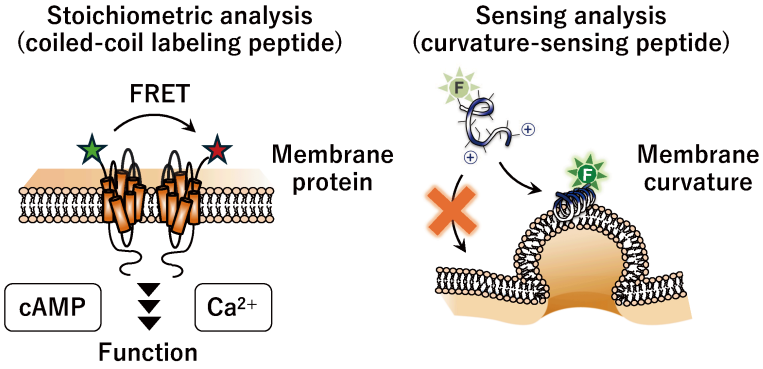

Part of the research eligible for 2024 Award for Young Investigator, The Japanese Peptide Society is described in this article.

Table 1. Functional peptides

Category	Type	Name	Sequence[a]	Net charge[b] pH 6.0	pH 7.3	pH 9.0
Coiled-coil labeling peptide	Tag	E3	EIAALEK-EIAALEK-EIAALEK-OH	−2.9	−3.0	−3.1
	Probe	K4	KIAALKE-KIAALKE-KIAALKE-KIAALKE-NH_2	+4.1	+4.0	+3.8
Curvature-sensing peptide	Unstapled EV-sensor	FAAV	GAGLLKXLNKBTDBLSKX-GSGSK-NH_2	+2.0	+2.0	+1.9
		nFAAV5	DKBLLKXLNKBTDBLSKX-GSGSK-NH_2	+2.0	+2.0	+1.9
	Stapled EV-sensor	stFAAV3	GAZLLKZLNKBTDBLSKX-GSGSK-NH_2	+2.0	+2.0	+1.9
		stFAAV9	GAGLLKXLNKBZDBLZKX-GSGSK-NH_2	+2.0	+2.0	+1.9
	pH-dependent EV-capture	NIC4	EZBLLZXLNZBTEBLSZX-GSGSC-NH_2	+0.7	−1.8	−2.0

a) The single letters of Z, X, and B indicate (*S*)-2-(4-pentenyl)alanine, norleucine, and 2-aminoisobutyric acid, respectively. Norleucine was used instead of methionine to prevent the oxidation. The C-termini of all peptides were amidated except for E3-tag. *b*) The charge of the N-terminus was not included the calculation of the peptide net charge.

Introduction

The first topic is the stoichiometric analysis of the oligomeric states of membrane proteins using a coiled-coil labeling peptide pair. The oligomeric state of membrane proteins is important for understanding their functions and for developing medical drugs because oligomer formation is proposed to allow faster signaling, specific crosstalk, or specific responses[1]. Analysis of the oligomerization of membrane proteins has traditionally relied on destructive methods, such as western blotting after cell lysis[2,3], or on non-destructive methods that involve fusing fluorescent or luminescent proteins of similar size to the target protein and measuring resonance energy transfer (FRET or BRET) in the cell[4–6]. However, conventional methods can cause conformational and functional perturbations in the membrane proteins. Fluorescent and luminescent fusion proteins sometimes have limitations in the stoichiometric analysis of membrane protein oligomerization because of difficulties in (*i*) distinguishing the noise signal of intracellular immature proteins from the true signal of membrane surface proteins, (*ii*) controlling the expression ratios of the FRET or BRET donor and acceptor, and (*iii*) avoiding the effects of steric hindrance from the fusion protein on the oligomerization and function of the target membrane protein.

To overcome these issues, we developed a novel in-cell FRET methodology[7] to precisely analyze the oligomeric state of membrane proteins based on FRET among proteins labeled using the coiled-coil tag–probe method[8] (Figure 1). This method utilizes the tight interactions between heterodimeric coiled-coil peptides, E3 tags and K4 probes (Table 1). It has the following advantages over conventional methods: (*i*) cell-surface-specific labeling because of the membrane-impermeable K4 probe binding to the E3 tag genetically introduced into the extracellular N-terminus of the target membrane proteins (Figure 1); (*ii*) precise control of the donor/acceptor labeling ratio of the target membrane protein by changing the ratio of donor and acceptor K4 probes; and (*iii*) minimal perturbation of membrane proteins because of the small size of the tag–probe peptides (approximately 5–6 kDa)[7]. Moreover, the K4 probe could rapidly label approximately 90% of the E3-tagged proteins within 1 min[8]. Commercially available Alexa Fluor 568 and 647 dyes were used as the FRET donor and acceptor, respectively, because this pair has a relatively long Förster distance of 82 Å, which is the distance between the donor and acceptor that yields 50% FRET efficiency. This enables highly sensitive detection of the oligomerization of large membrane proteins, such as GPCRs (*e.g.*, the β2-adrenergic receptor [β_2AR], which forms dimers with the size of approximately 80 Å)[9], and EGFR. We previously demonstrated that this in-cell FRET methodology enables stoichiometric analysis of the oligomeric state of membrane proteins in living cells using monomeric, dimeric, and tetrameric standard membrane proteins[7]. The observed apparent FRET efficiency (E_{app}) for the standard membrane proteins overlapped perfectly with each theoretical curve. After validating the accuracy of the

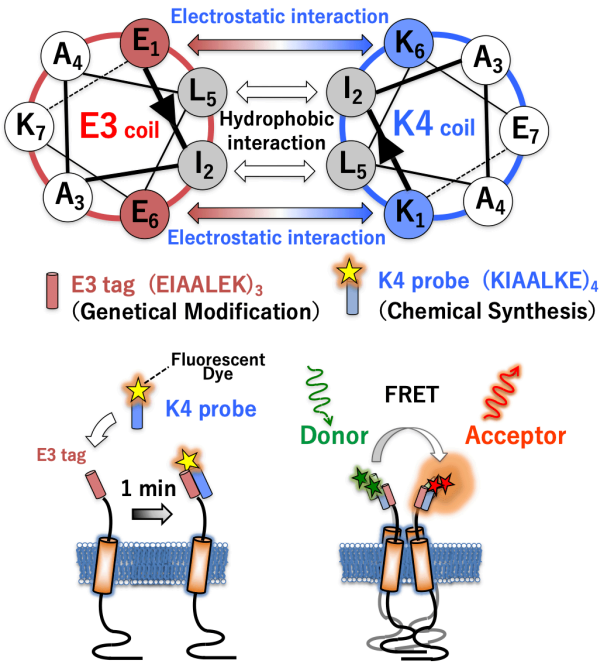

Figure 1. Schematic diagrams of the coiled-coil labeling method utilizing strong and specific interactions between the E3-tag and K4-probe, and the FRET phenomenon for stoichiometric analysis of oligomeric states of membrane proteins. The E3-tag is genetically introduced into the N-terminus of the target membrane protein, and the K4-probe, labeled with fluorescent dyes, binds to the E3-tagged protein within 1 min. If the membrane proteins form an oligomer, FRET occurs from the donor to the acceptor dye.

methodology, we applied it to the M2 proton channel of the influenza A virus, class-A GPCRs, and EGFR to investigate the relation between their oligomeric states and functions. Consequently, we found that membrane proteins in the native environments of living cells exhibited different behaviors than those of conventional models: (I) M2 exhibits a pH-dependent dimer–tetramer equilibrium state, and the minimal functional unit is the M2 dimer[10] (II) typical class-A GPCRs do not form constitutive homo-oligomers, and homo-oligomerization is not necessary for their receptor functions[7,11] and (III) EGFR exists as monomers but shows EGF-stimulation-induced dimerization followed by autophosphorylation[12].

The second topic is the sensing analysis of the membrane curvature of EVs using curvature-sensing peptides. EVs are biogenic lipidic nanoparticles secreted by both bacterial and mammalian cells and are known to be involved in cell–cell communication[13,14]. EVs from bacteria (bEVs) and small EVs from mammalian cells (sEVs or exosomes) have diameters of approximately 30–200 nm. EVs carry signaling molecules and biological information related to diverse diseases[15,16] therefore, they show great promise as sources of diagnostic and prognostic markers and as pharmaceutical targets[17–19]. However, the existing methods can still improve in terms of EV detection, isolation, and purification. It would be straightforward to measure the abundance of EVs in the presence of contaminants without purification; however, methods for detecting EVs directly in cultured media without isolating them are extremely limited. Antibody-based methods targeting specific protein markers on EVs could address this issue[15,20–22] however, they depend on the expression levels of antigens on EVs and cannot be used to detect EVs that lack these antigens because of gene modification or mutagenesis. Only a few potential protein markers are currently known in some EVs[23]. Moreover, since EVs constitute a heterogeneous population, the absence of housekeeping proteins complicates their detection. Although EV purification could provide a solution, high throughput and operational simplicity are required to process multiple samples simultaneously. For example, ultracentrifugation (UC) is a widely used strategy for isolating EVs from cell-cultured media by stepwise separation of vesicles according to their sedimentation coefficients. However, EVs isolated by UC exhibit relatively low purity because of the low selectivity and contamination with high-molecular-weight complexes[18,24]. Moreover, UC methods typically require 4–6 h or more for EV isolation, and the number of samples that can be handled simultaneously is limited, making it difficult to achieve high throughput and operational simplicity[24–26].

Therefore, to overcome these issues, we focused on highly curved membranes, which are common structures found in all EVs, and attempted to develop curvature-sensing peptides and applied them for the detection, isolation, and purification of EVs. (I) First, we screened the amphipathic helix region of the Bin/amphiphysin/Rvs (BAR)-domain family of proteins responsible for sensing membrane curvature[27]. The amino acid sequence of the peptide derived from sorting nexin 1 (SNX1), a BAR protein, was optimized based on a structure–activity correlation study to create a basal curvature-sensing peptide, FAAV (named after SNX1 with four mutations: F8L, A11B, A14B, and V15L; B = 2-aminoisobutyric acid [Aib])[28] (Table 1). FAAV has been demonstrated to successfully detect bEVs in cultured media without purification using the FRET method[29]. (II) α-Helix formation of the peptides was found to contribute to binding to the membrane surface of lipid vesicles[28,30]. A newly designed curvature-sensing peptide, N-terminus-substituted FAAV (nFAAV5) (Table 1), achieved higher sensitivity to bEVs than that of FAAV[31]. The random–α-helix transition of nFAAV5 upon binding to curved membranes was revealed to be an important factor for comprehensively binding to bEVs irrespective of the surface polysaccharides[32]. nFAAV5 has been successfully applied for the high-throughput screening of bEVs and identification of genes involved in bEV production[33]. (III) Furthermore, a net-charge invertible curvature-sensing peptide (NIC4) (Table 1), designed based on nFAAV5, allowed us to develop an EV catch-and-release isolation system (EV-CaRiS) that can reversibly capture and release EVs in a pH-dependent manner[34]. The EV-CaRiS achieved reproducible sEV isolation from three human cell lines and single-particle sEV imaging. This system is simple and convenient for isolating sEVs.

Stoichiometric analysis (I): M2 dimeric proton channel as a minimum functional unit

Contrary to the conventional model of M2 forming a stable tetramer, we found that M2 is in a pH-dependent dimer–tetramer equilibrium and forms a tetramer at acidic pH but exists as a dimer at neutral pH[10] (Figure 2A). Additionally, we found that the M2 dimer is the minimum proton-conducting unit and forms a complex with cholesterol in biomembranes, which is essential for its channel activity[10].

M2 is a single-membrane-spanning protein with 97 amino acid residues that forms a pH-dependent proton-selective channel in influenza A viruses[35] (Figure 2A). The M2 protein exhibits multiple functions essential for the virus infection process: (*i*) acidification of the virus interior (Figure 2A) in the endosome of host cells to promote the dissociation of viral nucleoproteins from the M1 matrix protein[36] (*ii*) prevention of premature conformational changes of biosynthesized hemagglutinin in host cells before virus budding[37] and (*iii*) support of virus budding and scission from host cell membranes by inducing membrane-curvature formation[38]. In the conventional model, the M2 protein is widely considered to form a tetrameric proton channel, supported by X-ray crystallography, ultraviolet resonance Raman spectroscopy, and NMR studies using fragment M2 peptides, including the transmembrane region in artificial environments[39–41], because the transmembrane region of the M2 protein functions as the core driving four-helix bundle formation for conducting protons. The antiviral drug amantadine hydrochloride (Am) binds to this transmembrane region. However, the native structure of the full-length M2 protein in biological membranes has not yet been elucidated.

We analyzed the oligomeric state of the full-length M2 protein [A/Udorn/72 virus (H3N2)] in the plasma membrane of living cells using in-cell FRET methodology and revealed their functional relevance[10]. E3-tagged M2 (E3-M2) was labeled with K4 probes at various FRET donor/acceptor ratios, and the E_{app} values at pH 4.9 perfectly overlapped with the tetrameric theoretical curves, indicating that E3-M2 forms a tetramer at acidic pH. Surprisingly, the E_{app} values at pH 7.3 overlapped with the dimeric theoretical curves, indicating that E3-M2 forms a dimer at neutral pH (Figure 2A). When the E_{app} values were plotted as a function of pH, it was revealed that E3-M2 existed as a dimer at pH > 5.5, whereas it forms a tetramer at pH 4.9. To confirm that M2 is in the dimer–tetramer equilibrium, the extracellular buffer was exchanged from pH 4.9 to 6.0 and lowered again to pH 4.9; E3-M2 exhibited interconversion between dimer and tetramer depending on external pH. We found that the driving force of M2 tetramerization arises from

the cation–π interaction between His37 and Trp41 residues in the transmembrane region (Figure 2A) because the H37A and W41A variants lost their tetramer formation ability even at pH 4.9. It is plausible that the His37 residue of one M2 protein forms a cation–π interaction with the Trp41 residue of a neighboring M2 protein, thereby stabilizing the tetrameric structure at acidic pH (Figure 2A). Although M2 has two Cys residues at the extracellular N-terminus, FRET analysis using Ala-substituted and N-terminus-truncated variants revealed that disulfide bonds are not involved in M2 tetramerization. FRET analysis using the C-terminus-truncated variant revealed that the amphipathic helix at the intracellular C-terminus of M2 is essential for M2 dimerization. Therefore, the amphipathic helix in the C-terminal region and His37 and Trp41 residues in the transmembrane region are responsible for M2 dimerization and tetramerization, respectively. In the presence of Am, M2 tetramerization was completely inhibited at pH 4.9, indicating that Am binds to the M2 dimer and prevents tetramer formation.

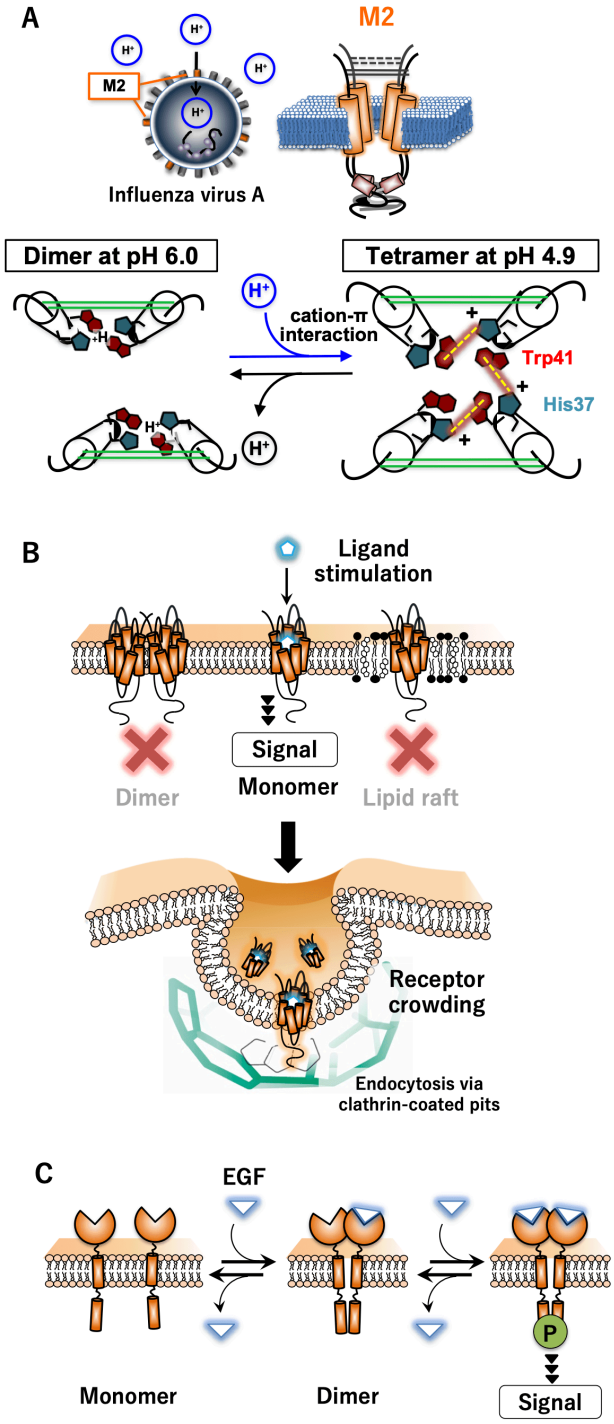

Figure 2. Schematic diagrams of (A) the pH-dependent dimer–tetramer equilibrium for the M2 channel of influenza A virus, (B) monomer as the functional unit transducing signals followed by receptor crowding in the endosome for four class-A GPCRs, and (C) ligand-induced monomer–dimer transition for EGFR in biomembranes. (A) Based on the Henderson-Hasselbalch equation, approximately 82% of His residues are protonated at pH 4.9; thus, three of four His residues (>75%) are interacting with Trp residues.

To elucidate the functional relevance of the oligomeric state, we measured the channel activity of the M2 monomer, dimer, and tetramer using a commercially available pH indicator dye, SNARF-4F[10]. If the M2 channel conducts protons inside cells, the SNARF-4F loaded into cells responds it and exhibits a pH-dependent emission spectral shift; thus, measurement of the SNARF-4F spectrum allows quantitative analysis of M2 channel activity. The extracellular buffer was changed from neutral to acidic pH; intracellular emission spectra were temporally acquired. The γ value ($s^{-1} \cdot protein^{-1}$) was used as an indicator of the channel activity normalized by the surface expression level of M2 proteins, which was determined by immunostaining. Consequently, E3-untagged and tagged M2 proteins exhibited similar levels of channel activity at pH 6.0 and 4.9, indicating that E3-tagging does not influence M2 function, and both the dimer and tetramer exhibit channel activity. Conversely, the M2 monomer (the C-terminus-truncated variant) did not show any activity, clearly demonstrating that the dimeric proton channel is the minimum functional unit of M2 proteins. We found that the removal of cholesterol from biomembranes remarkably affected dimeric channel activity but not M2 tetramerization. Alanine-scanning experiments revealed that the Ile35 residue in the transmembrane region lost its channel activity in a manner similar to cholesterol removal. It could be considered that the M2 dimeric channel forms a complex with cholesterol *via* the Ile35 residue for its channel activity. In the presence of Am, M2 channel activity was completely inhibited. Taken together with the FRET results, these findings demonstrate that Am binds to the M2 dimer and prevents both tetramer formation and channel activity. The present methodology, based on protein structural information, provides a new approach for elucidating the mechanisms of adamantane-based drugs and developing novel drugs with different modes of action.

Stoichiometric analysis (II): class-A GPCR oligomerization not required for their functional activities

We revealed that class-A GPCRs do not constitutively form homo-oligomers and that the monomers transduce second messenger signals upon agonist stimulation. Some receptors show high FRET signals, but this is due to receptor concentration in the endosome after stimulation[7,11] (Figure 2B).

GPCRs have six classes (A–F) and are seven membrane-spanning proteins coupled with heterotrimeric G-proteins for signal transduction. Class-A forms the largest group, accounting for 85% of GPCRs[42]. Most class-A GPCRs have 310–470 amino acid residues, consisting of a relatively short N-terminus and long C-terminal tail[43]. These proteins may represent some of the most important target proteins for medical drug discovery. Two decades ago, more than 30% of marketed clinical drugs

were active against this protein family[44]. While many drugs targeting GPCRs have been developed for different indications, including cardiovascular, metabolic, neurodegenerative, psychiatric, and oncological diseases, only limited exploration of structure-based drug design has been possible owing to the restricted structural information on GPCRs. Advances in scientific technology have made it possible to obtain the X-ray crystal structure of β_2AR[45], which is one of the typical class-A GPCRs; this breakthrough could accelerate the acquisition of structural information on GPCRs and facilitate the drug discovery process. However, the complicated signal transduction mechanism is regulated not only by the conformational change of a single receptor but also by dynamic oligomerization between receptors in the biomembrane. Because existing approaches have several limitations in precisely determining the oligomeric states of membrane proteins in the native environments of living cells, the acquisition of structural information remains challenging. For example, inconsistent results with BRET have been reported for the oligomeric state of β_2AR, resulting in marked controversy regarding whether oligomerization of β_2AR is required for signaling in living cells, as discussed previously[7].

Therefore, we extended our in-cell FRET methodology to stoichiometric analysis of four class-A GPCRs: β_2AR, C-X-C chemokine receptor (CXCR4), dopamine receptor D2 short isotype (D2R), and prostaglandin E receptor subtype 1 (EP1R). To confirm that E3-tagging does not deteriorate receptor functions, we prepared E3-tagged and untagged GPCRs to measure cyclic AMP responses for β_2AR and Ca^{2+} responses for CXCR4, D2R, and EP1R upon agonist treatment. The E3-β_2AR exhibited dose–response sigmoidal curves upon agonist stimulation and similar EC_{50} values to those in a previous report[46]. E3-CXCR4, E3-D2R, and E3-EP1R showed rapid Ca^{2+} responses as downstream signaling immediately following stimulation by their respective agonists, with response timing identical to that of the untagged GPCRs. These results demonstrated that E3-tagging does not affect receptor signaling. Subsequently, we measured FRET signals. These four E3-GPCRs displayed E_{app} values corresponding to the monomeric standard protein, with and without antagonist stimulation, indicating that they existed as monomers under these conditions. Conversely, E3-β_2AR, E3-CXCR4, and E3-EP1R showed a slight increase in E_{app} values upon agonist stimulation. To confirm whether the increase in the E_{app} values for these three receptors was related to receptor signal transduction, we measured the time-courses of cyclic AMP / Ca^{2+} responses and E_{app} values upon stimulation with each agonist. Consequently, increases in cyclic AMP / Ca^{2+} responses were observed before those in the E_{app} values, and increases in the E_{app} values occurred at the same time as receptor internalization, indicating that these GPCRs transduce signaling as monomers and that the increases in the E_{app} values are due to receptor crowding in the endosomes and are unrelated to signaling (Figure 2B). The removal of cholesterol did not influence the E_{app} values, presumably indicating that the increase in E_{app} values did not result from receptor clustering driven by a raft-like domain (Figure 2B). We conclude that oligomerization is not essential for receptor activation, at least for these four typical class-A GPCRs. Although considerable debates on class-A GPCR oligomerization are exemplified nowhere better than in β_2AR, the difference in these conclusions could be due to methodological precision.

Stoichiometric analysis (III): EGFR monomer–dimer transition triggered by ligand stimulation

We found that the majority of EGFRs exist as monomers without ligand stimulation and that approximately 10% of the population forms an inactive dimer (predimer), whereas over 60% of EGFR is converted to active dimers preceding autophosphorylation upon ligand stimulation, with the remainder persisting as monomers[12] (Figure 2C).

EGFR is a single-membrane-spanning glycoprotein with 1,186 amino acid residues[47], consisting of a large extracellular ligand-binding domain, transmembrane domain, tyrosine kinase domain, and tyrosine-containing C-terminal tail. EGFR ligands, including EGF and transforming growth factor-α, promote receptor activation[47], followed by cell differentiation, proliferation, and other physiological activities[48]. EGFR is overexpressed in certain cancer tissues, making it an important target for anticancer therapy[49]. Although its X-ray crystallographic structure has been determined[50], dynamic structural information on EGFRs in cell membranes is limited. The actual behavior upon ligand stimulation is more complex than that described by the conventional model, in which a simple transition from unliganded inactive monomers to liganded active dimers occurs. The relevance of EGFR oligomerization and activation remains controversial owing to a lack of quantitative analytical methods[12].

In this study, we used our in-cell FRET methodology to examine the relation between the oligomeric states of EGFRs and their autophosphorylation levels to elucidate the activation mechanism. Before FRET measurements, we confirmed that the E3-tagging and K4-labeling do not affect EGFR functions. EGF-induced autophosphorylation of E3-tagged EGFR in the absence of K4 probes was detected in a ligand concentration-dependent manner by western and dot blotting. Similar autophosphorylation levels were observed in EGF-stimulated E3-EGFR cells in the absence and presence of K4 probes. FRET analysis revealed that, in the absence of EGF, the E_{app} value for E3-EGFR was similar to or slightly higher than that for the monomeric standard protein, indicating that approximately 10% of E3-EGFR exists as an inactive dimer. In the presence of EGF, the E_{app} value for E3-EGFR was intermediate between those of the monomeric and dimeric standard proteins. To precisely estimate the monomer-to-dimer ratio, we used another FRET pair (tetramethylrhodamine and Cy5) with a relatively short Förster distance of 53 Å[51] and re-analyzed the FRET signals. Approximately 66% of E3-EGFRs formed dimers, and the remaining receptors still existed as monomers, even in the presence of EGF at a sufficient concentration. Time-course experiments revealed that EGFR dimerization preceded autophosphorylation. Upon EGF stimulation, the FRET signal immediately increased and reached a plateau level within 20 s; conversely, autophosphorylation exhibited a relatively slow response and required 90 s to reach a plateau. Interestingly, EGFR dimerization (EC_{50}: 1 nM) and autophosphorylation (EC_{50}: 8 nM) showed different sensitivities to EGF concentration. In conclusion, we propose a model in which EGF stimulation promotes EGFR dimerization and that single-EGF-occupied dimers may have low autophosphorylation activity, whereas double-EGF-occupied dimers have high autophosphorylation activity (Figure 2C). We excluded the involvement of functional modulators of EGFR, such as cholesterol and ganglioside GM3, in EGFR dimerization because the E_{app} values did not vary for E3-EGFR upon compactin (cholesterol depletion) and neuraminidase (GM3 degradation) treatments.

EV-sensing analysis (I): prototypic EV-sensor development and function assay

We created an initial curvature-sensing peptide, FAAV, as a prototype for EV sensors[28] (Table 1). FAAV selectively bound to bEVs, even in the presence of bacterial cells[29] (Figure 3A). We successfully developed a bEV detection method in cultured media by utilizing the FRET phenomenon in combination with FAAV-NBD and a membrane stain, FM4–64[29].

To create EV-sensing peptides, we focused on the well-studied BAR domain family, which functions as curvature-recognizing proteins. It was reported that 70 or more types of BAR proteins have been identified in various subcellular organelles and individually have characteristic amphipathic α-helix structures involved in the recognition of different curvatures[52]. Therefore, peptides derived from the amphipathic regions of BAR domain proteins have the potential to be superior membrane curvature sensors. Peptide-based curvature sensors are suitable for various biological research applications because they are small, easy to modify, and amenable to largescale production. We selected various amino acid sequences from the candidate peptides[28], which were derived from the amphipathic regions of each phylogenetic group of the BAR domain family. The side chains of the C-terminal lysine of the candidate peptides were labeled with 4-fluoro-7-nitrobenzofurazan (NBD), a hydrophobic environment-sensitive dye. The increase in the fluorescence intensity of the NBD dye was used as an indicator to evaluate the binding of the peptide to curved membranes. To investigate the curvature-sensing ability of the peptides, we prepared two types of liposomes with the same lipid composition but different diameters (50 and 120 nm) and examined whether they could distinguish between these slightly different particle sizes. The peptide derived from SNX1 was found to have high curvature-sensing ability among the 11 candidates at the initial screening. Moreover, the SNX1 peptide showed high α-helicity in the presence of liposomes, indicating that a highly α-helix-forming peptide could have strong binding ability to curved membranes. Hence, we performed a structure–activity correlation study by introducing mutations into the amino acid sequence of SNX1 and clearly demonstrated that improvement in α-helix formation is closely correlated with increased vesicle binding. Based on this correlation study, we created an initial curvature-sensing peptide, FAAV-NBD[28] (SNX1 with four mutations: F8L, A11B, A14B, and V15L; B = Aib) (Table 1), which is expected to be a promising EV sensor prototype.

To demonstrate the applicability of FAAV in detecting bEVs, *Shewanella vesiculosa* HM13 was selected as a model of biogenic secretory vesicles[53]. The HM13 strain is a gram-negative bacterium useful for studying bEVs because it produces large amounts of bEVs compared with those of other bacterial strains[53]. bEVs range in diameter from 30 to 100 nm and contain a single major cargo protein, P49. We showed that FAAV-NBD selectively binds to bEVs without separation from bEV-secretory cells, whereas it does not respond to bacterial cells, even at a 12-fold higher lipid content than that of bEVs[29]. This is because FAAV-NBD preferentially binds to curved membranes with rich lipid-packing defects, such as those of bEVs, but not to flat membranes with few defects, such as bacterial cells (Figure 3A). Furthermore, FAAV-NBD could fully detect bEVs within 5 min of peptide addition to the cultured media, and the presence of the cargo protein P49 had no effect on bEV binding by FAAV-NBD. This peptide has protease resistance against trypsin and proteinase K in the presence of bEVs for at least 1 h, owing to the introduction of the non-standard amino acid, Aib into the FAAV sequence, enabling FAAV-NBD to be used for long-term monitoring of changes in bEV levels. The amount of secreted bEVs varied from 45 to 70 μM in lipid concentration when bacterial cells were cultured in a 96-well plate. In the presence of bacterial cells, although FAAV-NBD

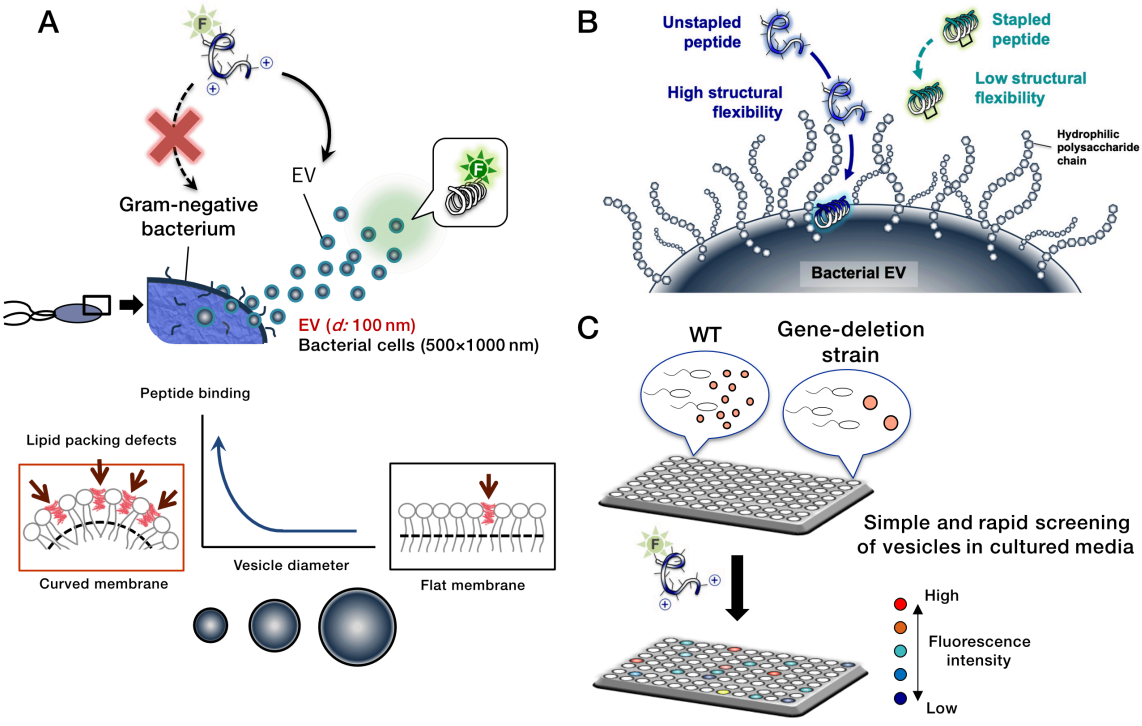

Figure 3. Schematic diagrams of (A) the curvature-sensing peptide selectively binding to bEVs but not to bEV-secretory cells; (B) the molecular mechanism by which the curvature-sensing peptide approaches the membrane surface of bEVs covered by hydrophilic polysaccharides; and (C) a simple and rapid screening system for bEVs in cultured media using the curvature-sensing peptide.

alone was able to response to the changes in the bEV amount, there was required to achieve the bEV detection with high sensitivity. Therefore, we adapted the FRET phenomenon to further improve sensitivity, using FAAV-NBD and FM4–64 as FRET donor and acceptor, respectively. Because FM4–64 staining is proportional to the bEV amount, it was assumed that the FRET signal would be highly sensitive to changes in the bEV amount due to the synergistic effect of FAAV-NBD and FM4–64. The FRET signal increased remarkably in proportion to small changes in the bEV amount. This study demonstrated the potential applicability of FAAV for bEV detection in cultured media using the FRET method without a bEV purification step[29].

EV-sensing analysis (II): simple and rapid screening system of EVs in cultured media

We designed the N-terminus-substituted peptide FAAV (nFAAV5-NBD) (Table 1), which has superior binding affinity for bEVs and detects changes in EV amount with a five-fold higher sensitivity than that of FAAV-NBD, even in the presence of bEV-secretory cells. This is because nFAAV5 forms a more stable α-helix structure than FAAV upon binding to vesicles[31]. Although the surfaces of bEVs are covered with polysaccharides, nFAAV5-NBD can easily approach the membrane surface. We found that the random coil–to–α-helix transition of nFAAV5 upon vesicle binding is an important factor for highly efficient detection of bEVs without being affected by polysaccharides[32] (Figure 3B). Using this nFAAV5-NBD, we achieved simple and rapid screening of bEVs from over 10,000 strains with random transposon mutations and identified genes involved in the hyper- and hypo-vesiculation production of bEVs[33] (Figure 3C).

Developing a simple and rapid detection system for bEVs in cultured media, including EV-secretory cells, is important for the comprehensive analysis of bEVs. The purpose of this study was to develop a quick, practical, and easy-to-use approach for detecting bEVs using an EV-sensing peptide in cultured media. To achieve this goal, it was necessary to design a novel curvature-sensing peptide with higher sensitivity than that of FAAV. α-Helix formation of the peptides was found to contribute to binding to the curved membrane of lipid nanovesicles[28,30]. We focused on the Gly-Ala-Gly sequence at the N-terminus of FAAV (Table 1), which presumably does not contribute to α-helix formation. The nFAAV5, with an α-helix-inducing amino acid sequence, Asp-Lys-Aib, was newly designed (Table 1). Asp at the N-terminus has been reported to induce α-helix formation in peptides *via* end-capping effects[54], whereby the side chains can form hydrogen bonds with the free NH group at the N-terminus and contribute to α-helix stabilization. Lys was used in the nFAAV5 sequence to maintain the same net charge as that of FAAV (+2) (Table 1). Aib, with its restricted side chain, contributed to facilitating α-helix formation[28]. Similar to FAAV-NBD, nFAAV5-NBD selectively binds to bEVs but not to bacterial cells[31]. In the presence of bacterial cells, nFAAV5-NBD exhibited a 15.2-fold higher relative fluorescence intensity when the EV amount was increased 16-fold, which was a five-fold higher sensitivity than that of FAAV-NBD, demonstrating that nFAAV5-NBD enables highly sensitive detection of bEVs in cultured media.

Subsequently, we adapted stapling to the sequence of FAAV by restricting its structure through intramolecular cross-linking, which afforded high α-helicity to the peptides, under the assumption that α-helix formation is important for the peptide to bind to vesicles. Stapling is one of the most promising and frequently employed strategies for improving peptide binding affinity for target molecules. Whereas nFAAV5 exhibited a random coil structure in the absence of liposomes, the representative stapled FAAV peptides (stFAAV3 and stFAAV9) listed in Table 1 showed high α-helicity[32], meaning that stFAAV3 and stFAAV9 adopt α-helical structures in solution. Although the surfaces of bEVs are covered with two types of polysaccharides[55,56], liposomes have a smooth surface. Contrary to our expectation, the stapled peptides with rigid α-helical structures showed lower binding affinities for bEVs than for liposomes. Conversely, the unstapled peptides (FAAV and nFAAV5) with flexible structures showed similar binding affinities for bEVs and liposomes regardless of surface conditions. In the bEV binding assay, the stapled peptides required 30 min to reach a plateau, whereas the unstapled peptides completely bound to bEVs within 5 min after addition. These results suggested that increased structural rigidity due to stapling makes it difficult for peptides to approach the membrane surface of bEVs covered with polysaccharide chains (Figure 3B). To prove this hypothesis, we defined a flexibility indicator as the ratio of α-helix contents of the peptides at 222 nm with and without liposomes. For example, flexibility indicators were arranged in the order of nFAAV5, stFAAV3, and stFAAV9, as shown in Table 2, indicating that the most flexible peptide was nFAAV5. Conversely, stFAAV9 showed less conformational change than nFAAV5 before and after liposome binding. To elucidate the binding mechanism, we estimated the number of peptides bound to the membrane surface per particle ($N_{peptide}$/bEV) according to a previous study[57], based on FRET between the FRET donor BODIPY FL-labeled 1,2-dilauroyl-*sn*-glycero-3-phosphorylethanolamine and acceptor Texas Red (TXR)-labeled curvature-sensing peptides. We found that the $N_{peptide}$/bEV values calculated based on the FRET method correlated with the flexibility indicators (Table 2), demonstrating that the peptide with a flexible structure easily approaches the membrane surface of bEVs, even when covered with polysaccharide chains. Collectively, these results indicate that the structural flexibility of curvature-sensing peptides is a governing factor in their comprehensive binding to vesicles under different surface conditions[32].

Finally, we demonstrated the utility of this novel EV screening method using nFAAV5-NBD to identify genes related to bEV production[33] (Figure 3C). The molecular mechanisms underlying bEV biogenesis have not been fully elucidated. Here, we extended nFAAV5-NBD to screen for bEVs secreted by *Shewanella vesiculosa* HM13[53]. More than 10,000 strains with random transposon mutations were prepared. If a gene inserted *via* random transposon mutagenesis is involved in bEV production, the strain should show differential bEV productivity. The strain can be readily identified by measuring NBD fluorescence intensity, which reflects bEV productivity in the cultured medium. The genes involved in bEV production

Table 2. Relationship between flexibility indicators and the number of the peptides accumulated on the bEVs ($N_{peptide}$/bEV)

Peptide	Flexibility indicator	$N_{peptide}$/bEV
nFAAV5-TXR	5.1	1308
stFAAV3-TXR	1.8	1005
stFAAV9-TXR	0.9	900

The C-terminal lysine of EV-sensors was labeled with TXR.

can be predicted by identifying the transposon insertion sites of the strain using inverse and single-primer PCR methods. We identified 16 and six genes related to hyper- and hypo-vesiculation transposon mutants, respectively[33]. Although further research is required to investigate how these genes are involved in bEV production at the molecular level, model screening using nFAAV5-NBD was successfully performed.

EV-sensing analysis (III): EV-CaRiS

We established a novel method for isolating sEVs, named EV-CaRiS (Figure 4A), which achieved reversible capture and release of sEVs in a pH-dependent manner using NIC4[34] (Table 1). EV-CaRiS allowed us to reproducibly isolate sEVs from three human cell lines within 1.5 h and visualize the catch-and-release of sEVs using single-particle imaging with anti-sEV biomarker antibodies on glass (Figure 4B). This system was demonstrated to be a simple and convenient method for isolating sEVs.

The subtypes of EVs released from mammalian cells can be classified as follows: exosomes with a relatively small and homogeneous diameter of 50 to 200 nm (also known as sEVs); microvesicles with a larger and heterogeneous size of 150 to 1,500 nm; other vesicle types, including apoptotic bodies with diameters of 100 to 2,000 nm released by cells undergoing apoptosis; blood-derived vesicles with diameters of 130 to 500 nm released upon platelet activation; and autophagosomes[13,14]. sEVs commonly exhibit high membrane curvature; however, the expression levels of biomarkers vary depending on the cell line and culture conditions. Novel sEV isolation methods are rapidly evolving owing to the efforts of various research groups. Nonetheless, achieving a balance between versatility and simplicity remains challenging because of the high cost and complexity of equipment used. Although UC methods are widely employed for sEV isolation, no gold standard has yet been developed that enables researchers to reproducibly isolate EVs by a simple method, in a short time, using standard laboratory equipment.

The concept of this research was to develop a novel sEV isolation method that combines versatility and simplicity in a way not previously demonstrated. To achieve this goal, we proposed a new methodology, EV-CaRiS, using the net-charge invertible curvature-sensing peptide, NIC4[34]. NIC4 was designed based on the sequence of nFAAV5 to enable pH-dependent control of sEV capture and release. NIC4 has a net positive charge (+0.7) at weakly acidic pH, allowing it to bind negatively charged sEVs through electrostatic interactions, whereas it converts to a net negative charge (– 2.0) at weakly basic pH, enabling dissociation from sEVs *via* electrostatic repulsion (Table 1) (Figure 4A). Similar to nFAAV5, NIC4 recognizes vesicles by binding to lipid-packing defects on highly curved membranes through hydrophobic interactions, regardless of biomarker expression levels. We coupled NIC4 onto agarose resins and used a batch method to isolate sEVs. sEVs are lipid nanoparticles with negatively charged lipids and highly curved membranes. To evaluate the properties of EV-CaRiS, a model liposome mimicking sEVs was prepared. This system captured 80% of the liposomes at pH 6 and released 70% of the captured liposomes when the buffer was replaced at pH 9. No liposomal membrane destruction was observed. Liposomes with a diameter of 200 nm or less, corresponding to the size of sEVs, were recovered. EV-CaRiS recovered both liposomes with and without negatively charged lipids. This is because NIC4 adopts an amphiphilic structure, and both electrostatic and hydrophobic interactions act as binding forces between NIC4 and the liposomes. Subsequently, we used EV-CaRiS to isolate sEVs from the cultured media of three human cell lines. EV-CaRiS achieved three-fold higher sEV isolation, in terms of particle number, with high purity, in one-third of the time required for conventional UC methods. The isolated EVs exhibited intrinsic immunomodulatory and anticancer activities against macrophages and cancer cells, respectively. This system showed high reproducibility, and the same NIC-coupled resin was used repeatedly for EV isolation at least five times[34]. Single-particle analysis of the catch-and-release of sEVs was visualized by labeling stereotypical exosome marker proteins, CD63 and CD81, with antibodies using total internal reflection fluorescence microscopy (Figure 4B). The fluorescent bright spots of Alexa 647-conjugated anti-

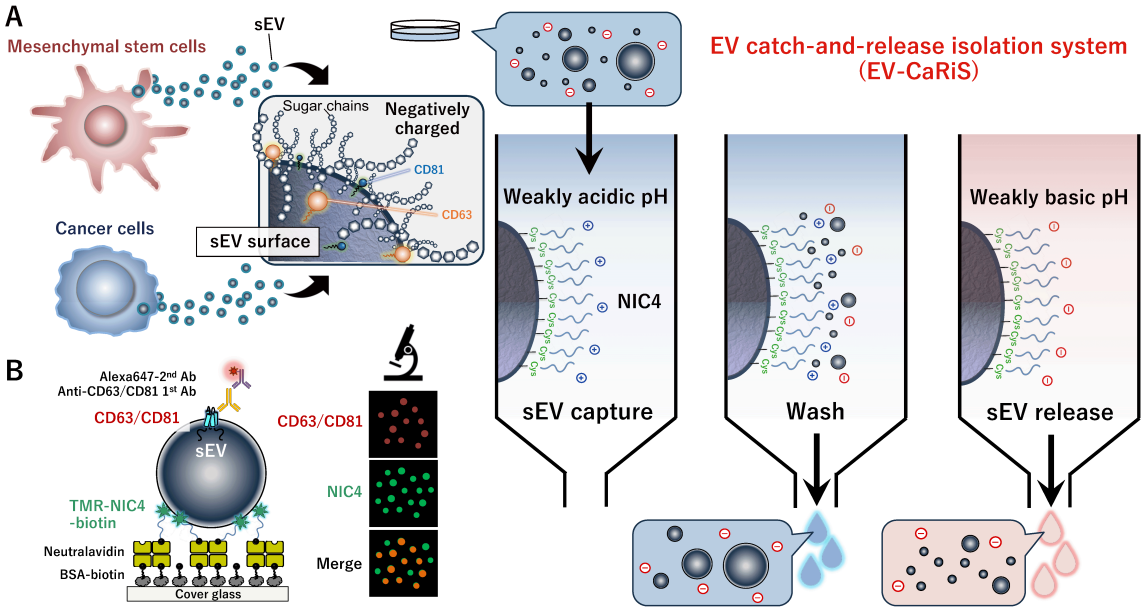

Figure 4. Schematic diagrams of (A) EV-CaRiS for sEV isolation and (B) for single-particle imaging, using a net-charge invertible curvature-sensing peptide. (A) sEVs in media are captured by NIC4 immobilized on a resin at weakly acidic pH, whereas larger EVs are washed out. The sEVs are then released from NIC4 at weakly basic pH. (B) The biomarkers CD63 and CD81 on sEVs are colocalized with NIC4 on glass.

bodies recognizing CD63 or CD81 colocalized with those of tetramethylrhodamine (TMR)-conjugated NIC4 immobilized on glass at pH 6, but not at pH 9 (Figure 4B). Upon treatment with Triton X-100 at pH 6, the fluorescent bright spots of Alexa 647-conjugated antibodies disappeared from the NIC4 spots, demonstrating that NIC4 captured biogenetic lipid nanoparticles secreted from living cells[34].

Overall, these results indicate that EV-CaRiS using NIC4 is a promising system for the isolation and single-particle observation of sEVs. The greatest advantage of this method is that anyone can easily isolate and purify sEVs at any time using only reagents and materials available in general laboratories, without the need for specialized equipment, including an ultracentrifuge. This methodology can be applied to the construction of a high-throughput sEV isolation system using a purification column and an efficient analysis system for sEV content using a microwell array chip in future work. We envision expanding this research to analyze bEVs derived from microorganisms and viral particles.

Conclusion

In the present study, we used two types of functional peptides for biomembrane research. The coiled-coil labeling of the E3–K4 peptide pair was combined with the FRET method to achieve stoichiometric analysis of the oligomeric states of membrane proteins in living cells. Using in-cell FRET methodology, we revealed the pH-dependent dimer–tetramer equilibrium for the M2 channel of influenza A viruses, monomer as a functional core transducing signals followed by receptor crowding in the endosome for four class-A GPCRs, and ligand-induced monomer–dimer transition for EGFR in the biomembrane. The in-cell FRET methodology holds potential for developing novel medical drugs based on structural information of membrane proteins. The curvature-sensing peptides enabled high-throughput screening of bEVs in cultured media without purification from EV-secretory cells and identification of genes involved in the hyper- and hypo-vesiculation of bEVs. This simple and rapid screening system for bEVs can also be applied to other bacterial species. EV-CaRiS, using a net-charge invertible curvature-sensing peptide, was demonstrated to be a simple and convenient sEV isolation system and useful for single-particle imaging of sEVs. EV-CaRiS offers potential for developing a high-throughput sEV isolation system and an efficient analysis platform for sEV content.

Acknowledgments

The author acknowledges Dr. Katsumi Matsuzaki (Kyoto University), Dr. Shiroh Futaki (Kyoto University), and Dr. Yoshiaki Yano (Mukogawa Women's University) for their direction to these works. The author sincerely thanks Dr. Tatsuo Kurihara (Kyoto University), Dr. Jun Kawamoto (Kyoto University), Dr. Fumiaki Yokoyama (University of Tokyo), Dr. Kouhei Kamasaka (Kobe University), Mr. Hiromu Inoue, Mr. Hirotaka Yamashita, Mr. Yuki Kuzuma, and Mr. Masaya Ogushi for their significant contributions to the present works. The authors thank Dr. Shinya Oishi (Kyoto Pharmaceutical University) and Dr. Nobutaka Fujii (Kyoto University), Dr. Ikuhiko Nakase (Osaka Metropolitan University), Dr. Shin-ya Morita (Shiga University of Medical Science Hospital) for their valuable technical advice. These researches were supported in part by the Takeda Science Foundation (K.K.), the ICR Grants for Promoting Integrated Research, Kyoto University (K.K.), the Chubei Itoh Foundation (K.K.), and JSPS KAKENHI (21K15254) (K.K.).

Conflict of Interest

The author declares no conflict of interest in this study.

References

1. Bockaert, J.; Pin, J. P., Molecular tinkering of G protein-coupled receptors: an evolutionary success. *EMBO J.* **1999**, *18* (7), 1723–1729.
2. Jordan, B. A.; Devi, L. A., G-protein-coupled receptor heterodimerization modulates receptor function. *Nature* **1999**, *399* (6737), 697–700.
3. Michineau, S.; Alhenc-Gelas, F.; Rajerison, R. M., Human bradykinin B2 receptor sialylation and N-glycosylation participate with disulfide bonding in surface receptor dimerization. *Biochemistry* **2006**, *45* (8), 2699–2707.
4. Angers, S.; Salahpour, A.; Joly, E.; Hilairet, S.; Chelsky, D.; Dennis, M.; Bouvier, M., Detection of beta 2-adrenergic receptor dimerization in living cells using bioluminescence resonance energy transfer (BRET). *Proc. Natl. Acad. Sci. USA* **2000**, *97* (7), 3684–3689.
5. Mercier, J. F.; Salahpour, A.; Angers, S.; Breit, A.; Bouvier, M., Quantitative assessment of beta 1- and beta 2-adrenergic receptor homo- and heterodimerization by bioluminescence resonance energy transfer. *J. Biol. Chem.* **2002**, *277* (47), 44925–44931.
6. James, J. R.; Oliveira, M. I.; Carmo, A. M.; Iaboni, A.; Davis, S. J., A rigorous experimental framework for detecting protein oligomerization using bioluminescence resonance energy transfer. *Nat. Methods* **2006**, *3* (12), 1001–1006.
7. Kawano, K.; Yano, Y.; Omae, K.; Matsuzaki, S.; Matsuzaki, K., Stoichiometric analysis of oligomerization of membrane proteins on living cells using coiled-coil labeling and spectral imaging. *Anal. Chem.* **2013**, *85* (6), 3454–3461.
8. Yano, Y.; Yano, A.; Oishi, S.; Sugimoto, Y.; Tsujimoto, G.; Fujii, N.; Matsuzaki, K., Coiled-coil tag–probe system for quick labeling of membrane receptors in living cell. *ACS Chem. Biol.* **2008**, *3* (6), 341–345.
9. Fung, J. J.; Deupi, X.; Pardo, L.; Yao, X. J.; Velez-Ruiz, G. A.; Devree, B. T.; Sunahara, R. K.; Kobilka, B. K., Ligand-regulated oligomerization of beta(2)-adrenoceptors in a model lipid bilayer. *EMBO J.* **2009**, *28* (21), 3315–3328.
10. Kawano, K.; Yano, Y.; Matsuzaki, K., A dimer is the minimal proton-conducting unit of the influenza a virus M2 channel. *J. Mol. Biol.* **2014**, *426* (14), 2679–2691.
11. Kawano, K.; Yagi, T.; Fukada, N.; Yano, Y.; Matsuzaki, K., Stoichiometric analysis of oligomeric states of three class-A GPCRs, chemokine-CXCR4, dopamine-D2, and prostaglandin-EP1 receptors, on living cells. *J. Pept. Sci.* **2017**, *23* (7–8), 650–658.
12. Yamashita, H.; Yano, Y.; Kawano, K.; Matsuzaki, K., Oligomerization-function relationship of EGFR on living cells detected by the coiled-coil labeling and FRET microscopy. *Biochim. Biophys. Acta.* **2015**, *1848* (6), 1359–1366.
13. Schwechheimer, C.; Kuehn, M. J., Outer-membrane vesicles from Gram-negative bacteria: biogenesis and functions. *Nat. Rev. Microbiol.* **2015**, *13* (10), 605–619.
14. Mathieu, M.; Martin-Jaular, L.; Lavieu, G.; Thery, C., Specificities of secretion and uptake of exosomes and other extracellular vesicles for cell-to-cell communication. *Nat. Cell Biol.* **2019**, *21* (1), 9–17.
15. Pegtel, D. M.; Cosmopoulos, K.; Thorley-Lawson, D. A.; van Eijndhoven, M. A.; Hopmans, E. S.; Lindenberg, J. L.; de Gruijl, T. D.; Wurdinger, T.; Middeldorp, J. M., Functional

delivery of viral miRNAs *via* exosomes. *Proc. Natl. Acad. Sci. USA* **2010**, *107* (14), 6328–6333.
16. Record, M.; Carayon, K.; Poirot, M.; Silvente-Poirot, S., Exosomes as new vesicular lipid transporters involved in cell-cell communication and various pathophysiologies. *Biochim. Biophys. Acta.* **2014**, *1841* (1), 108–120.
17. S, E. L. A.; Mager, I.; Breakefield, X. O.; Wood, M. J., Extracellular vesicles: biology and emerging therapeutic opportunities. *Nat. Rev. Drug Discov.* **2013**, *12* (5), 347–357.
18. Xu, R.; Greening, D. W.; Zhu, H. J.; Takahashi, N.; Simpson, R. J., Extracellular vesicle isolation and characterization: toward clinical application. *J. Clin. Invest.* **2016**, *126* (4), 1152–1162.
19. Jeppesen, D. K.; Zhang, Q.; Franklin, J. L.; Coffey, R. J., Extracellular vesicles and nanoparticles: emerging complexities. *Trends Cell Biol.* **2023**, *33* (8), 667–681.
20. Lo, T. W.; Zhu, Z.; Purcell, E.; Watza, D.; Wang, J.; Kang, Y. T.; Jolly, S.; Nagrath, D.; Nagrath, S., Microfluidic device for high-throughput affinity-based isolation of extracellular vesicles. *Lab. Chip* **2020**, *20* (10), 1762–1770.
21. Orozco, A. F.; Lewis, D. E., Flow cytometric analysis of circulating microparticles in plasma. *Cytometry A* **2010**, *77* (6), 502–514.
22. Jorgensen, M.; Baek, R.; Pedersen, S.; Sondergaard, E. K.; Kristensen, S. R.; Varming, K., Extracellular Vesicle (EV) Array: microarray capturing of exosomes and other extracellular vesicles for multiplexed phenotyping. *J. Extracell. Vesicles* **2013**, *2*, 20920.
23. Hong, J.; Dauros-Singorenko, P.; Whitcombe, A.; Payne, L.; Blenkiron, C.; Phillips, A.; Swift, S., Analysis of the Escherichia coli extracellular vesicle proteome identifies markers of purity and culture conditions. *J. Extracell. Vesicles* **2019**, *8* (1), 1632099.
24. Konoshenko, M. Y.; Lekchnov, E. A.; Vlassov, A. V.; Laktionov, P. P., Isolation of extracellular vesicles: general methodologies and latest trends. *Biomed. Res. Int.* **2018**, *2018*, 8545347.
25. Xu, R.; Greening, D. W.; Rai, A.; Ji, H.; Simpson, R. J., Highly-purified exosomes and shed microvesicles isolated from the human colon cancer cell line LIM1863 by sequential centrifugal ultrafiltration are biochemically and functionally distinct. *Methods* **2015**, *87*, 11–25.
26. Mathieu, M.; Nevo, N.; Jouve, M.; Valenzuela, J. I.; Maurin, M.; Verweij, F. J.; Palmulli, R.; Lankar, D.; Dingli, F.; Loew, D.; Rubinstein, E.; Boncompain, G.; Perez, F.; Thery, C., Specificities of exosome versus small ectosome secretion revealed by live intracellular tracking of CD63 and CD9. *Nat. Commun.* **2021**, *12* (1), 4389.
27. Habermann, B., The BAR-domain family of proteins: a case of bending and binding? *EMBO Rep.* **2004**, *5* (3), 250–255.
28. Kawano, K.; Ogushi, M.; Masuda, T.; Futaki, S., Development of a membrane curvature-sensing peptide based on a structure-activity correlation study. *Chem. Pharm. Bull. (Tokyo)* **2019**, *67* (10), 1131–1138.
29. Kawano, K.; Yokoyama, F.; Kawamoto, J.; Ogawa, T.; Kurihara, T.; Futaki, S., Development of a simple and rapid method for in situ vesicle detection in cultured media. *J. Mol. Biol.* **2020**, *432* (22), 5876–5888.
30. Groves, J. T., The physical chemistry of membrane curvature. *Nat. Chem. Biol.* **2009**, *5* (11), 783–784.
31. Kawano, K.; Yokoyama, F.; Kamasaka, K.; Kawamoto, J.; Ogawa, T.; Kurihara, T.; Futaki, S., Design of the n-terminus substituted curvature-sensing peptides that exhibit highly sensitive detection ability of bacterial extracellular vesicles. *Chem. Pharm. Bull. (Tokyo)* **2021**, *69* (11), 1075–1082.
32. Kawano, K.; Kamasaka, K.; Yokoyama, F.; Kawamoto, J.; Ogawa, T.; Kurihara, T.; Matsuzaki, K., Structural factors governing binding of curvature-sensing peptides to bacterial extracellular vesicles covered with hydrophilic polysaccharide chains. *Biophys. Chem.* **2023**, *299*, 107039.
33. Inoue, H.; Kawano, K.; Kawamoto, J.; Ogawa, T.; Kurihara, T., Rapid screening and identification of genes involved in bacterial extracellular membrane vesicle production using a curvature-sensing peptide. *J. Bacteriol. (in press)* **2025**, e0049724.
34. Kawano, K.; Kuzuma, Y.; Yoshio, K.; Hosokawa, K.; Oosugi, Y.; Fujiwara, T.; Yokoyama, F.; Matsuzaki, K., Extracellular-vesicle catch-and-release isolation system using a net-charge invertible curvature-sensing peptide. *Anal. Chem.* **2024**, *96* (9), 3754–3762.
35. Pinto, L. H.; Holsinger, L. J.; Lamb, R. A., Influenza virus M2 protein has ion channel activity. *Cell* **1992**, *69* (3), 517–528.
36. Helenius, A., Unpacking the incoming influenza virus. *Cell* **1992**, *69* (4), 577–578.
37. Maeda, Y.; Ide, T.; Koike, M.; Uchiyama, Y.; Kinoshita, T., GPHR is a novel anion channel critical for acidification and functions of the Golgi apparatus. *Nat. Cell Biol.* **2008**, *10* (10), 1135–1145.
38. Schmidt, N. W.; Mishra, A.; Wang, J.; DeGrado, W. F.; Wong, G. C., Influenza virus A M2 protein generates negative Gaussian membrane curvature necessary for budding and scission. *J. Am. Chem. Soc.* **2013**, *135* (37), 13710–13719.
39. Stouffer, A. L.; Acharya, R.; Salom, D.; Levine, A. S.; Di Costanzo, L.; Soto, C. S.; Tereshko, V.; Nanda, V.; Stayrook, S.; DeGrado, W. F., Structural basis for the function and inhibition of an influenza virus proton channel. *Nature* **2008**, *451* (7178), 596–599.
40. Schnell, J. R.; Chou, J. J., Structure and mechanism of the M2 proton channel of influenza A virus. *Nature* **2008**, *451* (7178), 591–595.
41. Okada, A.; Miura, T.; Takeuchi, H., Protonation of histidine and histidine-tryptophan interaction in the activation of the M2 ion channel from influenza a virus. *Biochemistry* **2001**, *40* (20), 6053–6060.
42. Wingert, B.; Doruker, P.; Bahar, I., Activation and Speciation Mechanisms in Class A GPCRs. *J. Mol. Biol.* **2022**, *434* (17), 167690.
43. Mirzadegan, T.; Benko, G.; Filipek, S.; Palczewski, K., Sequence analyses of G-protein-coupled receptors: similarities to rhodopsin. Biochemistry 2003, 42 (10), 2759-2767.
44. Wise, A.; Gearing, K.; Rees, S., Target validation of G-protein coupled receptors. *Drug Discov. Today* **2002**, *7* (4), 235–246.
45. Rasmussen, S. G.; DeVree, B. T.; Zou, Y.; Kruse, A. C.; Chung, K. Y.; Kobilka, T. S.; Thian, F. S.; Chae, P. S.; Pardon, E.; Calinski, D.; Mathiesen, J. M.; Shah, S. T.; Lyons, J. A.; Caffrey, M.; Gellman, S. H.; Steyaert, J.; Skiniotis, G.; Weis, W. I.; Sunahara, R. K.; Kobilka, B. K., Crystal structure of the beta2 adrenergic receptor-Gs protein complex. *Nature* **2011**, *477* (7366), 549–555.
46. Elster, L.; Elling, C.; Heding, A., Bioluminescence resonance energy transfer as a screening assay: Focus on partial and inverse agonism. *J. Biomol. Screen* **2007**, *12* (1), 41–49.

47. Ogiso, H.; Ishitani, R.; Nureki, O.; Fukai, S.; Yamanaka, M.; Kim, J. H.; Saito, K.; Sakamoto, A.; Inoue, M.; Shirouzu, M.; Yokoyama, S., Crystal structure of the complex of human epidermal growth factor and receptor extracellular domains. *Cell* **2002**, *110* (6), 775–787.
48. Sakaguchi, K.; Okabayashi, Y.; Kido, Y.; Kimura, S.; Matsumura, Y.; Inushima, K.; Kasuga, M., Shc phosphotyrosine-binding domain dominantly interacts with epidermal growth factor receptors and mediates Ras activation in intact cells. *Mol. Endocrinol.* **1998**, *12* (4), 536–543.
49. Okamoto, I., Epidermal growth factor receptor in relation to tumor development: EGFR-targeted anticancer therapy. *FEBS J.* **2010**, *277* (2), 309–315.
50. Ferguson, K. M.; Berger, M. B.; Mendrola, J. M.; Cho, H. S.; Leahy, D. J.; Lemmon, M. A., EGF activates its receptor by removing interactions that autoinhibit ectodomain dimerization. *Mol. Cell* **2003**, *11* (2), 507–517.
51. Ha, T.; Ting, A. Y.; Liang, J.; Caldwell, W. B.; Deniz, A. A.; Chemla, D. S.; Schultz, P. G.; Weiss, S., Single-molecule fluorescence spectroscopy of enzyme conformational dynamics and cleavage mechanism. *Proc. Natl. Acad. Sci. USA* **1999**, *96* (3), 893–898.
52. Simunovic, M.; Voth, G. A.; Callan-Jones, A.; Bassereau, P., When physics takes over: bar proteins and membrane curvature. *Trends Cell Biol.* **2015**, *25* (12), 780–792.
53. Chen, C.; Kawamoto, J.; Kawai, S.; Tame, A.; Kato, C.; Imai, T.; Kurihara, T., Isolation of a novel bacterial strain capable of producing abundant extracellular membrane vesicles carrying a single major cargo protein and analysis of its transport mechanism. *Front Microbiol.* **2019**, *10*, 3001.
54. Forood, B.; Feliciano, E. J.; Nambiar, K. P., Stabilization of alpha-helical structures in short peptides *via* end capping. *Proc. Natl. Acad. Sci. USA* **1993**, *90* (3), 838–842.
55. Di Guida, R.; Casillo, A.; Yokoyama, F.; Kawamoto, J.; Kurihara, T.; Corsaro, M. M., Detailed structural characterization of the lipooligosaccharide from the extracellular membrane vesicles of Shewanella vesiculosa HM13. *Mar. Drugs* **2020**, *18* (5), 231.
56. Casillo, A.; Di Guida, R.; Cavasso, D.; Stellavato, A.; Rai, D.; Yokoyama, F.; Kamasaka, K.; Kawamoto, J.; Kurihara, T.; Schiraldi, C.; Kulkarni, S.; Paduano, L.; Corsaro, M. M., Polysaccharide corona: The acetyl-rich envelope wraps the extracellular membrane vesicles and the cells of Shewanella vesiculosa providing adhesiveness. *Carbohydr. Polym.* **2022**, *297*, 120036.
57. Kaji, T.; Yano, Y.; Matsuzaki, K., In-cell FRET indicates magainin peptide induced permeabilization of bacterial cell membranes at lower peptide-to-lipid ratios relevant to liposomal studies. *ACS Infect. Dis.* **2021**, *7* (10), 2941–2945.

Biography

Dr. Kenichi Kawano was born in Hei-longjiang, China in 1985 and has lived in Okayama, Japan since 1991. He received his Bachelor's degree from Okayama University in 2009. He obtained his Ph.D. in Pharmacy from Kyoto University in 2014 under the direction of Professor Katsumi Matsuzaki. In 2014, he became a Project Assistant Professor in Professor Matsuzaki's group at Kyoto University. After a 6-month postdoctoral fellowship in Professor Akihiro Kusumi's group at Kyoto University, he was appointed Assistant Professor in Professor Shiroh Futaki's group at Kyoto University in 2016. Since 2021, he has served as Assistant Professor in Professor Matsuzaki's group. He will be promoted to Associate Professor at Graduate School of Biomedical and Health Sciences, Hiroshima University, in October 2025. He has received the Pharmaceutical Society of Japan Kinki-Branch Award for Young Scientists (2014), the Japan Peptide Society Award for Young Scientists (2024), and the Membrane Society of Japan Award for Young Scientists (2025). His research interests include peptides interacting with biomembranes, based on biophysical chemistry, medicinal chemistry, and chemical biology.

The 29th American Peptide Symposium and the 15th International Peptide Symposium 参加報告

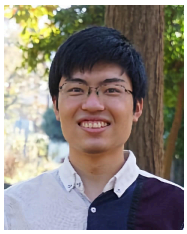

新城（永原）紳吾
しんじょう（ながはら）・しんご

東京農工大学 連合農学研究院
fv0940@go.tuat.ac.jp
https://web.tuat.ac.jp/~bio-org/index.html

東京農工大学生物有機化学研究室（北野克和先生・岡田洋平先生）所属、産学官連携研究員の新城（永原）紳吾と申します。この度、日本ペプチド学会の Travel Award のご支援を賜り、カリフォルニア州サンディエゴにて開催された the 29th American Peptide Symposium and the 15th International Peptide Symposium（6 月 15 日㈰から 19 日㈭の 5 日間）に参加してポスター発表を行いました。以下、現地での出来事や感じたことを記します。

1. 現地までの移動

6 月 15 日㈰、岡田先生、安達創太さん（D3）とともに成田空港を発ち、学会初日のお昼過ぎにサンディエゴ国際空港に到着しました。入国審査では、学会に参加することを伝えると“Peptide?”と尋ねられ、参加者が続々と入国していることがうかがえました。無事に審査を通過した後は、無料シャトルバスに乗り込み、学会会場兼宿泊地である Sheraton San Diego Hotel & Marina まで移動しました（写真 1（上））。リゾートホテルということで、部屋の目の前にはプールがあり（写真 1（下））、日中は宿泊客でにぎわっていました。また、現地は気温が 20 度前後で湿度は低めと、気温も湿度も高まる東京と比べて過ごしやすい気候でした。

写真 1. ホテル周辺の景色（上）、部屋の窓からの景色（下）

2. 学会期間中の食事

2 日目以降、ホテルで朝食としてベーグルやクロワッサン、フルーツと飲み物が準備されていました（写真 2（上））。ポスターセッション前には昼食も提供され、2 日目はタコス、4 日目はブリトーやサンドイッチを堪能しました（写真 2（下））。

最終日のバンケットを除き、夕食は各々で調達することになっていたので、Uber taxi でダウンタウンまで食べに出かけました。メキシコ料理店が多くありましたが、イタリア

写真 2. 会場での朝食（上）と昼食（下）

ンや日本食レストランもありました。どのお店で食べるにしても、日本の2倍近く費用がかかりましたが、ボリューム満点で美味しかったです。アルコールが飲めずアイスティーばかり飲んでいる傍ら、岡田先生と安達さんが美味しそうにビールを飲んでいるのは少しうらやましかったです。

3. 口頭発表

2日目と4日目の12時半から14時までのポスターセッションを除き、5日間にわたって口頭発表が行われました。28th APSに参加した時と比較して発表時間を守ることが強く求められており、質疑応答が全くない発表があったり、途中で打ち切られてしまう発表があったりしました。また、数百人が入る広いホールでの発表だったので、全体に伝わるように解像度の高い画像を使ったり、文字サイズを大きくしたりとスライド作りには工夫が必要だなと感じました。

4. ポスター発表

食事会場と同じ場所で開催され、建物の壁に沿ってポスターが並び、活発な議論が行われていました。私は、“Electrochemical Peptide Synthesis Applicable to Sterically Hindered Amino Acids Enabled by Electron-Rich Triaryl Phosphine”というタイトルで発表しました（写真3）。当研究室ではトリアリールホスフィンをリサイクル可能な縮合剤として用いる電気化学的液相ペプチド合成法の開発に取り組み、従来のペプチド合成法において大量の廃棄物が排出される課題の解決を目指しています。今回は、*N*-メチルアミノ酸をはじめとした嵩高いアミノ酸にも適用できる合成系の構築に成功したことについて発表しました。1時間半で約10人の参加者とディスカッションを行い、中にはあらかじめ論文を読んでから発表を聞きに来てくれた人や、発表を通じて論文に興味を持ってくれた人がいて嬉しかったです。決して流暢な英語ではありませんが、自分の研究内容を伝え、相手の求める回答がそれなりにできたと思います。

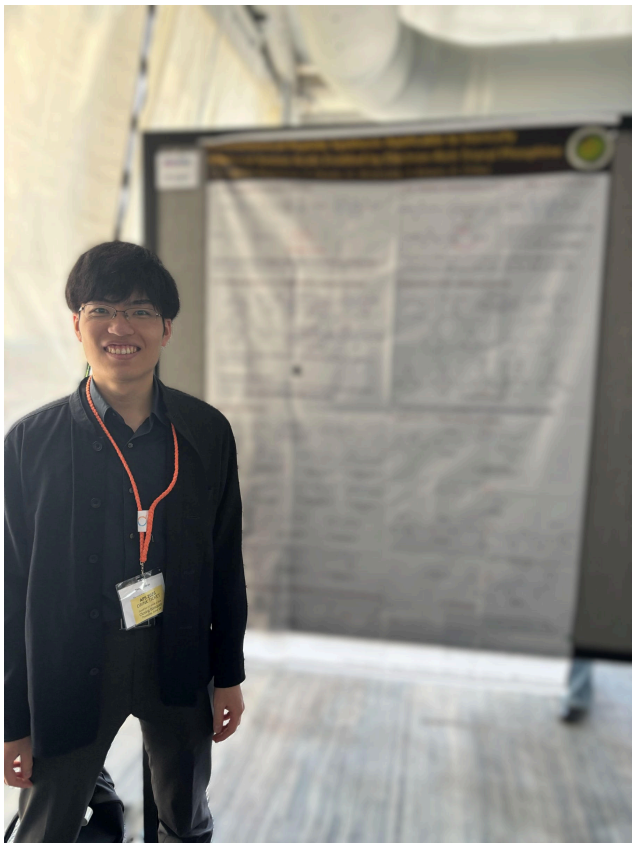

写真3. ポスター発表

5. 聴講や発表を通じて感じたこと

英語でのコミュニケーションは日本人参加者にとって大きな壁となることが多いと思いますが、発表練習さえ十分にしていれば、そこまで身構えなくてもよいと思います。参加者の3、4割程度は英語を第二言語としている印象で、それぞれ母国語の発音の癖を感じさせる話し方をしていました。日本人の英語のレベルが特別低いわけではないと思うので、参加するチャンスがあればぜひチャレンジしてみてください。

また、ペプチド液相合成法の知名度の低さを痛感しました。発表に登場するペプチドのほとんどは固相上で合成されており、サステナビリティに関するセッションでも液相合成法が話題の中心に上がることはありませんでした。自分たちとしては、液相合成法に大きな可能性を感じているだけに、歯がゆい思いをしました。液相合成法の良さをどれだけ広められるかは自分達次第ということで、アピールを続けようと決意を新たにしました。学会、論文等で積極的に発信するつもりなので、読者の皆様にも興味を持っていただけると幸いです。

写真4. San Ysidro周辺の景色（上）とメキシコとの国境（下）

6. サンディエゴ観光

3 日目が午前中で終了するスケジュールとなっていたため、午後は岡田先生、安達さんと観光を楽しみました。まず、路面電車に乗ってアメリカとメキシコの国境がある San Ysidro に向かいました。電車を降りると、英語以外の言語（おそらくスペイン語）が多く聞こえ、海から離れたこともあって宿泊地とは異なる雰囲気がありました（写真4（上））。案内に従って 5 分ほど歩いたところで、メキシコとの国境に到達しました（写真 4（下））。国境を渡っていく人を見ながら、門を通過した先は異国、というのは普段島国で生活している身としては不思議な気分でした。その後、門から引き返して散策し、たまたま見つけたハンバーガー屋に入りました。サンディエゴではありえない 3 ドルという価格でフライドチキンのハンバーガーを食べ、路面電車に乗って Old Town へと移動しました。

Old Town はサンディエゴの有名な観光地の一つで、歴史的背景からメキシコとアメリカの文化が入り混じった地域となっています。土産物屋や飲食店が点在しており、観光客でにぎわっていました。私たちは友人への誕生日プレゼントや家族へのお土産を買い、最後にメキシコ料理屋で夕食をとりました（写真 5）。ここでも液相ペプチド合成法の開発、論文化を頑張っていこうという話で盛り上がりました。

7. 学会での交流

会場は貴重な交流の場にもなり、Opening Reception ではミャンマー出身でアメリカの大学院に在籍している学生と相席しました。母国の情勢が落ち着かないため、博士号取得後も母国に帰らず、アメリカで職を探す予定だ、という話は学会中で最も印象に残ったことの 1 つです。

また、朝食や昼食、バンケットの際には日本からの参加者とお話する機会にも恵まれ、情報交換することができました。国外に出ると、初対面でも同郷であれば話しかけるハードルが下がり、新たな繋がりが生まれやすいのも国際学会ならではの良さではないかと思いました。現地でお世話になった皆様にはこの場を借りて御礼申し上げます。

8. 最後に

本学会参加を通して、ペプチド化学の最先端研究を学ぶだけでなく、様々な参加者と交流したり、現地の文化の一端に触れたりすることができました。参加を検討している皆様には、文章や写真を通じて APS 参加のイメージが少しでも伝われば幸いです。

写真 5. メキシコ料理屋にて（左から安達さん、岡田先生、筆者）

未筆になりますが、ペプチド学会の役員および Travel Award 選考委員の先生方、本誌 Essay の執筆機会を与えていただいた編集委員会の先生方に深く御礼申し上げます。

利益相反

利益相反はありません。

第 62 回ペプチド討論会のご案内
～ようこそ福岡へ～

伊東 祐二
いとう・ゆうじ

鹿児島大学 大学院理工学研究科
yito@sci.kagoshima-u.ac.jp

野瀬 健
のせ・たける

九州大学
nose@artsci.kyushu-u.ac.jp

松島 綾美
まつしま・あやみ

九州大学
ayami@chem.kyushu-univ.jp

第 62 回ペプチド討論会を、2025 年 10 月 21 日から 23 日の日程で、福岡市の福岡国際会議場にて開催させていただくことになりました世話人の、伊東祐二（鹿児島大学）、野瀬健（九州大学）、松島綾美（九州大学）です。多くの皆様のご参加をお待ちしております。

ご存知のように福岡市は、古くからも交易で栄え、産業や物流の拠点となってきました。人口も九州で最大の都市であり、近代化された街づくりや交通網によって、非常に活気が溢れ、多くの観光客によって年中賑わいを見せている観光都市でもあります。玄海灘からの美味しい海産物をはじめ、多くの質の高い食材によって作り出される料理を堪能できる街であり、夜には多くの屋台での食事文化も楽しめます。

さて、会場となります、福岡国際会議場は、福岡県福岡市博多区石城町という博多港内のベイサイドプレイス博多埠頭の近くに位置し、隣接する福岡国際センターと共に大きな学会でもよく使われてきた会場ですので、多くの方がご存じかと思います。最寄りの JR 博多駅は、福岡空港から地下鉄で 5 分であり、新幹線も直結しております。会場へは、この JR 博多駅からタクシーで 10 分足らずの距離ですが、地下鉄、バスでも 25 分以内で来ることも可能です（詳細は、https://www.marinemesse.or.jp/congress/faq/ にて）。この会議場の 3 階に位置するメインホール（1000 名収容）にて、討論会を開催し、2 階に位置する多目的ホールにて、ポスター発表とブース展示を行います。また、展示ブースは、最大 26 枠を予定し、昼食時には、ランチョンセミナーも開催いたします。懇親会ですが、国際会議場の 2 階から直結する福岡サンパレスホテルのパレスルームにて、10 月 22 日 ㈫ の夜に開催する予定です。

今回は、海外から、5 名の招待講演者に来ていただけることになりました。順不同でご紹介させていただきますと、Professor Mohammed Akhter Hossain（メルボルン大学、オーストラリア）、Associate Professor Christian W. Gruber（ウィーン医科大学、オーストリア）、Professor Paolo Rovero（フィレンツェ大学、イタリア）、Professor Anna Maria Papini（フィレンツェ大学、イタリア）、Professor Ines Neundorf（ケルン大学、ドイツ）の 5 名の先生方です。いずれの先生方もアクティブに研究を進めておられますので、大変講演が楽しみです。また、先生方は会期中を通して参加されますので、積極的な交流をお願いします。また、例年来ていただいている韓国 KPS からは、Professor Jiwon Seo（光州科学技術院）、Professor Yongju Kim（高麗大学校）に、参加・発表していただける予定です。また、日本ペプチド学会賞受賞講演では、林良雄教授（東京薬科大学）が「ペプチド化学を基盤とした創薬と化学修飾技術の革新」の演題で発表されます。さらに、日本ペプチド学会奨励賞受賞講演として、佐藤浩平助教（静岡大学）、辻耕平准教授（東京科学大学）のご講演も予定されています。発表数としては、若手口頭発表 33 件、一般講演と招待講演および受賞講演を含めた口頭発表は 27 件、ポスター発表は 169 件を予定しています。

討論会終了後の 10 月 25 日 ㈯ 13:30～16:30 には、九州大学医学部百年講堂（九州大学馬出キャンパス、福岡市東区馬出 3 丁目 1 番 1 号）にて、「ペプチドの世界へようこそ！ ―未来を変える分子からキャリア形成まで―」というテーマで、一般、高校生を対象にした日本ペプチド学会主催による市民フォーラムを開催いたします。本学会会長の大高章教授（徳島大学）をはじめ、アカデミアからは、鎌田瑠泉教授（長崎大学）、松島綾美教授（九州大学）、産業界からは、岡田浩幸博士（第一三共株式会社）にご講演いただきます。お時間の許す方は、是非、市民フォーラムにもご参加ください。

討論会の準備や運営にあたり、ご協力いただきました実行委員の先生方に心より感謝いたします。特に巣山慶太郎助教（九州大学）には、準備当初から会場の予約・設営にご協力いただき、田中正一教授（長崎大学）、鎌田瑠泉教授（長崎大学）、薬師寺文華教授（長崎大学）には、プログラムの策定・審査委員リストの作成などに、ご尽力いただきました。ペプチド学会事務局の宮嶋令子様ならびに森川和憲様には、事務処理全般、討論会ホームページの作成、演題登録など多岐にわたりサポートいただきました。この場をお借りして、心よりお礼申し上げます。また、限られた時間の中、若手口頭発表、ポスター発表の審査にご協力いただきます先生方にも、心より感謝申し上げます。

最後になりますが、本討論会の開催にあたり、本会の趣旨にご賛同いただき、多くの企業・財団から出展、協賛、ご寄附、要旨集広告等にお申込みいただきましたこと、厚くお礼申し上げます。本討論会は、共催として、日本化学会、日本薬学会、日本生化学会、日本蛋白質科学会に、また後援として、日本ケミカルバイオロジー学会、日本農芸化学会、有機合成化学協会、日本抗体学会にご協力いただきました。改めて深く感謝申し上げます。

Announcement of the 62nd Japanese Peptide Symposium — Welcome to Fukuoka

Yuji Ito

Kagoshima University
yito@sci.kagoshima-u.ac.jp

Takeru Nose

Kyushu University
nose@artsci.kyushu-u.ac.jp

Ayami Matsushima

Kyushu University
ayami@chem.kyushu-univ.jp

It is our great pleasure to announce that the 62nd Japanese Peptide Symposium will be held from October 21 to 23, 2025, at the Fukuoka International Congress Center in Fukuoka City. We, the organizers Yuji Ito (Professor, Kagoshima University), Takeru Nose (Professor, Kyushu University), and Ayami Matsushima (Professor, Kyushu University), warmly welcome your participation.

Fukuoka City has historically flourished as a hub for trade and logistics. As the largest city in Kyushu, it is renowned for its modern urban planning, advanced transportation networks, vibrant energy, and year-round popularity as a tourist destination. Visitors can enjoy exceptional cuisine featuring fresh seafood from the Genkai Sea, complemented by high-quality local ingredients, and experience the unique dining culture at numerous evening food stalls.

The symposium will take place at the Fukuoka International Congress Center, located near the Bayside Place Hakata Wharf in Sekijo-machi, Hakata-ku, Fukuoka. Many of you may already be familiar with this venue, often used alongside the adjacent Fukuoka International Center for large-scale academic conferences. The nearest railway station, JR Hakata, is accessible by subway from Fukuoka Airport in just 5 minutes and is directly connected to the Shinkansen network. From Hakata station, the venue can be reached within 10 minutes by taxi or approximately within 25 minutes by subway or bus (details at https://www.marinemesse.or.jp/eng/congress/faq/).

The main hall on the 3rd floor of the Congress Center (capacity: 1,000 people) will host the symposium, while poster presentations and exhibition booths will be set up in the multipurpose hall on the 2nd floor. Up to 26 exhibition booths are planned, and luncheon seminars will also be held. The reception is scheduled for the evening of Tuesday, October 22, at the Palace Room of the adjacent Fukuoka Sun Palace Hotel.

We are delighted to welcome five distinguished international speakers: Professor Mohammed Akhter Hossain (University of Melbourne, Australia), Associate Professor Christian W. Gruber (Medical University of Vienna, Austria), Professor Paolo Rovero (University of Florence, Italy), Professor Anna Maria Papini (University of Florence, Italy), and Professor Ines Neundorf (University of Cologne, Germany). These experts are highly active in their fields, and their talks promise to be exceptionally insightful. We encourage active interaction, as the speakers will participate throughout the entire symposium.

Additionally, from the Korean Peptide Society (KPS), we will welcome Professor Jiwon Seo (Gwangju Institute of Science and Technology) and Professor Yongju Kim (Korea University). Furthermore, we look forward to the Japanese Peptide Society Award lecture by Professor Yoshio Hayashi (Tokyo University of Pharmacy and Life Sciences), titled "Innovative drug discovery and chemical modification technologies based on peptide chemistry." We also have lectures by recipients of Young Investigator Award, Assistant Professor Kohei Sato (Shizuoka University) and Associate Professor Kohei Tsuji (Institute of Science Tokyo). The conference will include 33 oral presentations by young researchers, 27 oral presentations encompassing general, invited, and award lectures, and approximately 169 poster presentations.

Following the symposium, a public forum entitled "Welcome to the World of Peptides! – Molecules Changing the Future and Shaping Careers" will be held on Saturday, October 25, from 13:30 to 16:30 at Centennial Hall Kyushu University School of Medicine, (Maidashi Campus, 3-1-1 Maidashi, Higashi-ku, Fukuoka). Organized by the Japanese Peptide Society, this forum aims at general audiences and high school students, featuring talks by President Akira Otaka (Tokushima University), Professor Rui Kamada (Nagasaki University), Professor Ayami Matsushima (Kyushu University), and Dr. Hiroyuki Okada (Daiichi Sankyo Co., Ltd.). We encourage your participation if your schedule allows.

We sincerely thank all committee members who supported the preparation and management of this symposium. Special thanks to Assistant Professor Keitaro Suyama (Kyushu University) for venue arrangements, and Professor Masakazu Tanaka (Nagasaki University), Professor Rui Kamada (Nagasaki University) and Professor Fumika Yakushiji (Nagasaki University) for program preparation and reviewer coordination. We also deeply appreciate the extensive administrative support provided by Ms. Reiko Miyajima and Mr. Kazunori Morikawa from the Peptide Society Secretariat, who handled various tasks including website creation and abstract submissions. We also extend our gratitude to all reviewers involved in evaluating presentations.

Finally, we would like to express profound appreciation to numerous companies and foundations that supported this symposium through exhibitions, sponsorships, donations, and advertisements. This event is co-hosted by the Chemical Society of Japan, the Pharmaceutical Society of Japan, the Japanese Biochemical Society, and the Protein Science Society of Japan, and supported by the Japanese Society for Chemical Biology, the Japan Society for Bioscience, Biotechnology, and Agrochemistry, the Society of Synthetic Organic Chemistry, and the Antibody Society of Japan. Once again, our heartfelt thanks.

第 57 回若手ペプチド夏の勉強会開催報告

傳田 将也
でんだ・まさや

徳島大学 医歯薬学研究部
denda.masaya@tokushima-u.ac.jp
https://www.tokushima-u.ac.jp/ph/faculty/labo/syn/

猪熊 翼
いのくま・つばさ

徳島大学 医歯薬学研究部
tinokuma@tokushima-u.ac.jp
https://www.tokushima-u.ac.jp/ph/faculty/labo/org/

第 57 回若手ペプチド夏の勉強会が、兵庫県三木市にある三木ホースランドパーク エオの森研修センターで、8 月 3 日（日）から 8 月 5 日（火）にかけて開催されました。本勉強会は、傳田将也（徳島大学医歯薬学研究部）、猪熊翼（同大学医歯薬学研究部）が世話人となり、徳島大学 大高研究室の 11 名の学生スタッフと共に企画・運営致しました。徳島大学のスタッフで開催する勉強会であったため、可能であれば徳島もしくは四国での開催を目指しましたが、会場確保が困難であったため兵庫県三木市で開催致しました。北は北海道、南は九州から 39 団体、150 名の学生、教員、研究者、企業人の方々にご参加頂き、盛況のうちに会を終了することができました（写真 1）。なお、本会開催にあたり、日本ペプチド学会から運営費の一部をご支援頂くとともに、日本薬学会中国四国支部及び科研費学術変革領域研究（A）「新興硫黄生物学が拓く生命原理変革 ～硫黄生物学～」のご共催と Chem-Station のご協賛を頂きました。さらに、中辻創智社、加藤記念バイオサイエンス振興財団、サントリー生命科学財団から学会開催助成金をご援助頂くとともに、合計 14 社の企業様よりご協賛をいただきました。この場を借りて、関係者の皆様方に心より感謝申し上げます。

本会のプログラムとしては、多様な研究分野で活躍する研究者 10 名を講師としてお招きし、特別講演 4 件、依頼講演 5 件、留学体験記講演 1 件を行って頂きました。特別講演を行って頂いた、大高章先生（徳島大学、日本ペプチド学会会長）「たかがペプチド、されどペプチド、ペプチドに教えられた 40 年」、山西芳裕先生（名古屋大学）「生命情報と化学情報を活用した AI 創薬」、小松徹先生（東京大学）「ペプチドの代謝活性を 1 分子レベルで見て疾患を知る ～血液中 1 分子酵素活性計測に基づく膵臓がん早期診断技術の開発～」、片桐豊雅先生（国立研究開発法人医薬基盤・健康・栄養研究所）「副作用のない「がんペプチド創薬」～新たな概念に基づいたがん創薬への挑戦～」、依頼講演を行って頂いた、金本和也先生（東京科学大学）「N 末端選択的なアゾメチンイリド発生が拓くペプチドのピンポイント修飾」、外山喬士先生（東北大学）「生体内セレン輸送系のハッキングとエンジニアリング」、森本淳平先生（東京大学）「ペプチドの構造と受動的膜透過性の相関の理解」、山田雄二先生（東京薬科大学）「万能接着剤をめざして：細胞が“惚れる”ペプチド設計」、大洞光司先生（大阪大学）「ポリペプチドによる金属ポルフィリノイドの機能発現」、留学体験記についてご講演頂いた、牛丸理一郎先生（九州大学）「テキサスでの留学体験」に厚く御礼申し上げます。いずれのご講演も、先生方の最先端研究に関してご講演頂くだけでなく、本勉強会の趣旨に則して若手研究者への熱いメッセージ（研究人生で忘れらない体験や失敗談）を盛り込んでいただき、通常の学会とは異なる貴重なお話を拝聴することができました（写真 2）。参加者の非常に高い関心は、休憩時間も惜しんで講

写真 1

演者の先生方に質問や相談をする姿から伺うことができました。

招待講演に加え、学生を中心とした一般講演 14 件、ポスター発表 73 件も行い、いずれの発表でも白熱した議論が展開されておりました。さらに昨年度に続き同演題でのポスター発表を 8 月 3 日、4 日の二日間実施した結果、特に学生同士のより密なディスカッションが行われ、若手ペプチド勉強会特有の「交流の場」が提供出来たのではないかと世話人一同考えております。

また本勉強会では、学生参加者の研究意欲向上を指向し、優秀な一般講演・ポスター発表に対して「一般講演優秀発表賞」「ポスター発表優秀賞」、優れたアイディアに基づいた研究に対する「一般講演チャレンジング賞」「ポスター発表チャレンジング賞」、特に活発な質疑・討論を行った学生に対する「ベストディスカッション賞」とユーモアのある研究室紹介を行ったグループに対する「研究室紹介優秀賞」を設定し、計 24 件の賞を進呈致しました。受賞者多数のため、各賞の受賞者は本勉強会ホームページ（https://sites.google.com/view/wakatepeptide57）をご参照頂けたらと思います。学生の参加者にとって、当該受賞が研究の励みになれば幸いです。

昨年度に続き合宿形式での開催となり、活発な交流が行える勉強会を提供できるか世話人・スタッフ一同心配しておりましたが、研究の話、人生相談、たわいもない話などが盛り上がり、これぞ夏の勉強会という場面が多くみられる勉強会を作り上げることができたのではないかと考えております。本勉強会を通して、若手研究者が交流を深め、今後の研究活動を更に発展させるための一助になりましたら幸いです。改めまして、本勉強会にご参加頂きました皆様に感謝申し上げるとともに、本勉強会開催にご尽力頂きました徳島大学 大高研究室の学生の皆様にも厚く御礼申し上げます。

来年度の第 58 回若手ペプチド夏の勉強会は、東京薬科大学の山田雄二先生が世話人となり、計画、準備を進めておられますので、多数の方にご参加頂けたらと思います。今後も本勉強会が若手ペプチド研究者の交流の場となり、皆様の研究発展の一助になればと考えております。末筆ながら、次回以降も本勉強会への変わらぬご支援、ご協力の程、何卒宜しくお願い申し上げます。

写真 2

第 27 回ペプチドフォーラム 開催報告

伊東 祐二
いとう・ゆうじ

鹿児島大学 大学院理工学研究科
yito@sci.kagoshima-u.ac.jp

吉矢 拓
よしや・たく

ペプチド研究所
t.yoshiya@peptide.co.jp

第 27 回ペプチドフォーラムは、日本ペプチド学会のご支援のもと、2025 年 6 月 28 日に鹿児島大学・郡元キャンパスにて開催されました。ペプチドフォーラムとしては、コロナ禍の影響もあり、鳥取大学 松浦先生のお世話で 2019 年に鳥取大学にて開催されて以来の開催となりました。

本フォーラムでは「ペプチドの相互作用を活かした科学とその応用」と題して、幅広い分野の最先端で活躍する 5

写真 1. 講演中の会場の様子

写真 2. 講演者の先生方

名の先生方を講師としてお招きし講演を依頼しました。また、若手研究者2名にも発表をお願いしました。ご講演くださった秋葉宏樹先生（京都大学）「ペプチドデザインによるバイパラトピック抗体の機能制御」、相馬洋平先生（和歌山県立医科大学）「アミロイドペプチドの相互作用をつくる・壊す・活かす」、松島綾美先生（九州大学）「女性ホルモンが誘起する痛み関連神経ペプチド遺伝子の転写」、中馬吉郎先生（新潟大学）「抗体模倣分子を用いた疾患関連脱リン酸化酵素阻害剤の開発」、中瀬生彦先生（大阪公立大学）「膜透過性ペプチドを基盤とした生物物理学観点からのユニークな細胞内導入」にこの場を借りて深く御礼を申し上げます。いずれのご講演でも先端研究を基礎から丁寧にご説明いただき、大変学びの多い貴重な機会になったと感じます。また、若手研究者からは、Andrea Di Santo さんに抗体医薬に対する抗医薬品抗体に関して、Maria Chiara Maimone さんに抗SARS-CoV-2 ペプチドに関して、それぞれ英語でご発表いただきました。お二人ともイタリア フィレンツェ大学から日本に短期留学中の PhD student で、活発な質疑応答を含め若手聴講者の皆様にも大いに刺激になったと思います。

この度、初夏の鹿児島での本フォーラムに、鹿児島大学理工学研究科の大学院講義として取り扱わせていただいた経緯もあり、60 名を超える参加者にお集まりいただきました。本フォーラムを開催できたことは、日本ペプチド学会や関係の諸先生方のご協力あってこそのものです。講演者、参加者、関係者の皆様に改めて感謝申し上げます。また、開催を支えてくださった鹿児島大学 伊東研究室のスタッフの皆様と、ペプチド研究所の河上紘子氏に改めてお礼申し上げます。今後も、ペプチドフォーラムが継続的にペプチド研究の交流の場として活用され、日本のペプチド研究のさらなる発展につながることを祈念し、開催報告とさせていただきます。

学会からのお知らせ

《2025 年度行事予定》

2025 年 10 月 20 日 (月)
第 120 回理事会・第 44 回評議員会合同会議

2025 年 10 月 21 日 (火) ～ 23 日 (木)
第 62 回ペプチド討論会
場　所：福岡国際会議場
世話人：伊東 祐二（鹿児島大）、野瀬 健（九州大）、
松島 綾美（九州大）

2025 年 10 月 22 日 (水)
2025 年度日本ペプチド学会通常総会

2025 年 10 月 25 日 (土)
市民フォーラム 2025「ペプチドの世界へようこそ！－未来を変える分子からキャリア形成まで－」
場　所：九州大学 馬出キャンパス 百年講堂

2025 年 11 月
第 19 期評議員選挙公告

2025 年 12 月
第 19 期評議員選挙開票

2026 年 1 月
第 121 回理事会

訃　報

日本ペプチド学会名誉会員・中嶋暉躬先生（享年 91 歳）（東京大学名誉教授）が、本年 1 月 4 日にご逝去されました。日本ペプチド学会を代表して、中嶋暉躬先生のご逝去を悼み、ここに謹んでお悔やみを申し上げます。

中嶋暉躬先生は、東京大学薬学部および同大学院薬学系研究科で学ばれ教鞭を執られたのち、広島大学医学部総合薬学科、東京医科歯科大学医用器材研究所、東京大学薬学部の教授を歴任されました。この間、中嶋先生は、一貫して、その持ち前の分析知識・技能をフルに発揮されて、精力的に、昆虫等の小動物から数多くのペプチド性あるいはポリアミン性の毒成分を単離されました。薬学部での研究としては異を放っておられたのかもしれませんが、中嶋先生は「本来のホルモンのような生理活性物質ではないのに、なぜこれらの毒ペプチド等が細胞や生体に高い特異性をもって作用するのか」という強い学術的興味を抱いておられました。本学会の前身であるペプチド化学討論会の時代より、新たなペプチド毒を次々と発表されておられた中嶋先生のお姿を印象的に覚えておられる本学会員の方も多いでしょう。中嶋暉躬先生は、その非常に温厚なお人柄が常に周囲の人々を引きつけ、本学会内のコミュニティーでも数多くの共同研究を行って来られた先生のお一人です。その結果、中嶋先生が発見された多くの毒物は、単なる毒物学の研究対象であるばかりでなく、生化学・物理化学などの研究ツールとしても活用されることとなりました。1994 年には、ハチ毒やクモ毒の神経科学的側面に関する共同研究の業績が認められて、日本学士院賞も受賞されています。

東京大学を定年退官で退かれたあとは、中西香爾先生の後を継がれて財団法人サントリー生物有機科学研究所の所長となり研究を続けられていました。しかし、その卓越した人望がまわりに知られることになり、乞われてサントリー株式会社の専務取締役や星薬科大学の学長など要職にも就かれ、非常にお忙しい毎日を過ごされていました。中嶋先生ご自身は、もっともっと研究の現場にいることを望まれていたようですので、あの世では、またご研究を楽しまれているのではないかと思わずにはいられません。本学会に多くのペプチド研究の種を蒔かれて行かれた中嶋先生のご冥福を心よりお祈り申し上げます。

日本ペプチド学会
会長　大高 章